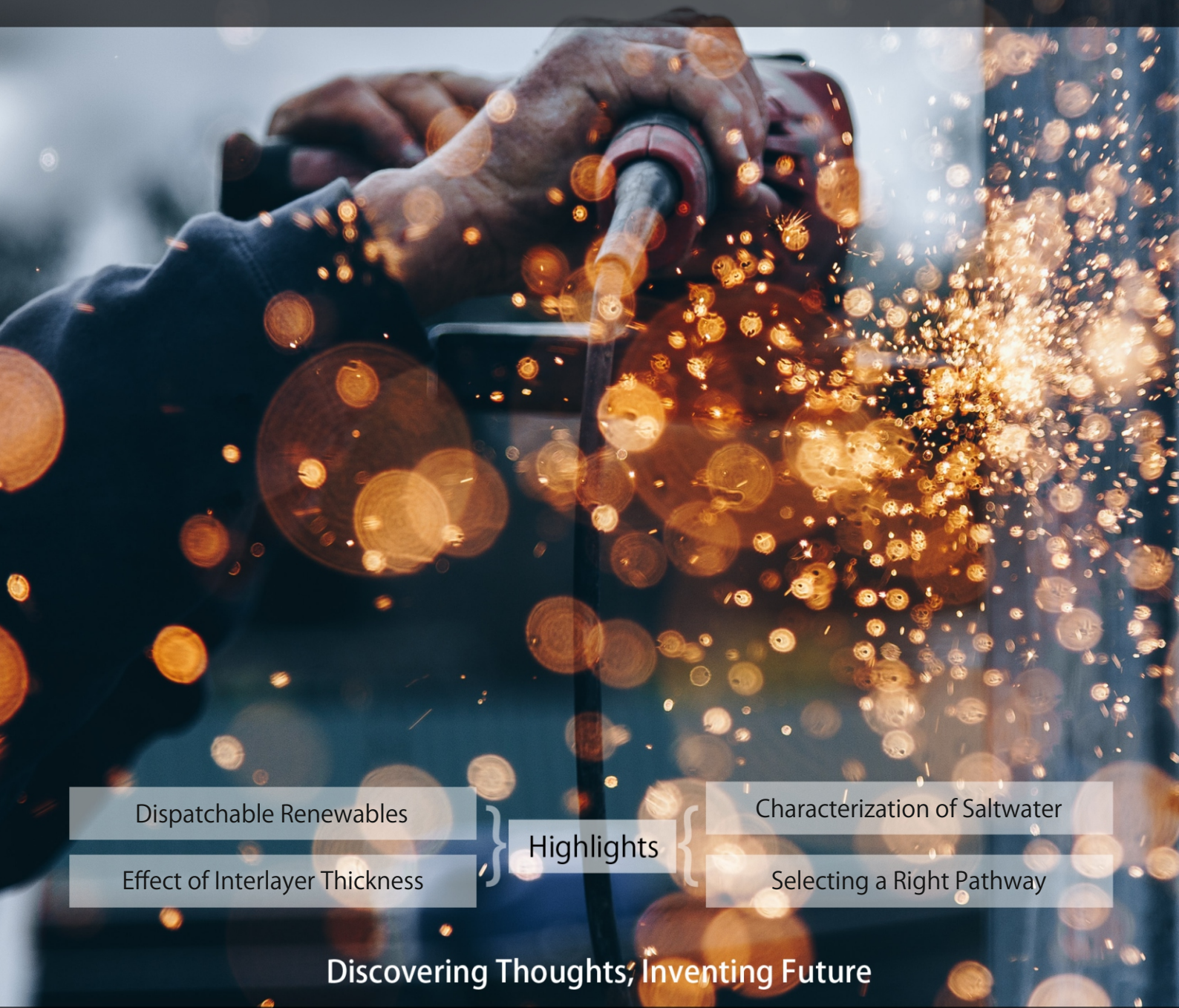


GLOBAL JOURNAL

OF RESEARCHES IN ENGINEERING: J

General Engineering



Dispatchable Renewables

Effect of Interlayer Thickness

} Highlights {

Characterization of Saltwater

Selecting a Right Pathway

Discovering Thoughts, Inventing Future

VOLUME 24 ISSUE 1 VERSION 1.0



GLOBAL JOURNAL OF RESEARCHES IN ENGINEERING: J
GENERAL ENGINEERING



GLOBAL JOURNAL OF RESEARCHES IN ENGINEERING: J
GENERAL ENGINEERING

VOLUME 24 ISSUE 1 (VER. 1.0)

OPEN ASSOCIATION OF RESEARCH SOCIETY

© Global Journal of
Researches in Engineering.
2024.

All rights reserved.

This is a special issue published in version 1.0
of "Global Journal of Researches in
Engineering." By Global Journals Inc.

All articles are open access articles distributed
under "Global Journal of Researches in
Engineering"

Reading License, which permits restricted use.
Entire contents are copyright by of "Global
Journal of Researches in Engineering" unless
otherwise noted on specific articles.

No part of this publication may be reproduced
or transmitted in any form or by any means,
electronic or mechanical, including
photocopy, recording, or any information
storage and retrieval system, without written
permission.

The opinions and statements made in this
book are those of the authors concerned.
Ultrapublishing has not verified and neither
confirms nor denies any of the foregoing and
no warranty or fitness is implied.

Engage with the contents herein at your own
risk.

The use of this journal, and the terms and
conditions for our providing information, is
governed by our Disclaimer, Terms and
Conditions and Privacy Policy given on our
website [http://globaljournals.us/terms-and-condition/
menu-id-1463/](http://globaljournals.us/terms-and-condition/menu-id-1463/).

By referring / using / reading / any type of
association / referencing this journal, this
signifies and you acknowledge that you have
read them and that you accept and will be
bound by the terms thereof.

All information, journals, this journal,
activities undertaken, materials, services and
our website, terms and conditions, privacy
policy, and this journal is subject to change
anytime without any prior notice.

Incorporation No.: 0423089
License No.: 42125/022010/1186
Registration No.: 430374
Import-Export Code: 1109007027
Employer Identification Number (EIN):
USA Tax ID: 98-0673427

Global Journals Inc.

(A Delaware USA Incorporation with "Good Standing"; Reg. Number: 0423089)

Sponsors: Open Association of Research Society

Open Scientific Standards

Publisher's Headquarters office

Global Journals® Headquarters
945th Concord Streets,
Framingham Massachusetts Pin: 01701,
United States of America

USA Toll Free: +001-888-839-7392

USA Toll Free Fax: +001-888-839-7392

Offset Typesetting

Global Journals Incorporated
2nd, Lansdowne, Lansdowne Rd., Croydon-Surrey,
Pin: CR9 2ER, United Kingdom

Packaging & Continental Dispatching

Global Journals Pvt Ltd
E-3130 Sudama Nagar, Near Gopur Square,
Indore, M.P., Pin:452009, India

Find a correspondence nodal officer near you

To find nodal officer of your country, please
email us at local@globaljournals.org

eContacts

Press Inquiries: press@globaljournals.org

Investor Inquiries: investors@globaljournals.org

Technical Support: technology@globaljournals.org

Media & Releases: media@globaljournals.org

Pricing (Excluding Air Parcel Charges):

Yearly Subscription (Personal & Institutional)
250 USD (B/W) & 350 USD (Color)

EDITORIAL BOARD

GLOBAL JOURNAL OF RESEARCH IN ENGINEERING

Dr. Ren-Jye Dzung

Professor Civil Engineering, National Chiao-Tung University, Taiwan Dean of General Affairs, Ph.D., Civil & Environmental Engineering, University of Michigan United States

Dr. Iman Hajirasouliha

Ph.D. in Structural Engineering, Associate Professor, Department of Civil and Structural Engineering, University of Sheffield, United Kingdom

Dr. Ye Tian

Ph.D. Electrical Engineering The Pennsylvania State University 121 Electrical, Engineering East University Park, PA 16802, United States

Dr. Eric M. Lui

Ph.D., Structural Engineering, Department of Civil & Environmental Engineering, Syracuse University United States

Dr. Zi Chen

Ph.D. Department of Mechanical & Aerospace Engineering, Princeton University, US Assistant Professor, Thayer School of Engineering, Dartmouth College, Hanover, United States

Dr. T.S. Jang

Ph.D. Naval Architecture and Ocean Engineering, Seoul National University, Korea Director, Arctic Engineering Research Center, The Korea Ship and Offshore Research Institute, Pusan National University, South Korea

Dr. Ephraim Suhir

Ph.D., Dept. of Mechanics and Mathematics, Moscow University Moscow, Russia Bell Laboratories Physical Sciences and Engineering Research Division United States

Dr. Pangil Choi

Ph.D. Department of Civil, Environmental, and Construction Engineering, Texas Tech University, United States

Dr. Xianbo Zhao

Ph.D. Department of Building, National University of Singapore, Singapore, Senior Lecturer, Central Queensland University, Australia

Dr. Zhou Yufeng

Ph.D. Mechanical Engineering & Materials Science, Duke University, US Assistant Professor College of Engineering, Nanyang Technological University, Singapore

Dr. Pallav Purohit

Ph.D. Energy Policy and Planning, Indian Institute of Technology (IIT), Delhi Research Scientist, International Institute for Applied Systems Analysis (IIASA), Austria

Dr. Balasubramani R

Ph.D., (IT) in Faculty of Engg. & Tech. Professor & Head, Dept. of ISE at NMAM Institute of Technology

Dr. Sofoklis S. Makridis

B.Sc(Hons), M.Eng, Ph.D. Professor Department of Mechanical Engineering University of Western Macedonia, Greece

Dr. Steffen Lehmann

Faculty of Creative and Cultural Industries Ph.D., AA Dip University of Portsmouth United Kingdom

Dr. Wenfang Xie

Ph.D., Department of Electrical Engineering, Hong Kong Polytechnic University, Department of Automatic Control, Beijing University of Aeronautics and Astronautics China

Dr. Hai-Wen Li

Ph.D., Materials Engineering, Kyushu University, Fukuoka, Guest Professor at Aarhus University, Japan

Dr. Saeed Chehreh Chelgani

Ph.D. in Mineral Processing University of Western Ontario, Adjunct professor, Mining engineering and Mineral processing, University of Michigan United States

Belen Riveiro

Ph.D., School of Industrial Engineering, University of Vigo Spain

Dr. Adel Al Jumaily

Ph.D. Electrical Engineering (AI), Faculty of Engineering and IT, University of Technology, Sydney

Dr. Maciej Gućma

Assistant Professor, Maritime University of Szczecin Szczecin, Ph.D.. Eng. Master Mariner, Poland

Dr. M. Meguellati

Department of Electronics, University of Batna, Batna 05000, Algeria

Dr. Haijian Shi

Ph.D. Civil Engineering Structural Engineering Oakland, CA, United States

Dr. Chao Wang

Ph.D. in Computational Mechanics Rosharon, TX, United States

Dr. Joaquim Carneiro

Ph.D. in Mechanical Engineering, Faculty of Engineering, University of Porto (FEUP), University of Minho, Department of Physics Portugal

Dr. Wei-Hsin Chen

Ph.D., National Cheng Kung University, Department of Aeronautics, and Astronautics, Taiwan

Dr. Bin Chen

B.Sc., M.Sc., Ph.D., Xian Jiaotong University, China. State Key Laboratory of Multiphase Flow in Power Engineering Xi'an Jiaotong University, China

Dr. Charles-Darwin Annan

Ph.D., Professor Civil and Water Engineering University Laval, Canada

Dr. Jalal Kafashan

Mechanical Engineering Division of Mechatronics KU Leuven, Belgium

Dr. Alex W. Dawotola

Hydraulic Engineering Section, Delft University of Technology, Stevinweg, Delft, Netherlands

Dr. Shun-Chung Lee

Department of Resources Engineering, National Cheng Kung University, Taiwan

Dr. Gordana Colovic

B.Sc Textile Technology, M.Sc. Technical Science Ph.D. in Industrial Management. The College of Textile? Design, Technology and Management, Belgrade, Serbia

Dr. Giacomo Risitano

Ph.D., Industrial Engineering at University of Perugia (Italy) "Automotive Design" at Engineering Department of Messina University (Messina) Italy

Dr. Maurizio Palesi

Ph.D. in Computer Engineering, University of Catania, Faculty of Engineering and Architecture Italy

Dr. Salvatore Brischetto

Ph.D. in Aerospace Engineering, Polytechnic University of Turin and in Mechanics, Paris West University Nanterre La Defense Department of Mechanical and Aerospace Engineering, Polytechnic University of Turin, Italy

Dr. Wesam S. Alaloul

B.Sc., M.Sc., Ph.D. in Civil and Environmental Engineering, University Technology Petronas, Malaysia

Dr. Ananda Kumar Palaniappan

B.Sc., MBA, MED, Ph.D. in Civil and Environmental Engineering, Ph.D. University of Malaya, Malaysia, University of Malaya, Malaysia

Dr. Hugo Silva

Associate Professor, University of Minho, Department of Civil Engineering, Ph.D., Civil Engineering, University of Minho Portugal

Dr. Fausto Gallucci

Associate Professor, Chemical Process Intensification (SPI), Faculty of Chemical Engineering and Chemistry Assistant Editor, International J. Hydrogen Energy, Netherlands

Dr. Philip T Moore

Ph.D., Graduate Master Supervisor School of Information Science and engineering Lanzhou University China

Dr. Cesar M. A. Vasques

Ph.D., Mechanical Engineering, Department of Mechanical Engineering, School of Engineering, Polytechnic of Porto Porto, Portugal

Dr. Jun Wang

Ph.D. in Architecture, University of Hong Kong, China Urban Studies City University of Hong Kong, China

Dr. Stefano Invernizzi

Ph.D. in Structural Engineering Technical University of Turin, Department of Structural, Geotechnical and Building Engineering, Italy

Dr. Togay Ozbakkaloglu

B.Sc. in Civil Engineering, Ph.D. in Structural Engineering, University of Ottawa, Canada Senior Lecturer University of Adelaide, Australia

Dr. Zhen Yuan

B.E., Ph.D. in Mechanical Engineering University of Sciences and Technology of China, China Professor, Faculty of Health Sciences, University of Macau, China

Dr. Jui-Sheng Chou

Ph.D. University of Texas at Austin, U.S.A. Department of Civil and Construction Engineering National Taiwan University of Science and Technology (Taiwan Tech)

Dr. Houfa Shen

Ph.D. Manufacturing Engineering, Mechanical Engineering, Structural Engineering, Department of Mechanical Engineering, Tsinghua University, China

Prof. (LU), (UoS) Dr. Miklas Scholz

Cand Ing, BEng (equiv), PgC, MSc, Ph.D., CWEM, CEnv, CSci, CEng, FHEA, FIEMA, FCIWEM, FICE, Fellow of IWA, VINNOVA Fellow, Marie Curie Senior, Fellow, Chair in Civil Engineering (UoS) Wetland Systems, Sustainable Drainage, and Water Quality

Dr. Yudong Zhang

B.S., M.S., Ph.D. Signal and Information Processing, Southeast University Professor School of Information Science and Technology at Nanjing Normal University, China

Dr. Minghua He

Department of Civil Engineering Tsinghua University Beijing, 100084, China

Dr. Philip G. Moscoso

Technology and Operations Management IESE Business School, University of Navarra Ph.D. in Industrial Engineering and Management, ETH Zurich M.Sc. in Chemical Engineering, ETH Zurich, Spain

Dr. Stefano Mariani

Associate Professor, Structural Mechanics, Department of Civil and Environmental Engineering, Ph.D., in Structural Engineering Polytechnic University of Milan Italy

Dr. Ciprian Lapusan

Ph. D in Mechanical Engineering Technical University of Cluj-Napoca Cluj-Napoca (Romania)

Dr. Francesco Tornabene

Ph.D. in Structural Mechanics, University of Bologna Professor Department of Civil, Chemical, Environmental and Materials Engineering University of Bologna, Italy

Dr. Kitipong Jaojaruek

B. Eng, M. Eng, D. Eng (Energy Technology, Asian Institute of Technology). Kasetsart University Kamphaeng Saen (KPS) Campus Energy Research Laboratory of Mechanical Engineering

Dr. Burcin Becerik-Gerber

University of Southern California Ph.D. in Civil Engineering Ddes, from Harvard University M.S. from University of California, Berkeley M.S. from Istanbul, Technical University

Hiroshi Sekimoto

Professor Emeritus Tokyo Institute of Technology Japan Ph.D., University of California Berkeley

Dr. Shaoping Xiao

BS, MS Ph.D. Mechanical Engineering, Northwestern University The University of Iowa, Department of Mechanical and Industrial Engineering Center for Computer-Aided Design

Dr. A. Stegou-Sagia

Ph.D., Mechanical Engineering, Environmental Engineering School of Mechanical Engineering, National Technical University of Athens, Greece

Diego Gonzalez-Aguilera

Ph.D. Dep. Cartographic and Land Engineering, University of Salamanca, Avilla, Spain

Dr. Maria Daniela

Ph.D in Aerospace Science and Technologies Second University of Naples, Research Fellow University of Naples Federico II, Italy

Dr. Omid Gohardani

Ph.D. Senior Aerospace/Mechanical/ Aeronautical,
Engineering professional M.Sc. Mechanical Engineering,
M.Sc. Aeronautical Engineering B.Sc. Vehicle
Engineering Orange County, California, US

Dr. Paolo Veronesi

Ph.D., Materials Engineering, Institute of Electronics,
Italy President of the master Degree in Materials
Engineering Dept. of Engineering, Italy

CONTENTS OF THE ISSUE

- i. Copyright Notice
- ii. Editorial Board Members
- iii. Chief Author and Dean
- iv. Contents of the Issue

1. Dispatchable Renewables: Selecting a Right Pathway. *1-31*
2. Comparative Characterization of Saltwater from Kula, Nembe, and Kwale in the Niger Delta, Nigeria. *33-41*
3. Evolution of the use of Nanoparticles in Cancer Diagnosis and Treatment. *43-50*
4. Effect of Interlayer Thickness on Mechanical Properties of Steel/Polymer/Steel Laminates Fabricated by Roll Bonding Technique. *51-72*

- v. Fellows
- vi. Auxiliary Memberships
- vii. Preferred Author Guidelines
- viii. Index



GLOBAL JOURNAL OF RESEARCHES IN ENGINEERING: J
GENERAL ENGINEERING
Volume 24 Issue 1 Version 1.0 Year 2024
Type: Double Blind Peer Reviewed International Research Journal
Publisher: Global Journals
Online ISSN: 2249-4596 & Print ISSN: 0975-5861

Dispatchable Renewables: Selecting a Right Pathway

By Alexandre Pavlovski

Abstract- Clean Grid readiness is a major objective of Canada's Clean Grid 2035 efforts and commitment to make all electricity generation in the country carbon net-zero. Making all the sources of electricity in power grids clean would be a tremendous step in Canada's energy transition and low carbon economy growth.

Deploying on a very large scale variable renewables such as wind and solar in Canada requires an extremely significant power dispatchability effort, allowing the country's power grids to maintain their reliability. Dispatchable generation refers to controllable and flexible sources of electricity that can promptly respond to demand at the request of power grid operators. The Clean Grid 2035 commitment assumes that all existing and new power dispatchability sources in Canada backing up variable renewables' operations are clean.

Keywords: carbon net zero, electric federalism, clean grid readiness, variable renewables, dispatchability reserves, hydro power, geothermal power, clean power generation, renewable dispatchable fleet, interchange.

GJRE-J Classification: LCC: TK3105



DISPATCHABLE RENEWABLES SELECTING A RIGHT PATHWAY

Strictly as per the compliance and regulations of:



RESEARCH | DIVERSITY | ETHICS

Dispatchable Renewables: Selecting a Right Pathway

Alexandre Pavlovski

Abstract- Clean Grid readiness is a major objective of Canada's Clean Grid 2035 efforts and commitment to make all electricity generation in the country carbon net-zero. Making all the sources of electricity in power grids clean would be a tremendous step in Canada's energy transition and low carbon economy growth.

Deploying on a very large scale variable renewables such as wind and solar in Canada requires an extremely significant power dispatchability effort, allowing the country's power grids to maintain their reliability. Dispatchable generation refers to controllable and flexible sources of electricity that can promptly respond to demand at the request of power grid operators. The Clean Grid 2035 commitment assumes that all existing and new power dispatchability sources in Canada backing up variable renewables' operations are clean.

Choosing to have the renewable segment of clean dispatchability sources lead in Canada's Clean Grid efforts and creating renewable dispatchable fleets – the clean power generation fleets that will make all variable renewables in the country dispatchable. Canada's extremely strong reservoir-based dispatchable hydro power generation in Newfoundland and Labrador, Quebec and Manitoba can participate in these fleets to back up variable renewables' growth in the country. Canada's unique geothermal power generation in the Pacific Rim, including the regions of northeastern British Columbia

and southern Yukon, northern Alberta and southern Northwest Territories, constitutes very high potential for highly dispatchable electricity generation to participate in renewable dispatchable fleets.

The proposed approach to using hydropower as a variable dispatchability reserve for Eastern Canada and combining hydropower and geothermal power as dispatchability reserves for Western Canada will make variable renewables dispatchable, upgrading all power grids in Canada to 100% Clean Grid readiness by 2035 and maintaining this Clean Grid commitment in 2050 and beyond. Using dispatchable hydropower and geothermal power together with wind and solar power in Renewable Dispatchable Fleets would make all renewable capacity dispatchable, establishing leading clean dispatchability practices in North America.

To agree on Renewable Dispatchable Fleets deployment and existing Renewable Dispatchability Reserves commitments from the provinces owning and operating large scale reservoir-based hydro power plants, Canada's "electric federalism" concept and approach should be demonstrated efficiently and promptly.

Keywords: carbon net zero, electric federalism, clean grid readiness, variable renewables, dispatchability reserves, hydro power, geothermal power, clean power generation, renewable dispatchable fleet, interchange.

Graphic Abstract



Author: Green Power Labs Inc., Dartmouth, Canada. e-mail: ampavlovski@greenpowerlabs.com

I. INTRODUCTION

a) *A Growing, Clean Economy*

Canada is currently competing globally for its share in a low carbon economy [1]. According to the Government of Canada vision, the country must capitalize on Canada's competitive advantages, including critical resources needed by the world, and the country's skilled and diverse workforce. Canada is bringing solutions for and "business bridges" between highest-quality manufacturing at home and exporting leading products and services globally.

To successfully grow the economy while averting the worst impacts of climate change, the Government of Canada is committed to meeting an ambitious climate target of 40-45% emissions reductions by 2030 and achieving net-zero emissions (where our economy either emits no greenhouse gas emissions or offsets its emissions) by 2050 [2].

b) *Total Electrification Targets and Steps*

Electricity is becoming the key fuel for low carbon economy activities in Canada. Today the country is committed to total electrification. By fully decarbonizing Canada's electricity grids by 2035, our country is enabling the rest of the economy to electrify by 2050 [3].

According to the 2023 federal budget, Canada's electricity demand is expected to double by 2050. To meet this increased demand with a sustainable, secure, and affordable grid, the country's electricity capacity must increase by 2.2 to 3.4 times compared to current levels. To achieve both objectives, the Government of Canada is committed to ensuring that an emissions-free grid ("Clean Grid") target has been achieved by 2035 [4]. These commitments expect phaseout of coal generation in 2030, clean grid deployment, with last sales of new internal combustion engine vehicles in 2035, and net-zero total emissions in 2050 [2].

c) *Energy Transition means Dispatchable Renewables*

Ensuring the increasing penetration of renewable power into the energy supply mix, towards total electrification, is very often referred to as an "energy transition" [5]. Moving from fossil fuel-based to clean electricity-based electricity sources and scaling the growth of clean electricity changed the role of renewables from historically "secondary" to today's "primary" in building Canada's low carbon economy.

This means that all clean electricity generation fleets on the grid, including variable renewables such as wind or solar, should be made dispatchable by keeping necessary clean dispatchability reserves.

Dispatchable renewables in Canada are presented by large reservoir-based hydro power strongly established in the country. Hydro power generating stations have been for many years contributing to electricity use at home as well as to

exporting electricity as a valuable product. This includes hydro power in Newfoundland and Labrador, Quebec, Manitoba, and British Columbia [6-10].

Dispatchable renewables opportunities in Canada are also presented by geothermal resources. Enhanced Geothermal Systems for power generation based on deep geothermal resources can provide power generation as well as clean dispatchability reserves. Geothermal power is economically attractive in energy transition process [11-14] that is seen as a longer-term objective in Canada. The high capacity factor of geothermal power makes it particularly attractive as a renewable resource for highly dispatchable electricity generation. Geothermal resources with high (> 150°C) temperatures allow very high potential for electrical generation in regions of northeastern and southern Yukon, northern Alberta, and southern Northwest Territories.

Using hydro and geothermal power sources and clean dispatchability resources for variable renewables allows for integrating dispatchable renewable fleets to address the Clean Grid goals in Canada in mid- and long-term.

d) *Realizing Electric Federalism*

Achieving net zero goals in Canada through energy transition requires an approach often referred to as electric federalism [15]. In the Canadian federation, electric federalism presents coherent policy actions from federal, provincial, and territorial governments focused on upgrading and aligning all electricity systems in Canada to meet net zero in a timely manner.

Currently, electricity in Canada is provincially regulated, and system planning still occurs in silos, leaving no overarching entity to enact policies and changes that ensure these benefits are realized. Instead, it is voluntary on the part of provinces and territories.

The electric federalism approach is seen as a core basis for moving forward in integrating renewable dispatchable fleets through regional integration and related close collaboration. Interregional integration through strong interties will improve economic efficiency due to the technical benefits of larger, integrated power systems.

Based on the understanding of electric federalism in 2024, policy interventions from federal, provincial, and territorial governments are expected to upgrade and transform electricity systems in Canada, allowing for growing renewable dispatchable fleets. This includes considerable policy leadership from the provinces, since they control many of the key policy levers, and an important enabling and accelerating role played by the federal government [15].

e) *Investment in Dispatchable Renewables: Calling for Actions*

Completing Renewable Dispatchable Fleets integration efforts and achieving Clean Grid goals and objectives within 2025-2035 time frame requires prompt and efficient investment decisions at federal and provincial levels.

The federal government can complement its policy efforts related to Renewable Dispatchable Fleets—including support for integration in the electricity sector—with financial support for clean dispatchable reserves deployment that incentivize provincial and territorial governments to exercise their policy tools. In return for coordinated provincial and territorial policy action focused on investments in Renewable Dispatchable Fleets, the federal government could offer more stable long-term funding for provincial and territorial electricity transformations [15].

As indicated in Canada's 2023 Budget, "...Given the long lead times and high upfront costs for electricity generation and transmission projects—and with our allies and partners set to invest heavily in preparing their own electrical grids for the future—Canada needs to move quickly to avoid the consequences of underinvestment" [1].

The Canada Infrastructure Bank is seen as an active partner in supporting these efforts by making investments in renewable energy, energy storage, and transmission projects. These investments may position the Canada Infrastructure Bank as the government's primary financing tool for supporting clean electricity generation, transmission, and storage projects, including for major Renewable Dispatchable Fleet Integration projects in Canada.

Overall, based on the electric federalism rooted in negotiated agreements of the federal government with provinces, as well as historical and current experiences of the provinces with power transmissions, intra-provincial interties and international interconnections, Renewable Dispatchable Fleets in Canada would provide a unique solution for the country to achieve its net zero goals and commitments "in a way that makes sense in the Canadian federation" [15].

This paper is focused on efficient and effective ways of growing Renewable Dispatchable Fleets in Canada's energy transition. It describes proposed changes in clean dispatchability reserves meeting clean generation mix and "Clean Grid 2035" objectives and commitments. Specifically, the following issues are discussed:

- Available dispatchability reserves for variable renewables planned in each of the provinces and territories by 2035;
- Review of existing Clean Dispatchability Reserves in each of the provinces;

- Review of new Renewable Dispatchable assets for each of the provinces using the experience with their existing renewable assets and geo-economical [16] resources;
- Review of an electric federalism [15] approach to potential shares of Clean Dispatchability Reserves considered by the provinces to meet the Canadian "Clean Grid 2035" commitment.

II. MATERIALS AND METHODS

a) *Approaching Dispatchable Renewables*

i. *Clean Grid Readiness Commitment*

A starting point for approaching dispatchable renewables vision in Canada is closely related to clean grid as a major goal. Indeed, among the ten provinces that have been using 99.8% of electricity in Canada, seven provinces, for different geo-economic reasons, historically committed to clean electricity generation, mostly based on hydro or/and uranium (even Ontario, the second largest electricity generation-wise in Canada, has only less than 7% of electricity from natural gas in 2022). Only three provinces (Alberta, Saskatchewan, and Nova Scotia) have had their electricity generation heavily based on fossil fuels and are currently addressing a unique task of deploying very large scale renewable fleets within a decade to contribute to Canada's Clean Grid 2035 commitment [17].

Table 1.1 below shows "clean grid" readiness targets (in percent) for each of the Canadian provinces. These targets indicate electricity generation projections of the Canada Energy Regulator (CER). Most recent data provided by CER is analysed in its Energy Future report of 2023 (further-EF2023) [18] presenting first long-term outlook. The report presents its key findings in Current Measures, Canada NetZero, and Global NetZero scenarios (Global NetZero scenario is not discussed in this paper).

Table 1.1: Clean Grid Readiness Targets by Province

Electricity Generation: Clean Grid Readiness, %	2030		2035	
	NetZero	Current	NetZero	Current
Alberta	36.6%	17.9%	95.1%	20.6%
British Columbia	81.0%	84.8%	96.4%	85.8%
Manitoba	99.8%	99.8%	99.9%	98.7%
New Brunswick	96.7%	98.0%	99.1%	99.1%
Newfoundland and Labrador	100%	100%	100%	100%
Northwest Territories	85.3%	95.1%	94.1%	96.7%
Nova Scotia	92.4%	35.2%	99.7%	39.8%
Nunavut	6.0%	6.1%	35.5%	39.4%
Ontario	87.3%	90.9%	97.6%	90.8%
Prince Edward Island	97.7%	98.3%	99.8%	99.6%
Quebec	99.2%	98.7%	99.3%	96.2%
Saskatchewan	52.2%	52.3%	98.3%	61.1%
Yukon	50.2%	54.6%	69.8%	74.2%

Shaded in Table 1.1 are the provinces of Alberta, Saskatchewan, and Nova Scotia which because of historical business development reasons require support in Clean Grid Readiness.

According for EF2023, in Canada NetZero scenario variable renewables Alberta, Saskatchewan and Nova Scotia are expected to deploy 50% of wind power generation and 63.7% of solar power generation in Canada. While, as a leading nation globally, Canada has committed to the clean electricity grid concept supporting a low-carbon economy and adaptation to climate change, thoughtful and strategic business and community approaches have to be supported in Alberta, Saskatchewan, and Nova Scotia to meet the federally proposed timelines.

These approaches have to keep all clean/renewable sources dispatchable, and to strengthen electricity export opportunities both in Eastern and Western Canada. Today these approaches clearly exist and are technically doable within the "clean grid 2035" time frame.

In Eastern Canada they are presented by large-scale onshore and/or offshore wind power in the Canadian part of the Atlantic Rim (e.g., off Sable Island and other related areas) that can be supported by hydro power from Newfoundland and Labrador (so called "Atlantic Axis" of power transmission).

In Western Canada they are also presented by large-scale deep geothermal power on the border of Alberta, British Columbia and Yukon in the Canadian part of the Pacific Rim overlapping the Pacific Ring of Fire. This major geothermal opportunity may be called the "Pacific Axis" of power transmission. The opportunity will not only address electricity needs in the regions, but it can also provide power dispatchability reserves much

beyond the target provinces in Western Canada. Technologies for enhanced geothermal systems have been developed and tested in Alberta and invested in globally (see [19,20]. It is expected that negotiations of the federal government with Alberta and Saskatchewan will bring this opportunity to the forefront of public policies and decision making at the federal and provincial levels.

While the EF2023 report reviewed five "What If" cases (such as wide-scale adoption of hydrogen, small modular reactor, direct air capture and carbon capture, utilization, and storage technologies maturity, and higher peak electricity demand due to electric vehicles charging) that may address uncertainties on the pathway to net-zero and possible changes in key assumptions in the report, it did not look into the ways of supporting the growth of variable renewables by available dispatchability reserves planned in each of the provinces and territories by 2035, the role of existing Clean Dispatchability Reserves in each of the provinces, including Renewable Dispatchability Reserves, and opportunities with Enhanced Geothermal systems and technologies based on Canadian geo-economical resources [16].

Although the future of energy in Canada is broader than the economic and technical factors driving the projections in EF2023, and many of these factors are beyond the scope of EF2023 analysis, some of these factors require critical attention and should be very promptly addressed as they touch very sensitive decisions of Canadian provinces and realities of electric federalism in Canada.

The following sections of this paper are dedicated to the two related factors: dispatchability of variable renewables, and enhanced geothermal systems

as a renewable dispatchable asset available for deployment and critically needed in Canada.

ii. *Data Sources and Assumptions*

a. *Data Sources*

For this publication the Author used the data on electricity demand, generation, capacity, interchange, and other related data for provinces in Canada provided publicly by the Canada Energy Regulator's (CER) [21]. Projections to 2050 were presented by CER in the "Canada's Energy Future 2023" (further - EF2023) report [18]. The data as of February 2024 was used.

The period for Energy Supply and Demand Projections was limited in this paper to 2023-2035 and focused on the Canadian "Clean Grid 2035" commitment.

The core data tables were limited to Canada NetZero and Current Measures scenarios presented in [18].

The core data tables included:

- End - Use Demand (petajoules)
- Electricity Generation by Primary Fuel (GWh)
- Electricity Generation by Technology (GWh)
- Electricity Capacity by Primary Fuel(MW)
- Electricity Capacity by Technology (MW)
- Electricity Interchange (GWh)

Electricity generation technology and its capacity included *fossil fuel* group, such as Carbon Capture, Utilization and Storage (CCUS) technology advancements that capture the greenhouse gas carbon dioxide (CO₂) and utilize it or store it safely underground (this includes Coal and Coke, Natural Gas, and Oil), *cleaner fuel* group (Bioenergy, Bioenergy with CCUS,

In Current Measures scenario (table 1.3.1):

Table 1.3.1: Electricity demand, generation, and interchange in target provinces: Current Measures

Current Measures Scenario, TWh	2025			2030			2035		
	Demand	Generation	Interchange	Demand	Generation	Interchange	Demand	Generation	Interchange
Alberta	83.83	93.01	9.18	92.17	105.74	13.57	100.55	112.39	11.84
Saskatchewan	27.00	26.60	-0.39	29.41	28.39	-1.01	31.68	30.77	-0.90
Nova Scotia	11.79	7.81	-3.98	12.92	9.53	-3.38	13.86	10.13	-3.73

and in Canada NetZero scenario (table 1.3.2):

Table 1.3.2: Electricity demand, generation, and interchange in target provinces: Canada NetZero

Canada Net-Zero Scenario, TWh	2025			2030			2035		
	Demand	Generation	Interchange and Loss	Demand	Generation	Interchange and Loss	Demand	Generation	Interchange and Loss
Alberta	81.61	90.39	8.77	97.15	106.78	9.63	117.17	128.49	11.32
Saskatchewan	26.08	25.75	-0.33	30.26	29.76	-0.50	36.41	35.38	-1.03
Nova Scotia	11.97	7.80	-4.17	13.70	14.10	0.40	15.52	21.66	6.15

Coal with CCUS, Natural Gas with CCUS) and *clean fuel* group of technologies (Hydro, Hydrogen, Onshore Wind, Offshore Wind, Solar (Distributed), Solar (Utility scale), Uranium, Uranium SMR).

The recent CER's EF2023 report [18] does not include geothermal electricity generation, a very powerful clean primary fuel and electricity generation technology with major energy resources in Canada.

b. *Assumptions*

Only existing and/or ready for deployment cleaner fuel and clean fuel technologies were used for "clean grid 2035" commitment.

Specifically, Cleaner Fuel included:

- Coal with CCUS and Natural Gas with CCUS
- Biomass with CCUS generation (conventional biomass was not included in "clean grid 2035" analysis)

In Clean Fuel the following assumptions were made:

- No tidal and wave generation was used in 2035 or earlier.
- No geothermal generation was used in EF2023 in the 2023-2035 period; in this paper Enhanced Geothermal Systems were proposed to be used starting 2031 after 7 years (2024 to 2030) of development.

iii. *Current Vision of Clean Grid Support*

Based on the Canada Energy Regulator's vision [18] of expected changes in Alberta, Saskatchewan and Nova Scotia, the situation in these three provinces defining a need for "clean grid" support to achieve the 2035 target is seen as follows:

EF2023 data for the 2025 to 2035 period including Electricity Demand, Generation, and Interchange in all Canadian provinces is summarised in Appendix A.

EF2023 electricity generation data by fuel for Alberta, Saskatchewan and Nova Scotia for NetZero and Current Measures scenarios is presented in Appendix B. Based on EF2023 data, the current vision of Canada's Clean Electricity Future presents an approach where

clean (Hydro, Onshore Wind, Offshore Wind, Solar (Distributed), Solar (Utility scale), Uranium SMR) and cleaner (e.g., Bioenergy with CCUS, Natural Gas with CCUS) fuels are planned to be used to achieve the "clean grid 2035" target in Alberta, Saskatchewan, and Nova Scotia.

In the NetZero scenario the following technology capacity for clean and cleaner fuels is expected as follows (table 1.3.3):

Table 1.3.3: Clean and Cleaner Fuel Capacity Total in target provinces: Canada NetZero

Alberta, Saskatchewan, and Nova Scotia - Total, MW	2025	2030	2035
Cleaner Fuels, MW	0	2,090	5,587
Cleaner Fuels, %	0%	13%	11%
Clean Fuels, MW	8,749	14,309	45,055
Clean Fuels, %	100%	87%	89%
Total clean/cleaner fuels, MW	8,749	16,399	50,642
Total clean/cleaner fuels, %	100%	100%	100%

Specifically, the total of clean technology capacity in the three provinces presents the major effort in the country in NetZero scenario - see tables 1.3.4 and 1.3.5 below:

Table 1.3.4: Clean and Cleaner Fuel Capacity in Target Provinces

Canada NetZero Scenario	Alberta		Saskatchewan		Nova Scotia	
	Deployed between		Deployed between		Deployed between	
	2026-2030	2031-2035	2026-2030	2031-2035	2026-2030	2031-2035
Solar (Distributed)	279.17	500	80	50	9	2.5
Solar (Utility scale)	750	11070	32	1354	0	0
Offshore Wind	0	0	0	0	2000	3000
Onshore Wind	1560	11440	850	1800	0	0
Natural Gas with CCUS	2090	2200	0	13.3	0	0
Bioenergy with CCUS	0	728	0	556	0	0
Uranium SMR	0	459	0	1070	0	0

Table 1.3.5: Clean and Cleaner Fuel Capacity Shares

Canada NetZero Scenario	CANADA		Alberta, Saskatchewan, and Nova Scotia TOTAL			
	Deployed between		Deployed between		Share, % Deployed between	
	2026-2030	2031-2035	2026-2030	2031-2035	2026-2030	2031-2035
Solar (Distributed)	1,237	1,329	368	553	30%	42%
Solar (Utility scale)	1,350	14,862	782	12,424	58%	84%
Offshore Wind	2,000	3,000	2,000	3,000	100%	100%
Onshore Wind	5,319	27,046	2,410	13,240	45%	49%
Natural Gas with CCUS	2,090	2,213	2,090	2,213	100%	100%
Bioenergy with CCUS	0	1,451	0	1,284	0%	89%
Uranium SMR	300	13,072	0	1,529	0%	12%

In the NetZero scenario the clean fuel effort made by Alberta, Saskatchewan, and Nova Scotia in 2035 is led by wind power (20.7 GW, 103.8 TWh) followed by solar power (14.1 GW, 21.6 TWh) and Uranium SMR (1.5 GW, 9.46 TWh).

Table 1.3.5 shows the provinces leadership in deployed capacity in Canada: 49% onshore wind, 100% offshore wind, 84% utility-scale solar.

To address the issues related to these capacities, the review and discussion in this paper is focused on clean fuels only, presenting close to 89% of the potential effort by 2035.

Variable renewables capacity data for Alberta, Saskatchewan and Nova Scotia planned by Canada Energy Regulator for 2030 and 2035 (see tables 1.3.4 and 1.3.5) is used in the following sections to define

available dispatchability reserves required and available in these target provinces.

b) *Making All Renewables Dispatchable*

i. *Power Dispatchability Definition and Applications*

Dispatchable sources are electricity sources that can be ramped up or down in a relatively short time – from milliseconds (e.g., grid batteries or spinning reserves) to minutes (e.g. natural gas and hydro turbines) and hours (e.g., coal, biomass, or nuclear plants), which is defined by electricity demand (load) and related operating conditions in the power grid [22,23].

Depending on the nature of dispatchable sources, they may be used for grid operations tasks such as load matching and peak matching, as well as supporting so-called “lead-in times” required by large coal or natural gas fueled electricity generators to reach full output.

This functionality of dispatchable sources may be extended to ancillary services that include active power/frequency control and reactive power/voltage control, on various timescales for maintaining grid stability and security [24].

ii. *Dispatchability of Renewables Today*

Today’s general understanding of the dispatchability of renewable power plants divides them into two major groups:

- *Non-dispatchable*: Solar photovoltaic (PV) and wind power plants
- *Dispatchable*: Hydroelectric, biomass, geothermal and ocean thermal energy conversion-based power plants.

For techno-economical reasons related to the temperature of the surface waters in Canada's Maritime Zones [25], ocean thermal energy conversion technology applications [26, 27] are not described in this paper.

Also, for local carbon economy reasons only natural gas-based and biomass power plants enabled with Carbon Capture, Utilization and Storage (CCUS) solutions are further discussed in this paper.

iii. *Capacity Value of Variable Renewables for Dispatchability Reserves*

When dealing with variable (“non-dispatchable”) renewable power sources such as wind or solar PV, grid operators have to keep ready-to-use dispatchable reserves to continuously maintain the balance between electricity generation (supply) and consumption (demand).

The amount of dispatchable reserves needed to be at hand in any utility service area with wind and/or solar power plants addressing the natural intermittency (variability) of these resources to smooth out electricity generation is defined by the Capacity Value of variable

generation plants. Capacity Value is the contribution that a plant makes toward the planning reserve margin [28] measuring the amount of generation capacity available to meet expected demand in planning horizon. For variable generation plants it means that a dedicated dispatchable reserves matching these plants will be added to the reserve margin.

When variable (wind or solar) generation is deployed, to ensure resource adequacy [29-32] of an electricity system grid operators determine Capacity Value of variable generation using reliability-based methods such as Effective Load Carrying Capability (ELCC), Equivalent Firm Capacity (EFC) or Equivalent Conventional Power (ECP) [33]. E.g., ELCC of a variable generation plant is defined as the amount by which the system’s loads can increase when the plant is added to the electricity system while maintaining the same system reliability of the system. Determined through a set of detailed calculations considering all possible intermittency and/or contingency scenarios for a utility, ELCC defines the required planning reserve that may or may not be available depending on the renewable generation output [34-37].

For growing penetration of wind and solar power in electricity generation, ELCC defines incremental changes in variable generation plants deployment and cumulative changes in variable generation.

An example of wind deployment is presented by Nova Scotia Power Inc. [38]. Adding 355 MW of wind power to 545 MW of wind power existing in the system brought incremental capacity value of 12% for this change and changed cumulative capacity value of wind power in the system from 26% (141.7 MW) at 545 MW level to 19% (171 MW) at 900 MW level. It is important to highlight that while cumulative capacity value of variable generation in terms of physical capacity (MW) is increasing with its penetration in the system, it is also decreasing as the fraction of its nameplate capacity (%).

Using the cumulative capacity value of wind power and solar power in Nova Scotia, Alberta, and Saskatchewan, and in Canada overall, we can define the level of dispatchable reserves to contribute to the planning reserve margins that are required for variable generation deployment towards Clean Grid 2035 targets in both Current Measures and Canada NetZero scenarios presented by EF2023 – see Tables 2.3.1 and 2.3.2 below.

Table 2.3.1: Determining Dispatchable Reserves for Variable Generation Capacity (Canada NetZero Scenario)

Canada NetZero Scenario, MW	Alberta			Saskatchewan			Nova Scotia		
	2025	2030	2035	2025	2030	2035	2025	2030	2035
Total capacity, MW	21,478	25,857	46,914	7,476	8,454	11,891	3,314	5,940	8,130
Solar (Distributed), MW	220.83	500	1000	20	100	150	1	10	12.5
Solar (Utility scale), MW	1180	1930	13000	84	116	1470	0.37	0.37	0.37
Total Solar Power, MW	1,401	2,430	14,000	104	216	1,620	1	10	13
Grid Penetration Solar, % of total capacity	6.5%	9.4%	29.8%	1.4%	2.6%	13.6%	0.0%	0.2%	0.2%
Capacity Value Solar, %	25.0%	18.0%	10.0%	32.0%	30.0%	15.0%	0.0%	35.0%	35.0%
Capacity Value Solar, MW	350	437	1,400	33	65	243	0	4	5
Offshore Wind, MW	0	0	0	0	0	0	0	2000	5000
Onshore Wind, MW	4,500	6,060	17,500	2,140	2,990	4,790	603	603	603
Total Wind Power, MW	4,500	6,060	17,500	2,140	2,990	4,790	603	2,603	5,603
Grid Penetration Wind, % of total capacity	21.0%	23.4%	37.3%	28.6%	35.4%	40.3%	18.2%	43.8%	68.9%
Capacity Value Wind, %	17.0%	17.0%	12.0%	19.0%	18.0%	17.0%	20.0%	19.0%	17.0%
Capacity Value Wind, MW	765	1030	2100	407	538	814	121	495	953
Total Variable Capacity Value, MW	1,115	1,468	3,500	440	603	1,057	121	498	957
Total Variable Capacity Value, % of grid capacity	5.2%	5.7%	7.5%	5.9%	7.1%	8.9%	3.6%	8.4%	11.8%

Table 2.3.2: Determining Dispatchable Reserves for Variable Generation Capacity (Current Measures Scenario)

Current Measures Scenario, MW	Alberta			Saskatchewan			Nova Scotia		
	2025	2030	2035	2025	2030	2035	2025	2030	2035
Total capacity, MW	20,115	24,327	26,277	6,926	7,614	9,208	3,423	4,219	3,250
Solar (Distributed), MW	188	300	550	64	96	811	1	5	8
Solar (Utility scale), MW	1,500.0	1,500.0	3,500.0	20	60	90	0.37	0.37	0.37
Total Solar Power, MW	1,688	1,800	4,050	84	156	901	1	5	8
Grid Penetration Solar, % of total capacity	8.4%	7.4%	15.4%	1.2%	2.0%	9.8%	0.0%	0.1%	0.2%
Capacity Value Solar, %	20%	21%	17.50%	30%	28%	19%	35%	35%	35%
Capacity Value Solar, MW	338	378	709	25	44	171	0.48	2	3

Onshore Wind, MW	2,850	3,750	3,750	1,800	2,630	3,280	603	657	828
Total Wind Power, MW	2,850	3,750	3,750	1,800	2,630	3,280	603	657	828
Grid Penetration Wind, % of total capacity	14.2%	15.4%	14.3%	26.0%	34.5%	35.6%	17.6%	15.6%	25.5%
Capacity Value Wind, %	18%	17%	17%	19%	18%	17%	19%	19%	19%
Capacity Value Wind, MW	513	638	638	342	473	558	115	125	157
Total Variable Capacity Value, MW	851	1,016	1,346	367	517	729	115	127	160
Total Variable Capacity Value, % of grid capacity	4.2%	4.2%	5.1%	5.3%	6.8%	7.9%	3.4%	3.0%	4.9%

Capacity value levels used in Tables 2.3.1, 2.3.2 are based on [35, Fig. 5] for wind power; and [37, Fig. 11] for solar PV.

Tables 2.3.1, 2.3.2 show that Variable Capacity Value indicates considerable dispatchability reserves required in every province adding variable generation to achieve the Clean Grid 2035 objective. This is specifically important in Alberta, Saskatchewan and Nova Scotia promptly growing their variable resources.

In the Canada NetZero scenario (table 2.3.1) within 2025 to 2035 period variable dispatchability reserves in Alberta will grow from 5.2% to 7.5%, in Saskatchewan – from 5.9% to 8.9%, and in Nova Scotia - from 3.6% to 11.8% of provincial grid capacity.

A summary of Variable Dispatchability Reserves needed in Canada and their growth in 2025-2035 in NetZero scenario is shown in Table 2.3.3 below:

Table 2.3.3: Variable Dispatchability Reserves needed in Canada by 2035

NetZero Scenario: Variable Dispatchability Reserves needed, MW	2025	2030	2035
<i>Eastern Canada:</i>			
Newfoundland and Labrador	16	18	19
Nova Scotia	121	498	957
Prince Edward Island	75	100	101
New Brunswick	93	107	442
Quebec	782	805	1,025
Ontario	1,879	2,223	3,211
<i>Subtotal Eastern Canada:</i>	<i>2,966</i>	<i>3,751</i>	<i>5,756</i>
<i>Western Canada:</i>			
Manitoba	68	102	105
Saskatchewan	440	603	1,057
Alberta	1,115	1,468	3,500
British Columbia	1,024	1,626	2,231
<i>Subtotal Western Canada:</i>	<i>2,647</i>	<i>3,798</i>	<i>6,894</i>
<i>Total Canada</i>	<i>5,613</i>	<i>7,549</i>	<i>12,649</i>

III. EXPECTED RESULTS AND OUTCOMES

a) Clean Electricity Sources for Dispatchability Reserves

i. Dispatchable Renewable Sources

Within the Clean Grid 2035 vision it is important that variable dispatchability reserves come from dispatchable renewable sources.

In Canada's environmental context two highly powerful dispatchable energy sources are available in the country: reservoir-based hydropower and deep geothermal power.

From an immediate readiness standpoint, *reservoir-based hydro power* can be seen as a strategic dispatchable renewable source available for load-

matching (within a few hours) and possibly for peak-matching (within a few minutes).

Specifically, major reservoir-based hydropower resources in Newfoundland and Labrador, Quebec and Manitoba may be used as dispatchability reserves for deploying variable resources in these – and neighbouring – provinces.

However, it is important to note that using shares of these hydropower sources as dispatchability reserves may reduce their ability to export electricity to the U.S.

Deep geothermal power sources, while not commercially tested in Canada, provide even higher opportunities for Clean Grid 2035 and beyond. Located in the area with very high geothermal resources bordering Alberta, British Columbia, and Yukon [geothermal references], these sources are realized with Enhanced Geothermal Systems (EGS). As a very efficient highly dispatchable resource with capacity factor of 90%, EGS is seen as a strong competitor to any clean electricity solutions considered in Western Canada. Technical and economic aspects of EGS are discussed in Section 4 of this paper.

ii. *Hydropower: Changing the Role*

Changing the role of reservoir-based hydropower resources from being export-focused to

becoming dispatchability reserves-focused to promptly deploy variable generation across the country presents a strategic opportunity for Clean Grid 2035.

From an economic angle, existing (and growing) power capacity should be seen firstly for meeting electricity demand and related dispatchability requirements, and only secondly for electricity exports. Because of the changes in variable capacity in each of the provinces' electricity generation mix, current export practices should be reviewed/upgraded to establish these priorities. Provincial generation capacity mix should clearly define changes in interconnections between the provinces to provide variable dispatchability reserves.

Favourable conditions for interchange with neighboring provinces should be established within the "electric federalism" context to make this a winning strategy for the provinces contributing variable dispatchability reserves, and for Canada in general.

iii. *Interchange Resources as a Key Asset*

Interchange resources including interprovincial out/in flows and exports/imports may be generally defined as a difference between Electricity Demand and Generation in the provinces. This difference includes transmission and distribution losses.

Table 3.3.1: Interchange Resources*

NetZero Scenario: Resources for Interchange, TWh	2025	2030	2035
<i>Eastern Canada:</i>			
Newfoundland and Labrador	32.84	32.47	32.43
Nova Scotia	-4.17	0.40	6.15
Prince Edward Island	-0.53	-0.51	-0.19
New Brunswick	-3.38	-6.67	-3.41
Quebec	20.56	35.06	36.72
Ontario	-9.60	-9.83	18.55
<i>Western Canada:</i>			
Manitoba	7.24	14.47	20.51
Saskatchewan	-0.33	-0.50	-1.03
Alberta	8.77	9.63	11.32
British Columbia	2.02	-5.07	-5.92

*Positive figures show interprovincial outflows and exports.
Negative figures show interprovincial inflows and imports.

A simplified methodology for defining a part of interchange resources available as variable dispatchability reserves using EF2023 data may be presented as follows.

$$G = D \times (1 + \text{TLF} + \text{DLF}) + \text{IF}, \text{ or}$$

$$\text{IF} = [G - D \times (1 + \text{TLF} + \text{DLF})], \text{ and}$$

$$I = \text{DR} + \text{IF} + \text{EF}, \text{ and}$$

$$\text{DRC} = \text{DR} / (\text{CF} \times 8760), \text{ where:}$$

TLF – Transmission loss factor (%)

DLF – Distribution loss factor (%)

G – Generation (TWh)

D – Demand (TWh)

IR – Interchange Resource (TWh),

IF – Interprovincial Flow (TWh),

EF – Export Flow (TWh),

DR – Dispatchability Reserves as a potential Interchange component (TWh)

DRC – Dispatchability Reserves Capacity (MW)

CF – Capacity factor of dispatchability reserve - related generation source, e.g., hydro power or geothermal power (%)

Calculations based on EF2023 data (see Table 3.3.1) show that Newfoundland and Labrador, and Quebec in Eastern Canada and Manitoba in Western Canada have interchange resources based on reservoir-based hydropower that can be used as dispatchability reserves. Nova Scotia and Alberta cannot use their resources for variable dispatchability planning.

However, due to long-term agreements between Newfoundland and Labrador and Quebec,

generation for variable dispatchability applications is limited to Muskrat Falls Generation Station (4.5 TWh annual at 62.3% capacity factor). With Quebec hydro capacity at 73.6% capacity factor (e.g., transmitting electricity from Churchill Falls station in NL) and Manitoba hydro capacity at 75% capacity factor, the sources for variable dispatchability reserves are seen as follows:

Table 3.3.2: Interchange Resources versus Variable Dispatchability Reserves Needed

NetZero Scenario: Interchange Resources Capacity, MW	2025	2030	2035
Newfoundland and Labrador	824	824	824
Quebec	941	2,769	2,319
Manitoba	830	1,880	2,734
Total Canada	2,595	5,473	5,877

NetZero Scenario: Variable Dispatchability Reserves needed, MW	2025	2030	2035
Subtotal Eastern Canada:	2,966	3,751	5,756
Subtotal Western Canada:	2,647	3,798	6,894
Total Canada	5,613	7,549	12,649

Comparing the dispatchability reserves sources and needs, we see that there is a clear gap between the sources and required uses in variable dispatchability reserves, and solutions should be discussed to address this dispatchability gap.

iv. *Realizing Clean Dispatchability Reserves Strategy*

Below are some examples describing possible realization of the “hydropower-as-a-clean-dispatchability-reserve” strategy in Eastern and Western Canada, using interchange capacity as a source of variable dispatchability reserves.

a. *Eastern Canada*

In the Canada NetZero scenario, the needs for dispatchability reserves may be as follows.

(1) *Variable generation growth in Nova Scotia*

In Eastern Canada, hydropower capacity in Newfoundland and Labrador presented by Muskrat Falls Generating Station may be considered as a major

source for variable dispatchability reserves for Nova Scotia.

By 2030 Nova Scotia plans to deploy 5 GW of offshore wind capacity to start exporting electricity. Dispatchability reserves required for variable capacity in Nova Scotia present 498 MW in 2030 and 957 MW in 2035 (see Table 2.3.3.). The installed capacity of Muskrat Falls Generating Station (NL) is 824 MW. It will provide 60% of its capacity to ensure related capacity value in Nova Scotia’s planning reserves only for 2.6 GW of wind power in 2030. In 2035 with expected 5.6GW of wind power in Nova Scotia, the full capacity of Muskrat Falls Generating Station will not be enough, and required difference in capacity would be required from Quebec.

Table 3.4.1: Variable dispatchability reserves for Nova Scotia

NetZero Scenario	2025	2030	2035
Muskrat hydro capacity, MW	824	824	824
Muskrat capacity factor, %	62.30%	62.30%	62.30%
Variable capacity in Nova Scotia, MW	604	2,613	5,616
Variable dispatchability reserves needed in Nova Scotia, MW	121	498	957
Muskrat hydro capacity available for electricity export, MW	703	326	0
Nova Scotia's purchase of dispatchability reserves from Quebec, MW	0	0	133

(2) *Clean dispatchability needs in Prince Edward Island, New Brunswick, and Ontario*

In Eastern Canada, the provinces of Prince Edward Island, New Brunswick and Ontario do not plan

to export electricity and do not have available reserves for variable capacity. The variable dispatchability needs of these provinces are as follows:

Table 3.4.2: Variable dispatchability reserves for Prince Edward Island, New Brunswick, and Ontario

NetZero Scenario	2025	2030	2035
Variable capacity in Prince Edward Island, MW	358.5	484.7	484.8
Dispatchability reserves for variable capacity required for PEI, MW	75.3	99.8	101.1
Variable capacity in New Brunswick, MW	430.2	488.2	2,297.7
Dispatchability reserves for variable capacity required for New Brunswick, MW	93.2	106.6	441.8
Variable capacity in Ontario, MW	10,750.6	13,792.7	23,199.7
Dispatchability reserves for variable capacity required for Ontario, MW	1,879.3	2,222.6	3,210.9

As shown in Table 3.4.2, while very minor support in 2025 may be needed to support dispatchability reserves in Prince Edward Island and New Brunswick, much higher need is seen with dispatchability reserves for variable capacity in Ontario.

(3) *Variable generation growth in Quebec*

According to Canada Energy Regulator [18], variable capacity in Quebec is expected to grow from

4,580 MW in 2025 to 5,840 MW in 2035. Availability to use interchange capacity based on hydro power for variable dispatchability reserves (calculated at 73.6% capacity factor) in Eastern Canada is shown in Table 3.4.3. It includes opportunities to address the needs of Nova Scotia, Prince Edward Island, New Brunswick, and Ontario.

Table 3.4.3: Quebec Interchange Capacity available for Eastern Canada

NetZero Scenario	2025	2030	2035
Quebec interchange availability, TWh	6.07	17.85	14.95
Quebec hydro capacity for electricity export/interprovincial outflows, MW	941	2,769	2,319
Variable capacity in Quebec, MW	4,580	4,660	5,840
Dispatchability reserves needed for variable capacity in Quebec, MW	782	805	1,025
Quebec interchange capacity available for dispatchability reserves, MW	159	1,964	1,294
Dispatchability reserves needed for variable capacity in Nova Scotia, MW	0	0	133
Dispatchability reserves needed for variable capacity in Prince Edward Island, MW	75	100	101

NetZero Scenario	2025	2030	2035
Dispatchability reserves needed for variable capacity in New Brunswick, MW	93	107	442
Dispatchability reserves needed for variable capacity in Ontario, MW	1,879	2,223	3,211
Quebec interchange capacity available after dispatchability reserves purchase by Nova Scotia, Prince Edward Island, New Brunswick and Ontario, MW	-1,889	-465	-2,593
Possible support from Manitoba, MW	762	1,778	2,629
Dispatchability reserves balance in Eastern Canada with Manitoba support, MW	-1,127	0	0
Interchange resources available in Manitoba after support to Ontario, MW	0	1,312	36

Summarizing dispatchability aspects in Canada NetZero scenario: figures in Tables 3.4.1-3.4.3 show that dispatchable hydropower resources in Eastern Canada (such as Newfoundland and Labrador, and Quebec) can provide variable dispatchability reserves for grid planning support for the Maritimes but are not sufficient for addressing the clean dispatchability reserves needs of variable capacity in Ontario (see Table 3.4.3). However, this may be addressed in 2030 and 2035 by receiving dispatchability reserves support from Manitoba.

b. Western Canada

In Western Canada opportunities to use hydropower as dispatchability reserve look as follows.

The reservoir-based hydropower resources of Manitoba have their total capacity of 2.3 GW (based on [39-41]). The hydro power resources in Manitoba, focused on electricity export, can be redirected to supporting dispatchability reserves in the province and beyond in Western Canada. A very small share of these resources can be supporting variable generation in Manitoba (see Table 3.4.4 below).

Table 3.4.4: Hydro Power sources in Manitoba supporting Dispatchability Reserves

Canada NetZero Scenario	2025	2030	2035
Manitoba hydro capacity, MW	6,070	7,590	7,670
Manitoba interchange capacity available, MW	830	1,880	2,734
Manitoba variable capacity, MW	320	466	476
Dispatchability reserves for variable capacity required for Manitoba, MW	68	102	105
Manitoba interchange capacity available after its dispatchability reserve adjustment, MW	762	1,778	2,629

The Manitoba hydro capacity available for export after its dispatchability reserve adjustment can be considered to support the clean dispatchability reserves needs of variable capacity in Ontario in coordination with

Quebec (Table 3.4.2). Or – it can be used to support dispatchability reserves needs of variable capacity in Saskatchewan:

Table 3.4.5: Variable dispatchability reserves for Saskatchewan

Canada NetZero Scenario	2025	2030	2035
Saskatchewan variable capacity, MW	2,244	3,206	6,410
Dispatchability reserves for variable capacity required for Saskatchewan, MW	440	603	1,057
Manitoba interchange capacity available after Saskatchewan dispatchability reserve adjustment, MW	322	1,175	1,572

However, Manitoba interchange capacity can only partially cover the needs for variable dispatchability reserves in Alberta:

Table 3.4.6: Variable dispatchability reserves for Alberta

Canada NetZero Scenario	2025	2030	2035
Alberta variable capacity, MW	5,901	8,490	31,500
Dispatchability reserves for variable capacity required for Alberta, MW	1,115	1,468	3,500
Manitoba interchange capacity available after Saskatchewan and Alberta dispatchability reserve adjustment, MW	-793	-293	-1,928

Also, the needs for dispatchability reserves for variable capacity required for British Columbia are not covered and have to be addressed by other clean dispatchability reserves sources:

Table 3.4.7: Variable dispatchability reserves for British Columbia

Canada NetZero Scenario	2025	2030	2035
British Columbia variable capacity, MW	5,721	11,710	16,890
Dispatchability reserves for variable capacity required for British Columbia, MW	1,024	1,626	2,231

Overall, should Manitoba provide their export-oriented capacity as clean dispatchability reserves to Ontario or sell electricity into the U.S., the following dispatchability reserves would be needed for Saskatchewan, Alberta, and British Columbia in total:

Table 3.4.8: Variable dispatchability reserves for Saskatchewan, Alberta, and British Columbia

Canada NetZero Scenario	2025	2030	2035
Dispatchability reserves for variable capacity required for Saskatchewan, Alberta, and British Columbia – total*, MW	2,579	3,696	6,789

*This is based on a hydropower capacity factor of 75% (close to hydropower in Manitoba).

As within the Clean Grid 2035 timeframe neither Saskatchewan nor Alberta or British Columbia probably will have available export or other clean dispatchability reserves supporting their variable capacity, other clean dispatchability resources can be used in Western Canada.

One of such sources that is seen as highly attractive for Western Canada's use is Enhanced Geothermal Systems (EGS) located in the area with very high geothermal resources bordering Alberta, British Columbia, and Yukon [11]. As a very efficient highly

dispatchable resource with capacity factor of 90%, EGS is seen as a strong competitor to any solutions being considered in Alberta and British Columbia. While technical and economic aspects of EGS are discussed in Section 4 of this paper, here we only indicate the figures relating to dispatchability reserve needs.

To establish EGS dispatchability reserve needs, reservoir-based hydro and enhanced geothermal capacity should be matched for electricity generation. This can be defined using a capacity factor ratio that can be applied in reserve planning:

$$\text{EGS capacity (MW)} = \text{hydropower capacity (MW)} \times \text{CFR},$$

where CFR = hydropower capacity factor/EGS capacity factor is capacity factor ratio.

Using hydropower capacity factor of 75% and EGS capacity factor of 90%, we determine capacity factor ratio of 0.8333 that is used for adjusting EGS dispatchability reserve:

3.4.9: Enhanced Geothermal Systems-based dispatchability reserves for Saskatchewan, Alberta, and British Columbia

Canada NetZero Scenario	2025	2030	2035
Enhanced Geothermal Systems-based dispatchability reserves for variable capacity in Saskatchewan, Alberta and British Columbia, MW	2,149	3,080	5,657

v. Integrating Dispatchable Renewable Fleets

Enhanced geothermal systems can be used not only in planning and deployment of clean dispatchability reserves, but they can also be effectively competing with other resources in EF2023 within the Clean Grid 2035 timeframe.

For example, Table 3.5.1 below shows the current Canada NetZero scenario for Alberta:

Table 3.5.1: Canada NetZero scenario for Alberta – current

Canada NetZero ALBERTA	Capacity, MW			Generation, TWh		
	2025	2030	2035	2025	2030	2035
Solar (Distributed)	221	500	1,000	0.33	0.76	1.51
Solar (Utility scale)	1,180	1,930	13,000	2.09	3.47	23.98
Onshore Wind	4,500	6,060	17,500	16.05	21.53	65.15
Hydro	894	894	894	1.65	1.65	1.35
Hydrogen	0	0	0	0.00	0.00	0.00
Natural Gas	14,300	14,000	8,660	68.85	66.07	5.28
Natural Gas with CCUS	0	2,090	4,290	0.00	11.70	21.23
Oil	7	7	7	0.02	0.00	0.00
Battery Storage	90	90	90			
Bioenergy	286	286	286	1.41	1.60	1.04
Bioenergy with CCUS	0	0	728	0.00	0.00	5.74
Geothermal with EGS						
Uranium SMR	0	0	459	0.00	0.00	3.20
Total	21,478	25,857	46,914	90.4	106.8	128.5

This scenario can be effectively transformed in a scenario with EGS deployment:

Table 3.5.2: Canada NetZero scenario for Alberta – adjusted by EGS capacity

Canada NetZero ALBERTA	Capacity, MW			Generation, TWh		
	2025	2030	2035	2025	2030	2035
Solar (Distributed)	221	500	1,000	0.33	0.76	1.51
Solar (Utility scale)	1,180	1,930	6,430	2.09	3.47	11.86
Onshore Wind	4,500	6,060	10,060	16.05	21.53	37.45
Hydro	894	894	894	1.65	1.65	1.35
Hydrogen	0	0	0	0	0	0
Natural Gas	14,300	3,000	0	68.85	14.16	0.00
Natural Gas with CCUS	0	2,090	4,290	0.00	11.70	21.23
Oil	7	7	7	0.02	0	0
Battery Storage	90	90	90			
Bioenergy	286	0	0	1.41	0.00	0.00
Bioenergy with CCUS	0	0	0	0	0	0
Geothermal with EGS	0	6,788	6,986	0	53.51	55.08
Uranium SMR	0	0	0	0	0	0
Total	21,478	21,359	29,758	90.4	106.8	128.5

Furthermore, Enhanced Geothermal Systems (EGS) located in the area with very high geothermal resources bordering Alberta, British Columbia, and Yukon [11], can be used for dispatchability resources/load matching not only in Western Canada, but will allow for addressing these needs in Ontario and in Eastern Canada (see Section 4).

Overall, the proposed approach to using hydropower as a variable dispatchability reserve from Newfoundland and Labrador, and Quebec for Eastern Canada, and combining hydropower in Manitoba and geothermal power in Alberta/Yukon as dispatchability reserves for Western Canada makes variable resources like wind and solar dispatchable, upgrading all power

grids in Canada to Clean Grid practices in 2035 and further in 2050.

Using dispatchable hydropower and geothermal power together with wind and solar power would make all generating capacity in Canada dispatchable and would establish its leading clean dispatchability practices in North America. It would also present an opportunity for Dispatchable Integrated Renewable Fleets in all Canadian provinces and beyond.

b) *Geothermal Technology as a Strategic Opportunity*

i. *Strategic Opportunities with Geothermal*

Dramatically scaling up clean electricity generation to meet the Clean Grid 2035 objective means leveraging and promptly deploying strategic solutions Canada has at hand. One of these very few strategic solutions for addressing the net-zero electricity gap in the country is Geothermal Power Generation.

While geothermal resources in Canada have massive potential to provide clean energy across the country, geothermal power generation has largely remained undeveloped [20]. Today, with Canada's leadership in energy transition and total electrification, and Canada Energy Regulator's detailed look into Canada's Energy Future, enhanced geothermal generation opportunities must be viewed from a crucial strategic angle.

It is generally well known that geothermal generation provides clean, renewable, round-the-clock electricity, not depending on weather, season, and time of day; it emits little or no greenhouse gases, and has a small environmental footprint, very competitive to renewable resources like wind, solar or hydro [42]. What is not often mentioned is that enhanced geothermal generation brings to power grids in Canada two unique opportunities: a powerful source of dispatchable baseload, and a "power storage" for dispatchability reserves allowing for unlimited growth of variable renewables like wind or solar. Understanding this in the context of the Clean Grid 2035 commitment, Canada must promptly strengthen geothermal power generation in Western provinces - moving from a "lagging behind" position in North America, and globally, to a world leader in exporting deep geothermal expertise and technology internationally [13].

ii. *Geothermal Resources in Canada*

High temperature geothermal resources in Canada are a part of the Pacific Ring of Fire, a tectonic belt of volcanoes and earthquakes [43], and the related Canada's Pacific Rim. Volcanic belts are common in the Canadian Cordillera [11, 14]. British Columbia, Yukon and Northwest Territories are home to a region of volcanoes and volcanic activity in the Pacific Ring of Fire.

Geothermal resources of the Pacific Rim are the most efficient and economic means to generate geothermal power, with high temperature resources (>150°C) typically targeted for highly dispatchable electricity generation.

These high temperatures allow very high potential for electricity generation in regions of northeastern British Columbia and southern Yukon, northern Alberta, and southern Northwest Territories. Regional temperatures suitable for electricity generation, 150°C or more, can be reached at relatively shallow depths of 3.5-4.5 km in northwestern Alberta and

northeastern BC. For communities in the southern Mackenzie Corridor and in southwest Yukon, temperatures >150°C can be reached at depths of 3.5-5 km.

To estimate the thermal energy, or heat content, for deploying geothermal power plants, a 4 x 4 km rock mass, 1 km thick (16 km³ total volume) was considered by S. E. Grasby et al in [11]. Cooling this rock mass from an initial temperature of 150°C to a final temperature of 30°C results in 5x10¹⁸ Joules, or 1.39 PetaWatt-hours (PWh).

The actual accessible and usable geothermal energy resource is estimated by applying a factor of 0.02 of in-place thermal energy, or 1 x 10¹⁷ J (27.8 TWh) for the same rock volume of 16 km³. Comparing 27.8 TWh power output of this geothermal unit with electricity demand in 2023 in British Columbia (65.10 TWh), Alberta (80.69 TWh) or Saskatchewan (25.45 TWh) shows a very limited number of units (e.g. one geothermal unit for transmission to Saskatchewan or three geothermal units in Alberta) that can cover the electricity needs in these provinces.

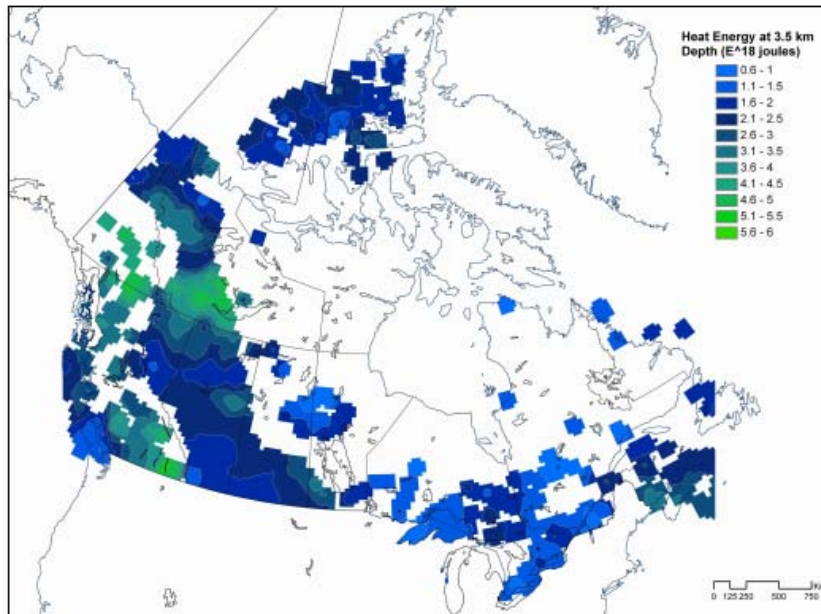


Fig. 4.2.1: Heat Energy at 3.5 km depth [11]

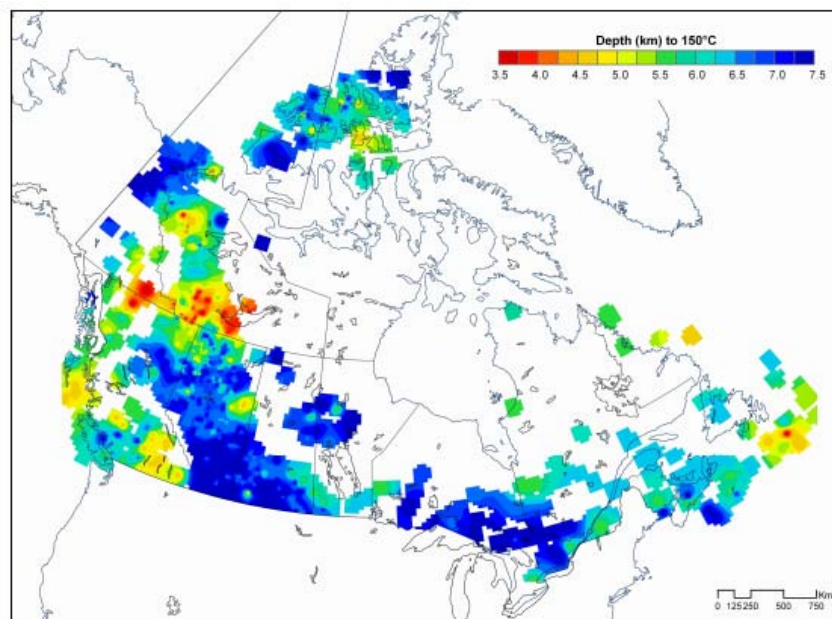


Fig. 4.2.2: Depth (km) to 150°C temperature [11]

It has been found [12] that multiple locations of heat value resources are available at moderate depths which have already been reached in oil and gas drilling operations. Based on petroleum industry experience in the Western Canadian Sedimentary Basin (WCSB), it is common to drill 4 to 6 km deep wells in deeper parts of this area, and technology to achieve such depths is readily available.

Many locations with enhanced geothermal generation potential in the WCSB occur in northeastern British Columbia, parts of northwestern Alberta and central Alberta (including the Lac La Biche high), and in Saskatchewan (Williston Basin high).

Also, in the WCSB these depths are mainly reached below the sedimentary cover. These sediments form an effective thermal blanket that decrease the depth required to reach effective temperatures for enhanced geothermal development. As drilling through sedimentary rocks is less expensive than in the areas of crystalline rock, enhanced geothermal deployment in these areas is more economically attractive.

Specifically, the Alberta Basin area is seen as a practical approach for geothermal electricity generation [12]. Opportunities of access to the Northern Lights Transmission line and the Edmonton-West coal power corridor were reviewed for power transmission within the

Alberta electricity system to make this geothermal power generation economic and leverage its highly efficient dispatch.

iii. Enhanced Geothermal Systems for Electricity Generation

Enhanced Geothermal Systems (EGS) bring geothermal energy for electricity generation from heat produced in the subsurface. This heat is generated from natural radiogenic decay of elements in the upper crust as well as primordial heat generated from the formation of the planet.

EGS use fluid injected deep underground under carefully controlled conditions; this fluid absorbs energy from hot rock formations and carries this energy to the surface to drive turbines and generate electricity in flash steam or binary-cycle geothermal power plants [44,45].

Modern EGS are divided into two major groups: open-loop and closed-loop systems. The open-loop systems have fluid pumped down injection wells into hot rock formations, migrate through the hot rock and while collecting heat, get captured by extraction wells, and

pumped back to the surface where the heat is converted into electricity [46]. The wells are often drilled horizontally to maximize the volume of hot rock exposed to the fluid. The closed-loop systems have the fluid pumped into a well contained within the underground pipes, recovered and re-used. The closed-loop EGS presents two approaches. A single-well approach uses concentric pipes to pump a heat transfer fluid down a vertical wellbore and along a directional wellbore, have it make U-turn and flow back within a concentric pipe. A multiple-well (doublet) approach has the fluid conveyed back to the surface up a second vertical wellbore to be pumped back to the injection wellbore.

Leading examples of EGS solutions in North America are presented by such technology developers as Fervo Energy (Houston, Texas) and Eavor Technologies Inc. (Calgary, Alberta) [47].

Fervo Energy presents first-of-a-kind EGS horizontal doublet well system, consisting of an injection and production well pair within a high-temperature, hard rock geothermal formation [48] (see Fig. 4.3.1).

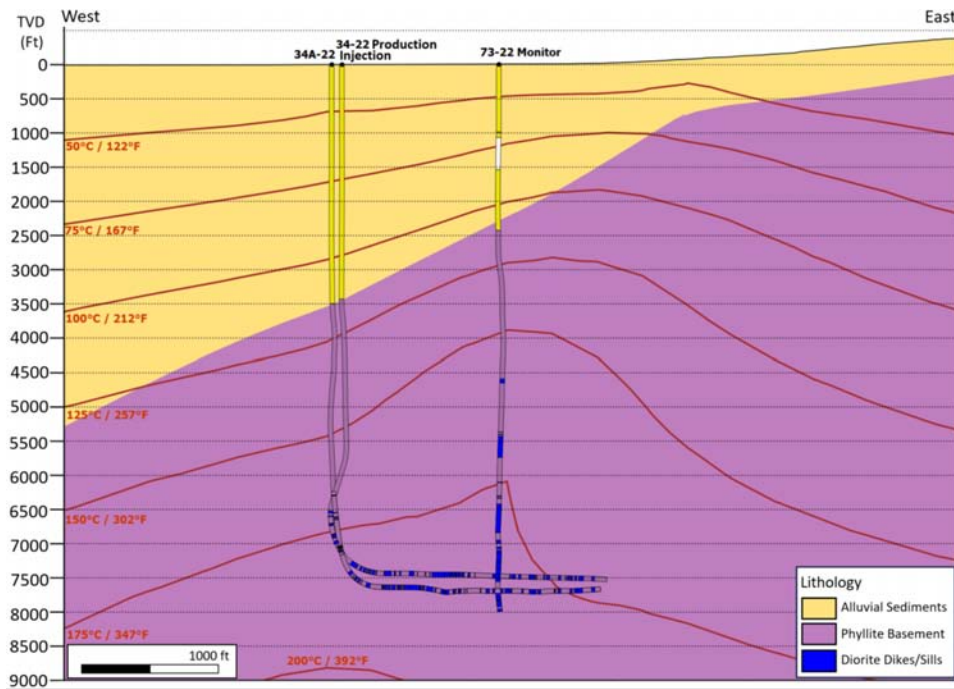


Fig. 4.3.1: A cross-section of the horizontal doublet EGS system and deep vertical monitoring well [48].

Credits to Fervo Energy

Eavor Technologies presents a Eavor-Loop™, consisting of large U-tube shaped well with 2 multilaterals. Eavor-Lite™ Pilot (see Figure 4.3.2) is a full-scale prototype of the Eavor-Loop™. The laterals are approximately 1700m long and are placed in the Rock Creek formation at depth of 2400m.

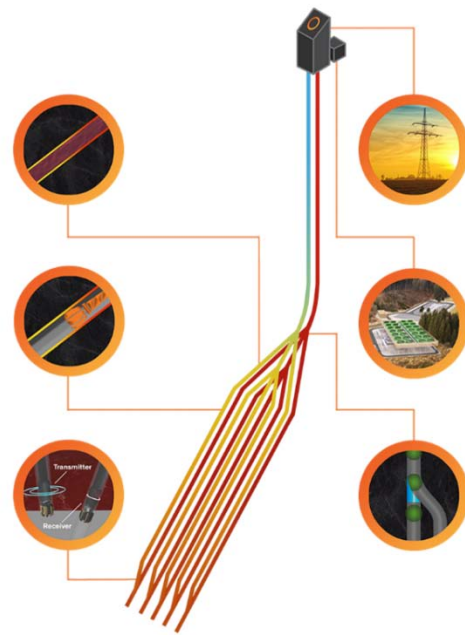
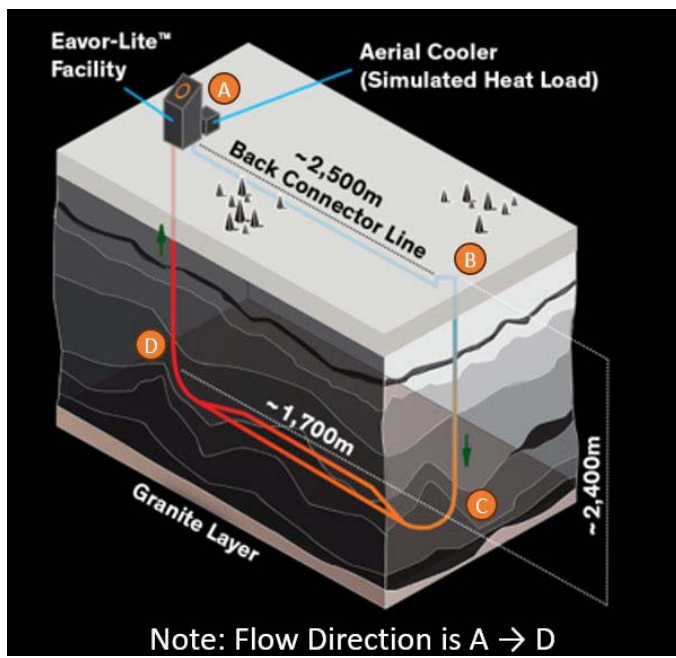


Fig. 4.3.2: Schematic of Eavor-Lite™ Pilot[49,50]. Credits to Eavor Technologies

EGS use human-made reservoirs to inject fluid and extract economical amounts of heat from low permeability and/or low porosity geothermal resources. The fluid in EGS carries energy to the surface through wells, driving turbines and generating electricity [44,45].

The high capacity factor of geothermal power (90%) makes it particularly attractive as a dispatchable renewable resource.

iv. Economics of Enhanced Geothermal Systems

While geothermal energy resources in Canada are unique and attractive because of their geo-economic positioning in Western Canada, Enhanced Geothermal Systems (EGS) for electricity generation in Canada present a longer-term objective in energy transition process towards Net Zero [11,14].

To support this statement, three major parameters of EGS should be reviewed to analyse costs and risk factors of deploying this technology: capital expenditures (CAPEX) covering equipment, engineering and deployment costs of a plant, operational expenditures (OPEX) covering fuel, maintenance, and support costs of this plant, and levelized cost of energy (LCOE) indicating the net present cost of electricity generation over the anticipated lifetime of the plant.

Table 4.4.4 below presented by [egs16] compares different power-station options based on their CAPEX and LCOE. CAPEX represents the upfront funds needed for plant development, and LCOE compares the lifetime costs of different energy systems using a 30-year payback period:

Table 4.4.4: Electricity source CAPEX and LCOE, USD [13]

	Electricity source	CAPEX (\$/kW)	LCOE (\$/kWh)	Cost Estimate Date, Notes, Source
1	Geothermal (hydrothermal)	2,400 – 6,200	0.07 – 0.12	(2019) ²
2	Geothermal ('near hydrothermal' EGS)	9,000 – 10,000	0.1 – 0.3	(2019) ²
3	Geothermal ('deep' [3-6km] EGS)	20,000 – 46,000	0.16 – 0.42	(2019) (low=flash, high=binary cycle) ³
4	Hydroelectric	2,500 – 16,000	0.06 – 0.36	(2019) ⁴
5	Solar (Utility PV)	~1,400	0.03 – 0.05	(2019) (w/o battery storage) ⁵
6	Wind (land)	~1,450	0.25 – 0.08	(2019) ⁶
7	Nuclear	~6,800	~0.08	(2019) ⁷
8	Coal	4,000 – 6,200	~0.09 - ~0.16	(2017) (low = new plant; high = with CCS (carbon capture + storage) ⁸
9	Natural Gas	920 – 3,300	~0.06 - ~0.16	(2017) (low = turbine combined cycle; high = same + CCS) ⁹
10	Tidal	"high"	0.2 – 0.45	(2020) (~ 535MW in operation worldwide; most 'tidal barrage' (~522MW) ¹⁰
11	Wave	"high"	0.3 – 0.55	(2020) (< 3MW in operation worldwide) ¹⁰

According to the Canada Energy Regulator [51], in 2021 the capacity cost for a geothermal power plant was estimated between US\$4,500 to \$6,050 per kilowatt (kW) of capacity, and the levelized cost of energy - US\$56 to \$93 per megawatt hour (MWh).

Geothermal plants, like hydroelectric and nuclear plants, are capital-intensive - in the case of near-hydrothermal and deep EGS plants, far more so than wind or solar installations [13]. However, as noted earlier, these plants can often be built out incrementally, starting with a small pilot plant and then scaling up. This option is not available with nuclear or hydroelectric plants.

In terms of geothermal CAPEX, drilling and well completion dominate the expenditures with on average 54 percent of all capital costs (see Fig. 4.4.1 [13, 52]):

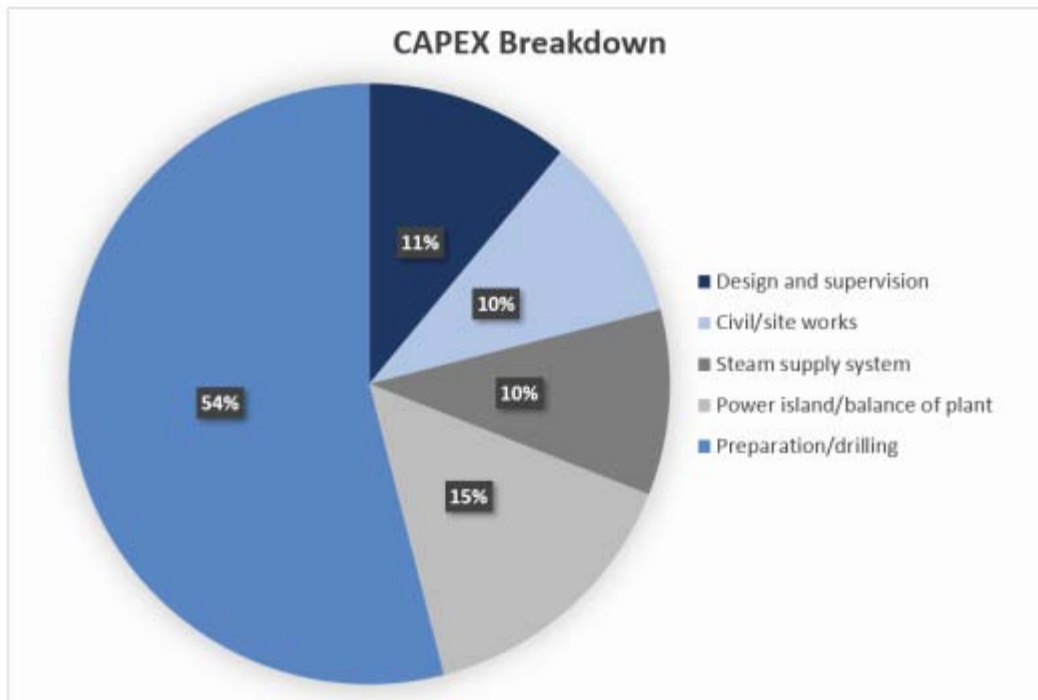


Fig. 4.4.1: CAPEX breakdown for geothermal projects (based on data from Belyakov 2019 [13, 52])

From environmental risk angle geothermal plants produce significantly less footprint and related landscape disturbance than solar, wind, and hydroelectricity indicating much smaller risks to lands

and ecosystems. Power density (in watts generated per square meter of power plant footprint) of competing clean electricity technologies is presented in Table 4.4.2 below [13]:

Table 4.4.2: Comparative Power densities of selected net-zero energy sources [13, 53]

Electricity source	Range of power density (W/m ²)	Mean power density (W/m ²)
Utility-scale PV	4.2 – 7.5	5.8
High-temp geothermal (>250°C)	1.6 – 8.4	4.9
Offshore wind	2.2 – 6.3	4.2
Onshore wind	2.4 – 3.8	3.1
Low-temp geothermal (<250°C)	0.5 – 2.9	1.6
Large hydro	0.2 – 1.0	0.5
Oil crops	N/A	0.2
Wood crops	N/A	0.2

v. Geothermal Fuel vision in North America

a. United States

On September 8th, 2022, the Enhanced Geothermal Shot was announced in Houston, Texas. Its target is to reduce the cost of EGS by 90%, to \$45 per megawatt hour by 2035.

The Enhanced Geothermal Shot is part of the U.S. Department of Energy's Earthshots™ Initiative to tackle key remaining technical challenges to reaching

U.S. climate goals and leverage economic opportunities [44, 45, 54].

While today a small portion of the geothermal energy is accessible with current technology in the U.S., research and innovation to advance enhanced geothermal systems (EGS), which create human-made reservoirs to access energy, is expected to unlock geothermal resources and put new, clean, dispatchable electricity on the grid.

According to the Advanced Technology Innovation approach considered with substantial drilling and EGS advancements, EGS power plants are assumed to be built with 100 MW of capacity to maximize project efficiency [54]. Based on GeoVision Analysis [55,56] EGS future growth is forecast.

Three scenarios are considered in this analysis: Business-as-Usual (BAU), Improved Regulatory Timeline (IRT) and Technology Improvement (TI). In the BAU scenario, installed geothermal capacity increases from 2,542 MWe in 2016 to 5,924 MWe by 2050. The IRT scenario estimates 12,891 MWe of total installed geothermal capacity by 2050. In the TI scenario, total installed geothermal capacity reaches 60,701 MWe by 2050.

As of 2019, developing, testing, and accelerating breakthroughs in EGS technologies to advance the uptake of geothermal resources has been led by the Frontier Observatory for Research in Geothermal Energy - Utah FORGE, a dedicated underground field laboratory sponsored by the U.S. Department of Energy. Working in coordination with Utah FORGE, in July 2023 Fervo Energy announced that it successfully completed a full-scale well test in Nevada that confirmed the commercial viability of its next-generation technology (see Fig. 4.5.1, 4.5.2). A next-generation geothermal plant backed by Google has started sending carbon-free electricity to the grid in Nevada, where the tech company operates some of its massive data centers [57].



*Fig. 4.5.1: Fervo Energy's 3.5-megawatt enhanced geothermal plant in Nevada.
Credits to Google/Fervo Energy*



Fig. 4.5.2: Fervo uses horizontal drilling techniques to tap the earth's heat. Credits to Fervo Energy

b. *Canada*

The Government of Canada is advancing the country's transition to a low-carbon economy in Canada through strategic investments and innovative partnerships including geothermal energy.

In June 2022, federal funding was provided to Novus Earth to execute a front-end engineering design (FEED) study for the Latitude 53 geothermal energy project with a closed-loop enhanced geothermal system in the community of Hinton, Alberta. This investment was provided by Natural Resources Canada's Smart Renewables and Electrification Pathways (SREPs) program that provides support for smart renewable energy and electrical grid modernization projects.

In October 2023, Eavor Technologies Inc. (Eavor), Calgary, Alberta, a pioneer in the field of advanced geothermal energy solutions, announced the successful completion of \$182 million in financing of its Eavor-Loop™ enhanced geothermal system solution. This significant investment will enable Eavor to accelerate the development and deployment of its revolutionary geothermal technology. The equity round was led by OMV AG, with participation from Canada Growth Fund ("CGF"), Japan Energy Fund, Monaco Asset Management and Microsoft's Climate Innovation Fund as well as from existing investors.

In February 2024 Eavor announced a significant add-on investment from Kajima Corporation, one of Japan's construction giants [58]. This strategic alliance

promises to accelerate the global transition to sustainable energy by facilitating the expansion of Eavor's innovative technology across various sectors (see Fig. 4.5.3).



Fig. 4.5.3: Eavor Technologies Secures Major Investment from Kajima for Geothermal Advancement [57]. Credits to Eavor Energy

As Canada's federal government is increasing its support of geothermal technology, provincial advances in geothermal are also matching this growth. Specifically, Alberta is strengthening its position to lead development and deployment and attract investment in geothermal industry with a natural geographical advantage, leadership in drilling technology, and extensive oil and gas expertise [59]. Geothermal Resource Tenure Regulation in Alberta [60] today is the primary regulation that deals with the tenure of geothermal leases in Alberta. This new regulation, and amendments to other regulations, took effect on January 1, 2022.

Also, while geothermal development efforts are growing in Canadian provinces, research is underway in Canada's three territories: Yukon, Northwest Territories and Nunavut, to assess geothermal resources of target communities [14]. This includes deep geothermal systems as a long-term objective that may provide sufficient energy to meet communities' heavy heating needs. Results suggest that geothermal technologies can provide important carbon reductions and are economically attractive.

IV. CONCLUSIONS AND RECOMMENDATIONS

1. Clean Grid readiness is a major objective of Canada's Clean Grid 2035 achievements and commitment to make all electricity generation in the country carbon net-zero. Making all the sources of electricity in power grids clean will make a

tremendous step in Canada's energy transition and low carbon economy growth.

2. A major effort in cleaning the grid within a decade is focused on decarbonizing power generation in three provinces historically using fossil fuels for growth: Alberta, Saskatchewan, and Nova Scotia.

An outstanding undertaking in cleaning energy generation mix in these three provinces is deploying variable renewables – wind and solar power at very large scale in the country. In the Canada NetZero scenario of energy future presented by Canada Energy Regulator, total capacity of variable renewables in Alberta, Saskatchewan, and Nova Scotia by 2035 is 27.9GW (49% of 56.7 GW) of wind power and 15.6 GW (59% of 26.4 GW) in Canada, and these variable renewables will generate 104TWh (50% of 207.5 TWh) of wind and 29 TWh (64% of 45TWh) of solar power in the country.

3. Deploying very large scale of variable renewables in Canada requires an extremely significant power dispatchability effort, allowing the country's power grids to maintain their reliability. Clean Grid 2035 commitment also assumes that all existing and new power dispatchability sources in Canada backing up variable renewables' operations are clean.
4. Choosing to have the renewable segment of clean dispatchability sources lead in Canada's Clean Grid efforts and creating renewable dispatchable fleets will make all variable renewables in the country dispatchable. This would make a tremendous change in upgrading Canada's power grids and its contribution to low carbon economy in general.

5. Canada is capable and committed to making this leadership change in dispatchability of variable renewables.

Indeed, Canada's electricity systems historically had been built on extremely strong reservoir-based hydro power in Newfoundland and Labrador, Quebec, Manitoba. These renewable dispatchable resources can be used to back up variable renewables' growth in Alberta, Saskatchewan, and Nova Scotia, and in the country in general.

Canada is also geographically built on geothermal resources. Geothermal resources in the Pacific Rim including the regions of northeastern British Columbia and southern Yukon, northern Alberta and southern Northwest Territories bring very high potential for highly dispatchable electricity generation. Due to their unique position in Western Canada, deep geothermal resources allow for deploying Enhanced Geothermal Systems (EGS) for electricity generation at high scale. Capabilities of Enhanced Geothermal power plants based on very high (90%) capacity factor and dispatchability will provide variable dispatchability reserves in Western Canada that will strengthen and support Canada's Clean Grid 2035 efforts. As a part of these leadership efforts, Canada must catch up with the U.S. in positioning and developing EGS partnerships and investments.

As Canada's federal government is increasing its support of geothermal technology, provincial advances in Enhanced Geothermal Systems led by Canadian clean technology companies such as Eavor Technologies Inc. are also matching this growth.

6. Opportunities with current and growing Clean Grid efforts may allow for changing the role of reservoir-based hydro power in Canada from electricity export-oriented to variable renewables dispatchability support-oriented. Backing up the growth of variable renewables will in turn allow for growing export of electricity in Eastern Canada (from offshore fleets in the Atlantic Rim such as Sable Island) and in Western Canada (from geothermal plants in the Pacific Rim such as in northern Alberta).
7. Comparison of the dispatchability reserves sources and needs for variable renewables shows that there is a clear gap between the sources and required uses in variable dispatchability reserves, and solutions should be discussed and agreed on to address this dispatchability gap.

Examples describing possible realization of the Clean Dispatchability Reserves Strategy in Eastern and Western Canada, using interchange capacity as a source for variable dispatchability reserves, are presented in Section 3 of this paper. They show that dispatchable hydropower resources in Eastern

Canada (such as Newfoundland and Labrador, and Quebec) can provide variable dispatchability reserves for grid planning support for the Maritimes but are not sufficient for addressing the clean dispatchability reserves needs of variable capacity in Ontario (see Tables 3.4.1-3.4.3). However, this may be addressed in 2030 and 2035 by receiving dispatchability reserves support from Manitoba. However, should Manitoba provide its export-oriented capacity as clean dispatchability reserves to Ontario or sell electricity into the U.S., dispatchability reserves would be needed for Saskatchewan, Alberta, and British Columbia (see Table 3.4.8).

8. The approach proposed here to using hydropower as a variable dispatchability reserve for Eastern Canada and combining hydropower and geothermal power as dispatchability reserves for Western Canada will make variable renewables dispatchable, upgrading all power grids in Canada to 100% Clean Grid readiness by 2035 and maintaining this Clean Grid commitment in 2050 and beyond. Using dispatchable hydropower and geothermal power together with wind and solar power in Renewable Dispatchable Fleets in Alberta, Saskatchewan and Nova Scotia would make all renewable capacity in these provinces dispatchable, establishing leading clean dispatchability practices in North America. It is an opportunity for Dispatchable Integrated Renewable Fleets present in all Canadian provinces.
9. To agree on renewable dispatchable fleets deployment and existing dispatchability reserves commitments from the provinces owning and operating large scale reservoir-based hydro power plants, Canada's "electric federalism" concept and approach should be demonstrated efficiently and promptly. A summary of Variable Dispatchability Reserves needed in Canada and their growth in 2025-2035 in NetZero scenario is shown in Section 2 of this paper. It brings attention to economic pricing solutions for hydro dispatchability assets in Manitoba, Quebec, and Newfoundland and Labrador.
10. Scaling up clean electricity generation to meet Clean Grid 2035 objectives means leveraging and promptly deploying strategic solutions Canada has at hand. Although the future of energy in Canada is broader than the economic and technical factors driving the projections in EF2023, some of these factors such as Renewable Dispatchability Reserves for variable renewables, and highly dispatchable Enhanced Geothermal systems and technologies require critical attention and should be very promptly addressed as they touch very sensitive decisions of Canadian provinces and realities of electric federalism in Canada.

ACKNOWLEDGMENTS AND CONFLICTS OF INTEREST

Acknowledgments: The author is extremely grateful to Marlene Moore for the concept discussions supporting the vision expressed in the manuscript.

The author is also much obliged to John Harker for his strategic review of the manuscript and for thoughtful editing.

Conflicts of Interest: The author declares no conflict of interest.

REFERENCES RÉFÉRENCES REFERENCIAS

1. Department of Finance Canada. (2023, March 28). *Chapter 3: A Made-In-Canada Plan: Affordable Energy, Good Jobs, and a Growing Clean Economy. Budget 2023*. <https://www.budget.canada.ca/2023/report-rapport/chap3-en.html#a5>
2. Service Canada. (2024, February 2). Net-zero emissions by 2050. Canada.ca. <https://www.canada.ca/en/services/environment/weather/climatechange/climate-plan/net-zero-emissions-2050.html>
3. Canada, N. R. (2023, August 31). *Powering Canada Forward: Building a clean, affordable, and reliable electricity system for every region of Canada*. <https://natural-resources.canada.ca/our-natural-resources/energy-sources-distribution/electricity-infrastructure/powering-canada-forward-building-clean-affordable-and-reliable-electricity-system-for/25259>
4. *Project of the Century - Public Policy Forum*. (2023, October 17). Public Policy Forum. <https://ppforum.ca/publications/net-zero-electricity-canada-capacity/>
5. *Fostering effective energy Transition 2023*. (2023, October 9). World Economic Forum. <https://www.weforum.org/reports/fostering-effective-energy-transition-2023>
6. Wikipedia contributors. (2024, March 28). *Churchill Falls Generating Station*. Wikipedia. https://en.wikipedia.org/wiki/Churchill_Falls_Generating_Station
7. Wikipedia contributors. (2024b, March 31). *Muskrat Falls Generating Station*. Wikipedia. https://en.wikipedia.org/wiki/Muskrat_Falls_Generating_Station
8. Hydro-Québec. (n.d.). *Generating stations*. <https://www.hydroquebec.com/generation/generating-stations.html>
9. Wikipedia contributors. (2023, January 26). *List of generating stations in Manitoba*. Wikipedia. https://en.wikipedia.org/wiki/List_of_generating_stations_in_Manitoba
10. Wikipedia contributors. (2024a, January 9). *List of generating stations in British Columbia*. Wikipedia. https://en.wikipedia.org/wiki/List_of_generating_stations_in_British_Columbia
11. Grasby, S. E., Allen, D., Bell, S. E., Chen, Z., Ferguson, G., Jessop, A. M., Kelman, M. C., Ko, M., Majorowicz, J., Moore, M. C., Raymond, J., & Therrien, R. (2012). *Geothermal energy resource potential of Canada*. <https://doi.org/10.4095/291488>
12. Majorowicz, J. & Moore, M.C. (2008 July). *Enhanced Geothermal Systems (EGS) Potential in the Alberta Basin*. Alberta Energy Research Institute. http://www.aeri.ab.ca/sec/new_res/docs/Enhanced_Geothermal_Systems.pdf
13. Cascade Institute. (2024, March 12). *Deep Geothermal Superpower: Canada's potential for a breakthrough in enhanced geothermal systems - Cascade Institute*. <https://cascadeinstitute.org/technical-paper/deep-geothermal-superpower/>
14. Miranda, M. M., Comeau, F., Raymond, J., Gosselin, L., Grasby, S. E., Wigston, A., Dehghani-Sanij, A., Sternbergh, S., & Perreault, S. (2022). *Geothermal resources for energy transition: A review of research undertaken for remote northern Canadian communities*. Zenodo (CERN European Organization for Nuclear Research). <https://doi.org/10.5281/zenodo.7882811>
15. Canadian Climate Institute. (2022, May 4). *Electric Federalism: Policy for aligning Canadian electricity systems with net zero*. <https://climateinstitute.ca/wp-content/uploads/2022/05/Electric-Federalism-May-4-2022.pdf>
16. Wikipedia contributors. (2024b, March 11). *Geoeconomics*. Wikipedia. <https://en.wikipedia.org/wiki/Geoeconomics>
17. Dryden, J. (2024, February 16). *Ottawa floats new options for electricity rules that drew ire of Alberta and Saskatchewan*. CBC. https://www.cbc.ca/news/canada/calgary/alberta-clean-electricity-regulations-ottawa-steven-guilbeault-1.7117495?__vz=medium%3Dsharebar
18. Government of Canada, Canada Energy Regulator. (2024, March 28). *CER – Canada's energy future*. <https://www.cer-rec.gc.ca/en/data-analysis/canada-energy-future/index.html>
19. Graham. (2024, February 28). *Eavor - the world's first scalable form of clean baseload power* [Video]. Eavor. <https://www.eavor.com/>
20. *Why Canada might finally seize its geothermal power potential - BNN Bloomberg*. (2023, December 27). BNN. <https://www.bnnbloomberg.ca/a-long-overlooked-climate-solution-geothermal-could-be-in-for-its-hottest-decade-yet-1.2015782>
21. Government of Canada, Canada Energy Regulator. (2024a, March 21). *CER – Access and Explore Energy Future Data*. <https://www.cer-rec.gc.ca/en/data-analysis/canada-energy-future/2023/access-and-explore-energy-future-data.html>
22. Harack, B., & Harack, B. (2016, February 24). *How can renewables deliver dispatchable power on demand? | Vision of Earth*. Vision of Earth | Shaping a Happy, Healthy, and Prosperous Future. <https://www.visionofearth.org/industry/renewable-en>

- ergy/renewable-energy-review/how-can-renewables-deliver-dispatchable-power-on-demand/
23. Wikipedia contributors. (2023b, July 25). *Dispatchable generation*. Wikipedia. https://en.wikipedia.org/wiki/Dispatchable_generation
 24. Wikipedia contributors. (2024a, January 3). *Ancillary services (electric power)*. Wikipedia. [https://en.wikipedia.org/wiki/Ancillary_services_\(electric_power\)](https://en.wikipedia.org/wiki/Ancillary_services_(electric_power))
 25. Government of Canada, Fisheries and Oceans Canada. (2007). *Canada's Ocean Estate. A Description of Canada's Maritime Zones*. <https://waves-vagues.dfo-mpo.gc.ca/library-bibliotheque/4-0622952.pdf>
 26. Wikipedia contributors. (2024d, March 19). *Ocean thermal energy conversion*. Wikipedia. https://en.wikipedia.org/wiki/Ocean_thermal_energy_conversion
 27. Ascari, M. B., Hanson, H. P., Rauchenstein, L. T., & Jansen, E. (2012). *Ocean Thermal Extractable Energy Visualization- Final Technical Report on Award DE-EE0002664*. October 28, 2012. *ResearchGate*. https://www.researchgate.net/publication/268506159_Ocean_Thermal_Extractable_Energy_Visualization_Final_Technical_Report_on_Award_DE-EE0002664_October_28_2012
 28. *M-1 reserve margin*. (n.d.). <https://www.nerc.com/pa/RAPA/ri/Pages/PlanningReserveMargin.aspx>
 29. Wikipedia contributors. (2024c, January 15). *Resource adequacy*. Wikipedia. https://en.wikipedia.org/wiki/Resource_adequacy
 30. *Resource adequacy*. (n.d.). NREL. <https://www.nrel.gov/research/resource-adequacy.html>
 31. Tuohy, A. (2024-02-26). *Probabilistic Resource Adequacy Methods*. ESIG/G-PST Webinar Presentation. <https://t.e2ma.net/click/csibkh/ki47uxb/odbh80>
 32. Willis, R. (2020, August 13). *Five Principles of Resource Adequacy for Modern Power Systems - ESIG*. ESIG. <https://www.esig.energy/five-principles-of-resource-adequacy-for-modern-power-systems/>
 33. *Comparison of capacity credit calculation methods for conventional power plants and wind power*. (2009, May 1). *IEEE Journals & Magazine | IEEE Xplore*. <https://ieeexplore.ieee.org/document/4806129>
 34. Madaeni, S., Sioshansi, R. & Denholm, P. (2012 July). *Comparison of Capacity Value: Methods for Photovoltaics in the Western United States*. Technical Report NREL/TP-6A20-54704 <https://www.nrel.gov/docs/fy12osti/54704.pdf>
 35. Keane, A., Milligan, M., D'Annunzio, C., Dent, C.J., Dagoon, K., Hasche, B., Holttinen, H., Samaan, N., Soder, L., O'Malley, M. (2011). *Capacity Value of Wind Power*. *IEEE Trans. Power Syst.* (26:2), 2011; pp. 564–572.
 36. Pelland, S., & Abboud, I. (2008). *Comparing Photovoltaic Capacity Value Metrics: A case study for the City of Toronto*. *Progress in Photovoltaics: Research and Applications*, 16(8), 715–724. <https://doi.org/10.1002/pip.864>
 37. Hoff, T.; Perez, R.; Ross, J.P.; Taylor, M. (2008). *Photovoltaic Capacity Valuation Methods*. SEPA REPORT # 02-08. Washington, DC: Solar Electric Power Association.
 38. Nova Scotia Power. (2014 April 3). *Capacity Value of Wind Assumptions and Planning Reserve Margin*. https://www.nspower.ca/docs/default-source/pdf-to-upload/20140423-wind-capacity-value-assumption-s.pdf?sfvrsn=2c12f8ab_0
 39. Wikipedia contributors. (2023c, September 24). *List of hydroelectric power stations in Canada*. Wikipedia. https://en.wikipedia.org/wiki/List_of_hydroelectric_power_stations_in_Canada
 40. Wikipedia contributors. (2023b, January 26). *List of generating stations in Manitoba*. Wikipedia. https://en.wikipedia.org/wiki/List_of_generating_stations_in_Manitoba#Off-grid
 41. *Generating stations*. (n.d.). https://www.hydro.mb.ca/corporate/facilities/generating_stations/
 42. *About*. (n.d.). Energy.gov. <https://www.energy.gov/eere/geothermal/about>
 43. Wikipedia contributors. (2024f, March 19). *Ring of fire*. Wikipedia. https://en.wikipedia.org/wiki/Ring_of_fire
 44. *Enhanced geothermal systems*. (n.d.). Energy.gov. <https://www.energy.gov/eere/geothermal/enhanced-geothermal-systems>
 45. *Electricity generation*. (n.d.). Energy.gov. <https://www.energy.gov/eere/geothermal/electricity-generation>
 46. Hughes, J. (2023, August 22) *Optimized CO2 Sequestration and Enhanced Geothermal System*. Patent No. US11,732,929B2.
 47. Bloomberg NEF. (2023, May 10). *Next-Generation geothermal technologies are heating up*. Bloomberg NEF. <https://about.bnef.com/blog/next-generation-geothermal-technologies-are-heating-up/>
 48. Norbeck, J., & Latimer, T. M. (n.d.). *Commercial-Scale demonstration of a First-of-a-Kind enhanced geothermal system*. <https://www.semanticscholar.org/paper/Commercial-Scale-Demonstration-of-a-First-of-a-Kind-Norbeck-Latimer/47d8751660affe73da68d1f5a44edbdd14cc14e1#citing-papers>
 49. Zatonski, V. & Brown, C., Eavor Technologies Inc. (2024a, January 11). *Eavor-Lite™ update after four years of operation*. <https://www.eavor.com/what-the-experts-say/eavor-lite-update-after-four-years-of-operation/>
 50. Toews, Matthew D. R. (2020). *Case Study of a Multilateral Closed-Loop Geothermal System*. World Geothermal Congress. Reykjavik.
 51. Government of Canada, Canada Energy Regulator. (2023, November 24). *CER – Market Snapshot: Geothermal Power is stable and low carbon, but what is its potential in Canada?* <https://www.cer->

- rec.gc.ca/en/data-analysis/energy-markets/market-snapshots/2023/market-snapshot-geothermal-power-stable-low-carbon-what-is-potential-canada.html
52. Belyakov, N. (2019). Geothermal energy. In *Elsevier eBooks* (pp. 475–500). <https://doi.org/10.1016/b978-0-12-817012-0.00034-7>
 53. Van Zalk, J., & Behrens, P. (2018). The spatial extent of renewable and non-renewable power generation: A review and meta-analysis of power densities and their application in the U.S. *Energy Policy*, 123, 83–91. <https://doi.org/10.1016/j.enpol.2018.08.023>
 54. *Geothermal | Electricity | 2022 | ATB | NREL*. (n.d.). <https://atb.nrel.gov/electricity/2022/geothermal>
 55. Augustine, C., Sarah Fisher, Jonathan Ho, Ian Warren & Erik Witter. (2023 January). *Enhanced Geothermal Shot Analysis for the Geothermal Technologies Office*. Technical Report. NREL/TP-5700-84822. <https://www.nrel.gov/docs/fy23osti/84822.pdf>
 56. Augustine, C., Ho, J., & Blair, N. (2019). *GeoVision Analysis Supporting Task Force Report: Electric Sector Potential to Penetration*. <https://doi.org/10.2172/1524768>
 57. Gallucci, M. (2023, November 28). America's first 'enhanced' geothermal plant just got up and running. *Canary Media*. https://www.canarymedia.com/articles/geothermal/americas-first-enhanced-geothermal-plant-just-got-up-and-running?utm_medium=email
 58. Trujillo, M. A. (2024, February 20). Eavor Technologies Secures Major Investment from Kajima for Geothermal Advancement. *BNN*. <https://bnnbreaking.com/tech/eavor-technologies-secures-game-changing-investment-from-kajima-corporation-to-advance-geothermal-energy>
 59. Government of Alberta, Canada. Geothermal Resource Development (2023). <https://www.alberta.ca/geothermal-resource-development>
 60. *Geothermal Resource Tenure Regulation - Open government*. (n.d.). https://open.alberta.ca/publications/2021_251

Appendix A: Electricity Futures by Province – Summary of the CER Findings (based on EF2023data [21])

Newfoundland and Labrador

Newfoundland and Labrador, TWh	2025	2026	2027	2028	2029	2030	2031	2032	2033	2034	2035
Demand											
Canada Net-Zero	12.5	12.6	12.8	12.9	13.1	13.2	13.3	13.3	13.4	13.5	13.5
Current Measures	12.3	12.4	12.5	12.5	12.6	12.7	12.7	12.8	12.8	12.9	13.0
Generation											
Canada Net-Zero	45.4	45.4	45.5	45.7	45.7	45.6	45.7	45.8	45.8	45.9	46.0
Current Measures	45.1	45.2	45.2	45.3	45.3	45.2	45.2	45.3	45.3	45.3	45.3
Interchanges											
Canada Net-Zero	32.3	32.2	32.1	32.1	31.9	31.7	31.7	31.6	31.5	31.4	31.3
Current Measures	32.6	32.6	32.5	32.6	32.4	32.3	32.3	32.2	32.2	32.2	32.2

Prince Edward Island

Prince Edward Island, TWh	2025	2026	2027	2028	2029	2030	2031	2032	2033	2034	2035
Demand											
Canada Net-Zero	1.9	1.9	2.0	2.0	2.1	2.2	2.2	2.3	2.4	2.4	2.5
Current Measures	1.9	1.9	2.0	2.0	2.0	2.1	2.1	2.2	2.2	2.3	2.3
Generation											
Canada Net-Zero	1.3	1.4	1.5	1.5	1.6	1.7	1.7	1.7	1.7	1.8	2.3
Current Measures	1.2	1.3	1.4	1.5	1.6	1.7	1.7	1.8	1.9	2.0	2.2
Interchanges											
Canada Net-Zero	-0.6	-0.6	-0.6	-0.6	-0.6	-0.6	-0.7	-0.8	-0.8	-0.9	-0.4
Current Measures	-0.7	-0.7	-0.6	-0.6	-0.6	-0.5	-0.5	-0.4	-0.4	-0.4	-0.2

Nova Scotia

Nova Scotia, TWh	2025	2026	2027	2028	2029	2030	2031	2032	2033	2034	2035
Demand											
Canada Net-Zero	12.0	12.3	12.6	13.0	13.4	13.7	14.1	14.4	14.8	15.1	15.5
Current Measures	11.8	12.0	12.2	12.5	12.7	12.9	13.1	13.3	13.5	13.7	13.9
Generation											
Canada Net-Zero	7.8	9.6	11.7	13.0	13.9	14.1	15.8	17.6	19.1	20.4	21.7
Current Measures	7.8	8.4	9.1	9.4	9.5	9.5	9.6	9.9	10.0	10.0	10.1
Interchanges											
Canada Net-Zero	-5.0	-3.5	-1.8	-0.9	-0.4	-0.7	0.6	1.8	2.8	3.5	4.1
Current Measures	-4.7	-4.5	-4.0	-3.9	-4.0	-4.2	-4.4	-4.3	-4.4	-4.6	-4.6

New Brunswick

New Brunswick, TWh	2025	2026	2027	2028	2029	2030	2031	2032	2033	2034	2035
Demand											
Canada Net-Zero	15.7	15.8	16.0	16.3	16.6	16.8	17.0	17.2	17.5	17.7	18.0
Current Measures	15.3	15.5	15.6	15.8	16.0	16.2	16.4	16.5	16.7	16.9	17.1
Generation											
Canada Net-Zero	12.3	12.1	12.1	11.0	11.0	10.1	11.0	12.0	13.1	13.8	14.6
Current Measures	12.0	12.2	12.4	11.2	11.2	10.0	11.0	12.1	13.2	14.2	15.0
Interchanges											
Canada Net-Zero	-4.0	-4.3	-4.6	-6.1	-6.4	-7.6	-7.0	-6.4	-5.8	-5.4	-5.2
Current Measures	-4.3	-4.2	-4.2	-5.6	-5.9	-7.1	-6.3	-5.4	-4.4	-3.6	-3.0

Quebec

Quebec, TWh	2025	2026	2027	2028	2029	2030	2031	2032	2033	2034	2035
Demand											
Canada Net-Zero	214.2	218.2	221.4	224.6	228.3	231.8	235.2	238.5	241.6	244.5	247.1
Current Measures	215.8	219.5	222.8	225.9	229.7	233.2	236.6	239.8	242.9	245.8	248.8
Generation											
Canada Net-Zero	234.7	243.7	250.4	257.3	261.9	266.9	270.8	273.1	275.3	277.6	283.9
Current Measures	235.6	244.2	250.7	257.8	262.3	268.9	271.2	274.1	277.6	281.8	285.3
Interchanges											
Canada Net-Zero	6.1	10.7	13.6	16.8	17.0	17.9	16.4	14.9	13.3	12.0	15.0
Current Measures	4.2	8.5	11.0	14.5	14.6	17.1	15.6	15.2	15.2	16.1	16.5

Ontario

Ontario, TWh	2025	2026	2027	2028	2029	2030	2031	2032	2033	2034	2035
Demand											
Canada Net-Zero	155.8	161.6	168.0	174.6	182.6	190.1	198.3	207.2	216.7	226.3	235.5
Current Measures	156.0	159.8	164.0	167.9	172.7	176.9	181.0	185.1	189.4	193.7	198.4
Generation											
Canada Net-Zero	146.2	148.4	153.0	161.1	167.1	180.2	193.1	208.8	223.6	241.4	254.1
Current Measures	148.4	150.6	153.1	157.8	159.8	164.3	167.0	172.1	174.8	179.5	182.1
Interchanges											
Canada Net-Zero	-2.4	-6.3	-8.9	-8.8	-11.9	-9.1	-11.5	-10.3	-10.8	-8.8	-12.7
Current Measures	-0.5	-3.1	-4.5	-3.7	-5.9	-4.9	-6.2	-5.5	-7.2	-7.1	-9.2

Manitoba

Manitoba, TWh	2025	2026	2027	2028	2029	2030	2031	2032	2033	2034	2035
Demand											
Canada Net-Zero	24.2	24.7	25.4	26.1	26.9	27.6	28.4	29.2	30.1	31.0	31.8
Current Measures	24.3	24.7	25.1	25.6	26.1	26.6	27.0	27.4	27.9	28.3	28.7
Generation											
Canada Net-Zero	31.4	32.3	34.5	35.5	40.8	42.1	43.1	44.4	45.6	46.9	52.3
Current Measures	31.5	32.1	33.8	34.2	38.4	38.9	39.3	39.8	40.1	40.3	40.7
Interchanges											
Canada Net-Zero	11.3	11.6	14.5	14.6	18.5	18.6	18.3	18.2	18.0	17.6	21.7
Current Measures	11.3	11.5	14.3	14.2	17.5	17.5	17.4	17.4	17.2	17.0	16.9

Saskatchewan

Saskatchewan, TWh	2025	2026	2027	2028	2029	2030	2031	2032	2033	2034	2035
Demand											
Canada Net-Zero	26.1	26.9	27.7	28.5	29.4	30.3	31.3	32.4	33.7	35.1	36.4
Current Measures	27.0	27.6	28.1	28.4	29.0	29.4	29.9	30.3	30.7	31.2	31.7
Generation											
Canada Net-Zero	25.8	26.5	27.5	27.9	28.8	29.8	31.8	33.2	34.8	36.9	35.4
Current Measures	26.6	27.6	28.0	27.6	28.1	28.4	28.9	29.3	29.8	30.4	30.8
Interchanges											
Canada Net-Zero	-2.1	-2.1	-2.0	-2.3	-2.3	-2.2	-2.5	-2.6	-2.6	-2.3	-5.4
Current Measures	-2.2	-2.3	-2.3	-3.1	-3.2	-3.3	-3.3	-3.3	-3.3	-3.2	-3.2

Alberta

Alberta, TWh	2025	2026	2027	2028	2029	2030	2031	2032	2033	2034	2035
Demand											
Canada Net-Zero	81.6	83.5	87.5	90.3	93.7	97.1	101.9	105.6	109.3	113.3	117.2
Current Measures	83.8	85.1	87.6	88.9	90.6	92.2	95.0	96.4	97.9	99.5	100.6
Generation											
Canada Net-Zero	90.4	92.4	96.1	100.0	103.4	106.8	112.9	116.5	119.3	122.3	128.5
Current Measures	93.0	95.3	98.3	101.3	103.8	105.7	108.3	109.5	110.8	112.0	112.4
Interchanges											
Canada Net-Zero	4.7	5.2	5.2	6.5	6.9	7.1	6.3	5.9	4.8	3.7	6.2
Current Measures	4.7	5.3	5.8	7.5	8.5	8.9	8.9	9.2	9.4	9.3	9.1

British Columbia

British Columbia, TWh	2025	2026	2027	2028	2029	2030	2031	2032	2033	2034	2035
Demand											
Canada Net-Zero	70.7	73.4	75.9	79.0	84.5	89.4	92.2	94.9	97.3	99.7	101.9
Current Measures	69.5	71.9	73.8	76.3	79.4	82.1	84.1	87.4	90.6	92.4	94.1
Generation											
Canada Net-Zero	72.7	73.6	74.9	75.9	80.4	84.3	88.9	92.1	95.3	98.8	96.0
Current Measures	72.4	73.4	74.1	74.8	77.0	78.8	80.9	83.9	86.4	88.2	89.6
Interchanges											
Canada Net-Zero	3.7	2.6	2.0	0.4	-0.1	-0.6	0.6	1.1	1.7	2.6	-2.5
Current Measures	-0.9	-2.2	-3.1	-4.6	-5.3	-5.9	-5.7	-5.9	-6.5	-6.3	-6.4

Appendix B: Electricity Generation Data by Fuel for Alberta, Saskatchewan, and Nova Scotia (based on Canada Future 2023 data)

Alberta

In NetZero scenario, wind power deployment will include 750 MW in 2025, 313 MW per year in 2026-2030, and very powerful 2285 MW per year deployment in 2031-2035. Solar power deployment will include 150 MW per year in 2026-2030, and 2216 MW per year in

2031-2035. Uranium SMR will be deployed at 91.8 MW per year in 2031-2035.

In Current Measures scenario, wind power deployment of 900 MW in 2028, and solar power deployment of 231 MW in 2026, and 400 MW per year

(2000 MW total) in 2031-2035. No Uranium SMR deployment expected.

Alberta Generation, TWh	Canada NetZero			Current Measures		
	2025	2030	2035	2025	2030	2035
Coal and Coke	0	0	0	0.00	0.00	0.00
Solar (Distributed)	0.33	0.76	1.51	0.28	0.45	0.83
Solar (Utility scale)	2.09	3.47	23.98	2.66	2.66	6.48
Onshore Wind	16.05	21.53	65.15	10.16	14.17	14.17
Hydro	1.65	1.65	1.35	1.65	1.65	1.65
Hydrogen	0.00	0.00	0.00	0.00	0.00	0.00
Bioenergy	1.41	1.60	1.04	1.59	1.19	0.86
Uranium SMR	0.00	0.00	3.20	0.00	0.00	0.00
Bioenergy with CCUS	0.00	0.00	5.74	0.00	0.00	0.00
Natural Gas	68.85	66.07	5.28	76.65	85.61	88.40
Natural Gas with CCUS	0.00	11.70	21.23	0.00	0.00	0.00
Oil	0.02	0.00	0.00	0.02	0.00	0.00
Total, including:	90.39	106.78	128.49	93.01	105.74	112.39
Clean Generation, TWh	20.12	39.11	122.17	14.75	18.93	23.13
Clean Generation, %	22.3%	36.6%	95.1%	15.9%	17.9%	20.6%
Non-Clean Generation, TWh	70.27	67.67	6.32	78.25	86.80	89.26
Non-Clean Generation, %	77.7%	63.4%	4.9%	84.1%	82.1%	79.4%

Saskatchewan

In NetZero scenario, wind power deployment expects a huge push of 1468 MW in 2024, 450MW in 2025, followed by 170 MW per year in 2026-2030, and 340 MW per year in 2031-2035. This is followed by solar power deployment: 20 MW in 2025, 32 MW in 2030, and then 270 MW per year in 2031-2035. Uranium SMR will be deployed at 214 MW per year from 2031 to 2035.

In Current Measures scenario, the same push of 1468 MW is indicated in 2024, 106 MW in 2025, 167 MW per year in 2026-2030, and 109 MW per year in 2031-2035 (209 MW in 2034). Solar power deployment will plan 32 MW in 2030, and 143 MW per year in 2031-2035

(53% of what is planned in NetZero). No Uranium SMR deployment expected.

Nova Scotia

In NetZero scenario, wind power will be deployed at 400 MW per year in 2026 to 2030, and then at 600 MW per year in 2031-2035.

In Current Measures scenario, wind power will increase annually by 38.5 MW per year from 2026 to 2030 and will continue growing: from 128.3 MW per year in 2031 to 122.5 MW per year in 2035.

No Uranium SMR deployment is expected in both scenarios.

Nova Scotia Generation, TWh	Canada NetZero			Current Measures		
	2025	2030	2035	2025	2030	2035
Coal and Coke	3.34	0.00	0.00	3.34	0.00	0.00
Solar (Distributed)	0.00	0.01	0.02	0.00	0.01	0.01
Solar (Utility scale)	0.00	0.00	0.00	0.00	0.00	0.00
Offshore Wind	0.00	10.03	19.46	0.00	0.00	0.00
Onshore Wind	2.16	2.11	1.89	2.16	2.35	2.98
Hydro	0.98	0.87	0.23	0.98	0.99	0.99
Oil	0.00	0.00	0.00	1.23	5.82	5.67
Natural Gas	1.16	0.81	0.03	0.00	0.00	0.00
Bioenergy	0.15	0.27	0.04	0.10	0.33	0.36
Total, including:	7.79	14.10	21.66	7.81	9.49	10.01
Clean Generation, TWh	3.14	13.03	21.59	6.48	3.35	3.98
Clean Generation, %	40.3%	92.4%	99.7%	83.0%	35.2%	39.8%
Non-Clean Generation, TWh	4.65	1.07	0.07	1.33	6.15	6.03
Non-Clean Generation, %	59.7%	7.6%	0.3%	17.0%	64.8%	60.2%

This page is intentionally left blank



GLOBAL JOURNAL OF RESEARCHES IN ENGINEERING: J
GENERAL ENGINEERING
Volume 24 Issue 1 Version 1.0 Year 2024
Type: Double Blind Peer Reviewed International Research Journal
Publisher: Global Journals
Online ISSN: 2249-4596 & Print ISSN: 0975-5861

Comparative Characterization of Saltwater from Kula, Nembe, and Kwale in the Niger Delta, Nigeria

By Aprioku, P. S., Usiabulu, G. I., Djoï, N. A., Okoh I. E., Egwuatu C. A. & Aguebor D. E.
University of Port Harcourt

Abstract- Three samples of water from Kwale, Nembe, and Kula in the Niger Delta were collected and characterized, and the following properties: pH, Temperature, Dissolved Oxygen, Turbidity, Acidity, Alkalinity, Electrical conductivity, Salinity, Oil and Grease, Total Hydrocarbon (THC), Heavy metals, BTEX and Poly Aromatic Hydrocarbon (PAH) were determined. The result of some of the key parameters showed that the Salinity of the Kula water sample is highest with a salt concentration of 13,115mg/L (at 30°C) followed by the Nembe water sample with a salt concentration of 2,500mg/L (at 29.68°C) and Kwale with a small salt concentration of 60mg/L (at 28.67°C). The electrical conductivity of the three water samples followed the same trend as salinity with Kula, Nembe, and Kwale water samples having electric conductivity of 20,101 μ S/cm (at 30°C), 1,489 μ S/cm (at 29.68°C), and 122 μ S/cm (at 28.67°C) respectively.

Keywords: *characterization, seawater, physiochemical and heavy metal, polyaromatic hydrocarbon, total petroleum hydrocarbon, BTEX.*

GJRE-J Classification: LCC: QC809-945.35



Strictly as per the compliance and regulations of:



© 2024. Aprioku, P. S., Usiabulu, G. I., Djoï, N. A., Okoh I. E., Egwuatu C. A. & Aguebor D. E. This research/review article is distributed under the terms of the Attribution-NonCommercial-NoDerivatives 4.0 International (CC BYNCND 4.0). You must give appropriate credit to authors and reference this article if parts of the article are reproduced in any manner. Applicable licensing terms are at <https://creativecommons.org/licenses/by-nc-nd/4.0/>.

Comparative Characterization of Saltwater from Kula, Nembe, and Kwale in the Niger Delta, Nigeria

Aprioku, P. S.^α, Usiabulu, G. I.^σ, Djoï, N. A.^ρ, Okoh I. E.^ω, Egwuatu C. A.[¥] & Aguebor D. E.[§]

Abstract- Three samples of water from Kwale, Nembe, and Kula in the Niger Delta were collected and characterized, and the following properties: pH, Temperature, Dissolved Oxygen, Turbidity, Acidity, Alkalinity, Electrical conductivity, Salinity, Oil and Grease, Total Hydrocarbon (THC), Heavy metals, BTEX and Poly Aromatic Hydrocarbon (PAH) were determined. The result of some of the key parameters showed that the Salinity of the Kula water sample is highest with a salt concentration of 13,115mg/L (at 30°C) followed by the Nembe water sample with a salt concentration of 2,500mg/L (at 29.68°C) and Kwale with a small salt concentration of 60mg/L (at 28.67°C). The electrical conductivity of the three water samples followed the same trend as salinity with Kula, Nembe, and Kwale water samples having electric conductivity of 20,101μS/cm (at 30°C), 1,489μS/cm (at 29.68°C), and 122μS/cm (at 28.67°C) respectively. The polyaromatic hydrocarbon content in the three water samples showed that the Nembe water sample has the highest polyaromatic hydrocarbon of 0.969mg/L followed by the Kwale water sample with 0.705mg/L and Kula water sample with 0.229mg/L. Interestingly the results also showed that n-pentacosane concentration is the highest component of the Total Petroleum Hydrocarbon (TPH) in the Kula and Kwale samples while n-hexacosane concentration is the highest component of the TPH in the Nembe water sample. This explains why the Nembe water sample is cloudier than the Kwale and Kula water samples. But in BTEX composition the total BTEX is highest in Nembe water, followed by Kwale and the least of these components is in Kula water.

Keywords: *characterization, seawater, physiochemical and heavy metal, polyaromatic hydrocarbon, total petroleum hydrocarbon, BTEX.*

I. INTRODUCTION

Seawater, or salt water, is water from a sethe or ocean. On average, seawater in the world's oceans has a salinity of about 3.5% (35 g/L, 599

mM). This means that every kilogram (roughly one litre by volume) of seawater has approximately 35 grams (1.2 oz) of dissolved salts (predominantly sodium (Na⁺) and chloride (Cl⁻) ions). The average density at the surface is 1.025 kg/L. Seawater is denser than fresh and pure water (density 1.0 kg/L at 4°C (39°F) because the dissolved salts increase the mass by a larger proportion than the volume. The freezing point of seawater decreases as salt concentration increases. At typical salinity, it freezes at about -2 °C (28°F) (Chester & Roy, 2012). The coldest seawater ever recorded (in a liquid state) was in 2010, in a stream under an Antarctic glacier, and measured -2.6°C (27.3°F). Seawater pH is typically limited to a range between 7.5 and 8.4. However, there is no universally accepted reference pH scale for seawater and the difference between measurements based on different reference scales may be up to 0.14 units (Chester & Roy, 2012).

Most of the seawater has a salinity of between 31 g/kg and 38 g/kg, which is 3.1–3.8%, seawater is not uniformly saline throughout the world. Where mixing occurs with fresh water runoff from river mouths, near melting glaciers, or vast amounts of precipitation (e.g. Monsoon), seawater can be substantially less saline. The most saline open sea is the Red Sea, where high rates of evaporation, low precipitation, low river run-off, and confined circulation result in unusually salty water. The salinity in isolated bodies of water can be considerably greater still - about ten times higher in the case of the Dead Sea. Historically, several salinity scales were used to approximate the absolute salinity of seawater. A popular scale was the "Practical Salinity Scale" where salinity was measured in "practical salinity units (PSU)". The current standard for salinity is the "Reference Salinity" scale with the salinity expressed in units of "g/kg" (Corwin & Lesch, 2013).

The density of surface seawater ranges from about 1020 to 1029 kg/m³, depending on the temperature and salinity. At a temperature of 25°C, salinity of 35 g/kg, and 1 atm pressure, the density of seawater is 1023.6 kg/m³ (Feistel, 2008). Deep in the ocean, under high pressure, seawater can reach a density of 1050 kg/m³ or higher. The density of seawater also changes with salinity. Brines generated by seawater desalination plants can have salinities up to 120 g/kg. The density of typical seawater brine of 120 g/kg salinity

Author α: Department of Chemical/Petrochemical Engineering, Rivers State University, Nkpolu Port Harcourt, Nigeria.

*Author σ: World Bank Africa Centre of Excellence, Oilfield Chemicals and Research, University of Port Harcourt, Rivers State, Nigeria.
e-mail: godsdaysiabuuulu@gmail.com*

Author ρ: Reservoir Engineer and Data Scientist, Directorate of Hydrocarbons and Other Energy Resources, Republic of Benin.

Author ω: FHN 26 Limited (First Hydrocarbon) Block W Shell Estate Ecjeba, Warri, Delta State Nigeria.

Author ¥: Chemical Engineering Department, Federal University of Petroleum Resources, Effurun, Delta State, Nigeria.

Author §: Department of Petroleum Engineering, Southern Alberta Institute of Technology, Calgary AB Canada.

at 25°C and atmospheric pressure is 1088 kg/m³ (Millero et al., 2008).

The pH of seawater is limited to the range of 7.5 to 8.4 while thermal conductivity is 0.6 W/mK at 25°C and a salinity of 35 g/kg. The thermal conductivity decreases with increasing salinity and increases with increasing temperature (Shargawy et al., 2010). Seawater contains more dissolved ions than all types of freshwaters (Millero et al., 2008). However, the ratios of solutes differ dramatically. For instance, although seawater contains about 2.8 times more bicarbonate than river water, the percentage of bicarbonate in seawater as a ratio of all dissolved ions is far lower than in river water. Bicarbonate ions constitute 48% of river water solutes but only 0.14% of seawater (Millero, et al., (2008). Differences like these are due to the varying residence times of seawater solutes; sodium and chloride have very long residence times, while calcium (vital for carbonate formation) tends to precipitate much more quickly. The most abundant dissolved ions in seawater are sodium, chloride, magnesium, sulfate, and calcium. Its osmolarity is about 1000m/l (Millero et al., 2008).

Small amounts of other substances are found, including amino acids at concentrations of up to 2 micrograms of nitrogen atoms per liter which are thought to have played a key role in the origin of life.

The composition of the total salt component is Cl⁻ (55%), Na⁺ (30.6%), SO₂⁻ (7.7%), Mg²⁺ (3.7%), Ca²⁺ (1.2%), K⁺ (1.1%), and Others (0.7%). Note that the unit of the above composition is in wt/wt, not wt/vol or vol/vol. Sea water elemental composition is given below.

The ocean has a long history of human waste disposal on the assumption that its vast size makes it capable of absorbing and diluting all noxious material (Larson & Carl-Fedrik 2021). While this may be true on a small scale, the large amounts of sewage routinely dumped have damaged many coastal ecosystems, and rendered them life-threatening. Pathogenic viruses and bacteria occur in such waters, such as *Escherichia coli*, *Vibrio cholerae* the cause of cholera, hepatitis A, hepatitis E, and polio, along with protozoans causing giardiasis and cryptosporidiosis. These pathogens are routinely present in the ballast water of large vessels, and are widely spread when the ballast is discharged (Larson & Carl-Fedrik 2021).

Nkoro River is in Rivers State in the Niger Delta area of Nigeria. The Salinity, dissolved oxygen, pH, and surface water temperature conditions of this River were studied for a period of one year (January – December 2008), and the following results were obtained (Abowei, 2009) The response of estuarine fishes to changes in salinity, dissolved oxygen, pH and surface water temperature conditions does not only enhance our biological understanding of estuarine fish but contributes to the understanding of the potential effects of anthropogenic impacts on estuarine fish species.

Dissolved oxygen meter of the model: Oxy-Guard Handy MK II was used in measuring dissolved oxygen and temperature. pH was measured using a pH meter (model: Hanna Instrument model No. H1 8915 ATC) while salinity was measured using a saline meter, model: New S-100. for each of the parameters. The probe end of the meter was dipped into the river while the value at the pointer of the scale was read off and recorded. The measurements were taken while inside the canoe along Nkontoru – Job Ama, which is part of the Nkoro river system. Dissolved oxygen (DO) was measured in milligrams per liter (mg/l); temperature in °C (degrees centigrade); and salinity in parts per thousand (ppt). Salinity values ranged from 5% (September) to 17% (February and March). Dissolved Oxygen values ranged from 6mg/l (January, April, July, and October) to 10mg/l (September). pH values ranged from 6.1(August) to 8.5 (November) and Temperature values ranged from 24.0°C (July) to 32.0°C (March).

Salinity values ranged from 12.8±0.30 (%) (Station 4) to 13.3±0.10 (%) (Station 3). Dissolved Oxygen values ranged from 3.2±0.1 mg/l (Station 3) to 7.3±0.16 mg/l (Station 1). pH values ranged from 7.3±0.17 (Station 1) to 7.7±0.14 (Station 3) and Temperature values ranged from 27.3±0.24 (Station 1) to 33.7±0.21 (Station 3). There was no significant difference in salinity and pH between stations, but dissolved oxygen, and temperature showed significant differences between stations (P#0.05). The results of the correlation matrix analysis showed a significant correlation between the variables at different stations. The association between the environmental variables in the Nkoro River was generally similar because the water at the stations was seemingly from the same source, the Atlantic Ocean through the Bonny River. A positive association was observed indicating functional similarity. The varying magnitude of the relationship between the water variables in the lower Bonny River of the Niger Delta was attributed to the micro habit difference study of Salinity, Dissolved Oxygen, PH, and surface temperature conditions in the Nkoro River the of Niger Delta.

The study area for this research is Kwale, Nembe, and Kula Rivers.

a) KWALE

Kwale is the most populous community of the Ukwuani-speaking people of Delta State, Nigeria, and is located within the colonial Warri province (FRN, 2006). Kwale is generally considered a city especially considering its oil and gas reserves which can be utilized to transform the town and neighboring communities into a modern city (Mart Oil Resources Launches New Brand Identity, 2018). Kwale is host to oil and gas companies, some of which have a presence in different parts of the African city such as a gas flow facility which is situated at Ebedei nearby the Umukwuta

area, and another at Ebendo and Umusadege with a pipeline running from Aboh and river Ase creek (TheNation, 2018). The location of the Kwale city in the Nigerian map is shown in fig 1.



Fig. 1: Location of Kwale on the Nigerian map. (Ukwuani, 2021)

b) NEMBE

Nembe is the headquarters of the Nembe Local Government of Bayelsa State in Nigeria. Its geographical coordinates are 4° 32'23" North, 6° 24' East (The Bayelsa State Oil & Environmental Commission, 2022). It is a low-lying coastal area in the mangrove swamp rural area of the Niger Delta. The Nembe kingdom hosts international oil and gas companies like SPDC and ENI Nigeria. The presence of these companies has given rights to a lot of oil exploration and exploitation activities (NLGA, 2021). They also lamented years of oil spillages that have destroyed their environment, aquatic life, as well as air and water pollution and called on the Bayelsa State Oil and Environmental Commission (BSOEC) and international communities to come to their rescue (The Guardian Nigeria News, 2019). The location of the Nembe city in the Nigerian map is shown in fig. 2.



Fig. 2: Location of Nembe on the Nigerian map. (NAD, 2022)

c) KULA

The Kula tribe of the Ijaw people lives in Akuku Toru Local Government Area, southwestern Rivers State, Nigeria (Talbot, 1932). The Kula people did not originally speak Kalabarias their language but have lost their real language due to trade and close interactions with the Kalabari. The small Kalabari-speaking tribe is sometimes classified as a Kalabari community rather than its tribe (Alagoa, 2001). The tribe seat is the town of Kula (also known as Anyame-Kula or Anyaminama-Kula) founded and established by King Sara. Kula is situated in the southwestern axis of Rivers State of Nigeria – under the Akuku – Toru Local Government Area of Rivers State (Alagoa, 1971). Its geographical coordinates are 4° 20' 29' North and 6° 38' 46" East. It is a low-lying coastal area in the mangrove swamp region of the Niger Delta, with a few feet above the mean sea level, located very close to the Atlantic Ocean (Alagoa, 1964). The location of the Kula city in the Nigerian map is shown in Fig. 3.





Fig. 3: Location of Kula in the Nigerian map. (Pacheco Pereira, 1505–1520)

This research aims to compare the characteristics of the saltwater in Kwale, Kula, and Nembe water which would form the framework for further research work by scholars on the one hand and enable the marine and construction industry to take the correct decision from the design and conceptual stage of marine projects to be sited as well as marine vessels and equipment to be used in this region in particular and the Niger Delta in general.

II. MATERIALS AND METHOD

a) Sample Collection

Saltwater samples were collected from the Rivers in Nembe (Bayelsa), Kula (Rivers), and Kwale

(Delta) as follows. Water sampling bottles were thoroughly washed and dried. The sampling bottles were then dipped into the seawater at sampling points to collect the required volume of the water sample. Three samples have been collected from each area (Nembe, Kula, and Kwale).

b) Characterization of Salt Water Samples

The standard methods below were used to characterize the saltwater samples to determine the presence and composition of the marine saltwater components that were relevant to the study and listed in Table 1.

Table 1: Standard Parameters for the Characterization of Salt Water Samples

S/N	Parameters	Standard Method
1	pH	APHA 4500A
2	Temperature	APHA 4500A
3	Dissolved oxygen (DO)	APHA 4500-0
4	Turbidity	APHA 5.0NTU
5	Acidity	APHA 2310B
6	Alkalinity	APHA 2320B
7	Electrical conductivity	APHA 2510 B
8	Salinity	ASTM D6529
9	Oil & grease	EPA 418.1/413.2
10	Total hydrocarbon content (THC)	EPA 418.1/413.2
11	Heavy metals	AAS UNICAMM 939
12	BTEX	ASTM D3328
13	PAH	ASTM D 3328-78

Source: APHA 2013

III. RESULTS AND DISCUSSIONS

The results of the physiochemical and heavy metal characterization of the salt water samples are stated in Table 2, Table 3, Table 4, and Figure 5. The results in Table 2 showed that the salinity of the Kula

water sample is highest with a salt concentration of 13,115mg/L (at 30°C) followed by the Nembe water sample with a salt concentration of 2,500mg/L (at 29.68°C) and Kwale with a little salt concentration of 60mg/L (at 28.67°C).

Table 2: Physiochemical and heavy metal characterization of salt water sample (Physiochemistry and heavy metals)

S/N	Parameters	Method	Kwale	Nembe	Kula	Dpr Limits	Fmenv Limits
1	pH	APHA 4500-HB	7.68	7.37	7.26	6.5-8.5	6.5-8.5
2	Temperature (°C)	APHA 2550B	28.67	29.68	30.01	30	35
3	EC(μ/cm)	APHA 2510B	122	1489	20101		
4	Salinity (Mg/L)	APHA 25208	60	2,500	13,115	-	2000
5	DO(Mg/L)	APHA 4500OC	5.14	4.49	4.85	10.50	
6	Turbidity (NTU)	APHA 2130C	10.00	35.50	25.50	10	
7	Alkalinity (Mg/L)	APHA 2320B	41.00	35.00	51.00		
8	Acidity (Mg/L)	APHA 2310B	9.00	0.50	11.00		
9	(THC) (Mg/L)	API 45 & EPA 4184/4132	0.114	0.410	0.727		
10	As (Mg/L)	APHA 3111C	<0.011	<0.011	0.030		
11	Cd (Mg/L)	APHA 3111C	0.009	0.114	0.681	-	0.5
12	Ni (Mg/L)	APHA 3111C	0.021	0.087	0.059		
13	Fe (Mg/L)	APHA 3111C	2.072	4.424	10.099	1	
14	Zn (Mg/L)	APHA 3111C	1.126	2.575	6.037	01	0.02
15	Hg (Mg/L)	APHA 3111D	<0.015	<0.015	<0.015	01	
16	Ba (Mg/L)	APHA 3111D	<0.013	0.078	0.145		
17	V (Mg/L)	APHA 3111D	<0.019	<0.019	<0.019		

Expectedly and as shown in Table 2 the electric conductivity of the three water samples followed the same trend as the salinity with Kula, Nembe, and Kwale water samples having electric conductivity of 20,101 μ S/cm (at 30°C), 1,489 μ S/cm (at 29.68°C), and 122 μ S/cm (at 28.67°C) respectively. This is because the more saline water body contains more quantity of ions that help to conduct charges in the water hence soluble salts are usually added to water to improve the electrical conductivity of the water often used as electrolyte. This is consistent with the work by Fedorov (2002) who established that the salinity of seawater is proportional to the conductivity of the water. The iron content in the three water samples was observed to also follow a similar trend with the Kula water sample having an Iron concentration of 10.099mg/L while Nembe and Kwale water samples had an Iron concentration of 4.424mg/L and 2.072mg/L respectively.

The Polyaromatic hydrocarbon content in the three water samples is shown in Table 3. The result

showed that the Nembe water sample has the highest polyaromatic hydrocarbon of 0.969mg/L (with traces of pyrene) followed by the Kwale water sample with 0.705mg/L (with traces of acenaphthylene, phenanthrene, anthracene, and fluoranthene) and the Kula water sample with 0.229mg/L polyaromatic hydrocarbon (with traces of pyrene). One of the main differences in the areas of saltwater is that Kwale water is richer pyrene than those of Nembe and Kula and the inverse is noticed for acenaphthylene, phenanthrene, anthracene, and fluoranthene components.

Table 3: Polyaromatic Hydrocarbon characterization of salts water sample

S/N	Parameters (PAH Components (mg/L))	Methods	Kwale	Nembe	Kalu
1.	Naphthalene	EPA 8100	0.006	0.002	<0.001
2.	Acenaphthene	EPA 8100	0.004	0.033	0.065
3.	Acenaphthylene	EPA 8100	<0.001	0.013	<0.001
4.	Fluorine	EPA 8100	0.010	0.008	0.012
5.	Phenanthrene	EPA 8100	<0.001	0.011	0.013
6.	Anthracene	EPA 8100	<0.001	0.006	0.006
7.	Fluroanthene	EPA 8100	<0.001	0.012	0.008
8.	Pyrene	EPA 8100	0.018	<0.001	<0.001
9.	Benz (a) anthracene	EPA 8100	0.023	0.029	0.006
10.	Chrysene	EPA 8100	0.028	0.010	0.008
11.	Benzo (b) fluoranthene	EPA 8100	0.044	0.108	<0.001
12.	Benzo (k) fluoranthene	EPA 8100	0.030	0.038	0.010
13.	Benzo (a) pyrene	EPA 8100	0.031	0.103	0.022
14.	Indeno (1,2,3-c,d) pyrene	EPA 8100	0.179	0.168	0.023
15.	Dibenz (a,h) anthracene	EPA 8100	0.170	0.172	0.025
16.	Benzo (g,h,i) perylene	EPA 8100	0.162	0.250	0.024
	Total (Mg/L)		0.705	0.964	0.229

Table 4 shows the total petroleum hydrocarbon concentration in each of the three water samples. The result showed that the Kula water sample has the highest total petroleum hydrocarbon giving 5.450mg/L (with traces of C8-C12), followed by the Nembe water sample with a total petroleum hydrocarbon concentration of 3.626mg/L (with traces of C8-C11) and the Kwale water sample with a TPH of 1.001mg/L (with traces of C8-C13, C15, C17 and pristine). This is consistent with the initial total hydrocarbon result of 7.27mg/L, 4.10mg/L, and 1.14mg/L for Kula, Nembe, and Kwale water samples respectively as stated in Table 4.

Table 4: Total Petroleum Hydrocarbon, TPH characterization of salts water sample

S/N	Parameters Aliphatic Components (Mg/L)	Methods EPA 3510C	Kwale	Nembe	Kula
1	n-Octane (C8)	EPA 3510C	<0.001	<0.001	<0.001
2	n-Nonane (C9)	EPA 3510C	<0.001	<0.001	<0.001
3	n-Decane (C10)	EPA 3510C	<0.001	<0.001	<0.001
4	n-Undecane (C11)	EPA 3510C	<0.001	<0.001	<0.001
5	n-Dodecane (C12)	EPA 3510C	<0.001	0.001	<0.00
6	n-Tridecane (C13)	EPA 3510C	<0.001	0.001	0.007
7	n-Tetradecane (C14)	EPA 3510C	0.005	0.002	0.004
8	n-Pentadecane (C15)	EPA 3510C	<0.001	0.006	0.006
9	n-Hexadecane (C16)	EPA 3510C	0.009	0.002	0.004
10	n-Heptadecane (C17)	EPA 3510C	<0.001	0.002	0.006
11	Pristine	EPA 3510C	<0.001	0.009	0.009
12	n-Octadecane (C18)	EPA 3510C	0.005	0.003	0.006
13	Phytane	EPA 3510C	0.008	0.010	0.022
14	n-Nonadecane (C19)	EPA 3510C	0.009	0.004	0.012
15	n-Eicosane (C20)	EPA 3510C	0.007	0.002	0.005
16	n-Henelcosane (C21)	EPA 3510C	0.011	0.009	0.022
17	n-Docosane (C22)	EPA 3510C	0.011	0.030	0.071
18	n-Tricisane (C23)	EPA 3510C	0.010	0.047	0.110
19	n-Tetracosane (C24)	EPA 3510C	0.015	0.074	0.218
20	n-Pentacosane (C25)	EPA 3510C	0.196	0.139	0.502
21	n-Hexacosane (C26)	EPA 3510C	0.173	0.077	0.421
22	n-Heptacosane (C27)	EPA 3510C	0.031	0.108	0.410
23	n-Octacosane (C28)	EPA 3510C	0.019	0.246	0.426
24	n-Nonacosane (C29)	EPA 3510C	0.061	0.226	0.450
25	n-Triacontane (C30)	EPA 3510C	0.028	0.397	0.710
26	n-Hentriacontane(C31)	EPA 3510C	0.106	0.302	0.505
27	n-Dotriacontane (C32)	EPA 3510C	0.052	0.197	0.501
28	n-Tritracontane (C33)	EPA 3510C	0.015	0.117	0.246
29	n-Tetracontane (C34)	EPA 3510C	0.034	0.235	0.217
30	n-Pentatriacontane (C35)	EPA 3510C	0.023	0.729	0.254
31	n-Hexatriacontane (C36)	EPA 3510C	0.021	0.377	0.150
32	n-Heptatriacontane (C37)	EPA 3510C	0.021	0.191	0.296
33	n-Octatriacontane (C38)	EPA 3510C	0.037	0.031	0.198
34	n-Nonatriacontane (C39)	EPA 3510C	0.025	0.062	0.062
35	n-Tetracontane (C40)	EPA 3510C	0.028	0.052	0.048
	Total TPH (Mg/L)		1.001	3.662	5.450

The above result also showed that n-pentacosane concentration is the highest component of the TPH in the Kula and Kwale water sample while n-hexacosane concentration is the highest component of the TPH in the Nembe water sample. This explains why the Nembe water sample is cloudier than the Kwale and Kula water samples.

Table 5 shows the BTEX composition of the three water samples. The result showed that Benzene and Xylene concentrations were highest in the Nembe water sample and lowest in the Kula water sample while

the Ethylbenzene concentration was highest in Kwale than Nembe water sample.

Table 5: BTEX components characterization of salts water sample

S/N	Parameters	Methods	Kwale	Nembe	Kalu
	BTEX Components	EPA 8021			
1.	Benzene	EPA 8021	0.14	0.37	0.06
2.	Toluene	EPA 8021	<0.01	0.09	0.04
3.	Ethylbenzene	EPA 8021	0.11	0.04	<0.01
4.	(m, p, o)-Xylene	EPA 8021	0.15	0.19	0.08
	Total BTEX (Mg/L)		0.40	0.69	0.18

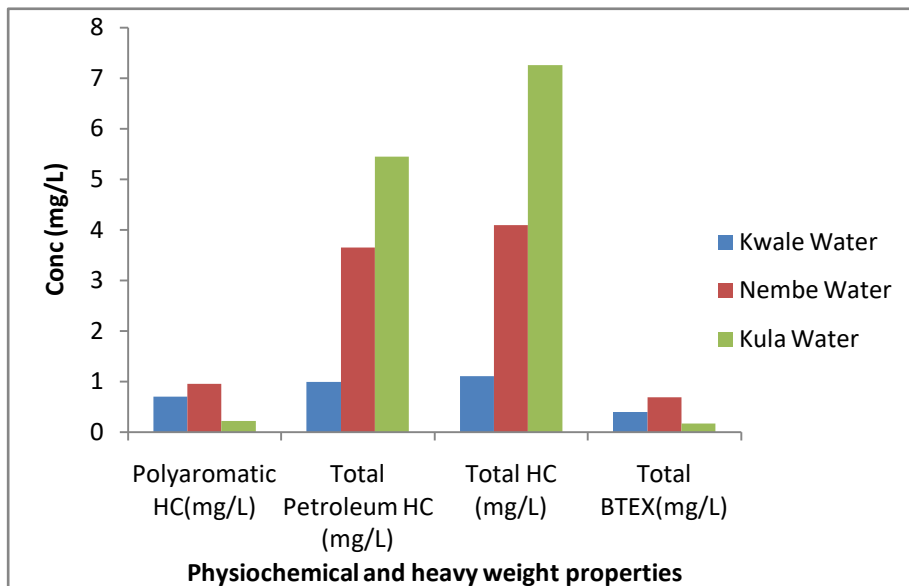


Fig. 4: Initial concentration of the major hydrocarbon family and heavy metal in Kwale, Nembe, and Kula water Samples

Figure 4 is a column chart showing the result summary of the initial composition of the major hydrocarbon family and heavy metal in the three different water samples. The result showed that the aliphatic and poly aromatic hydrocarbon composition in the water samples is highest in Nembe water followed by Kula water while Kwale has the least of these components. But in BTEX composition the total BTEX is highest in Nembe water, followed by Kwale and the least of these components is in Kula water.

IV. CONCLUSION

The main parameters used in the characterization of Kwale, Nembe, and Kula water bodies are Salinity, electric conductivity, polyaromatic hydrocarbon, and BTEX have shown that these parameters showed that the three water bodies are significantly different from one another even though they are all part of the Niger Delta. The salinity value for Kula River which is closest to the Atlantic Ocean and takes its source from the Atlantic Ocean was shown to have the highest (13,115mg/l at 30°C) followed by Nembe (2,500mg/l at 29.68°C) water body and the least salinity value is from Kwale water body (60mg/l at 28.67°C). This is expected because the closer you are to the ocean the higher its salinity value. Kwale is fresh water with very

little salinity value as it is the most distant from the Atlantic Ocean among the three water bodies. The electric conductivity of the three water samples is also consistent with the salinity trend with Kula, Nembe, and Kwale water samples having electric conductivity of 20,101µS/cm (at 30°C), 1,489µS/cm (at 29.68°C), and 122µS/CM (at 28.67°C) respectively. This is expected because electric conductivity is a function of the availability of ions in water which is proportional to the salinity of water. Based on this result corrosion is relatively expected to be highest around the Kula area more than the other two marine environments if all other factors that can cause corrosion remain the same. On the other hand, Kula could be the preferred environment to site a salt-producing industry. The Total Hydrocarbon (THC) content in the Kula water sample is the highest (0.727mg/l) followed by Nembe (0.411mg/l) and the least for the Kwale water sample. This may be due to increased oil spill and bunkering activities in the Kula environment with a lot of crude oil production activities followed by Nembe and then Kwale. Among the three water bodies the various hydrocarbon family composition of the three water bodies showed that Polyaromatic hydrocarbon in the Nembe water sample has the highest value of 0.969mg/l (with traces of pyrene) followed by the Kwale water sample with

0.705mg/l (with traces of acenaphthylene, phenanthrene, anthracene and fluoranthene) and Kula water sample with 0.229mg/l (with traces of pyrene). Interestingly the results also showed that n-pentacosane concentration is the highest component of the Total Petroleum Hydrocarbon (TPH) family in the Kula and Kwale water samples while n-hexacosane concentration is the highest component of the TPH in the Nembe water sample. This explains why the Nembe water sample is cloudier than the Kwale and Kula water samples. Finally, in BTEX composition, the total BTEX is highest in Nembe water, followed by Kwale and the least of these components is in Kula water.

REFERENCES RÉFÉRENCES REFERENCIAS

- "Delta to build three modular refineries". The Nation. February 22, 2018. Retrieved April 21, 2018.
- "Federal Republic of Nigeria: 2006 Population Census" (PDF). Archived from the original (PDF) on 5 March 2012. Retrieved 25 July 2016.
- "Mart oil resources launches new brand identity". This Day. March 23, 2018. Retrieved April 21, 2018. https://en.wikipedia.org/wiki/Kwale,_Nigeria
- "Nembe Local Government Area". www.manpower.com.ng Retrieved 2021-09-12.
- "Nigeria: Administrative Division (States and Local Government Areas) - Population Statistics, Charts, and Map". www.citypopulation.de. Retrieved 2022-03-11.
- "Oil Spill: Bayelsa communities slam oil firms over neglect". The Guardian Nigeria News - Nigeria and World News. 2019-07-13. Retrieved 2021-09-18.
- "The Bayelsa State Oil & Environmental Commission". The Bayelsa State Oil & Environmental Commission. Retrieved 2022-03-10.
- "Ukwuani: An ethnic people and language". 26 November 2021.
- Fedorov, K (2018) Formula for converting the electrical conductivity of seawater into salinity with digital temperature salinity probe under average ocean conditions *Oceanology* 11, 622-626.
- APHA 2013, Standard Parameters for the Characterization of Saltwater Samples. <https://academicjournals.org/journal/AJEST/article-full-text-pdf/C71880855964>
- Feistel, R. (2008). A Gibbs function for Seawater Thermodynamics from -6 to 80°C and Salinity up to 120 g kg^{-1} , *Deep-Sea Part I*, 55 (12), 1639–1671.
- Larson J. D. G & Carl-Fredrik F. (2021). Antibiotics Resistance in the Environment *Nature Reviews Microbiology* 20, 257-269.
- Millero, F. J., Feistel, R. & Write, D. G. (2008). The Composition of Standard Sea Water and the Definition of Reference Composition Salinity Scale Deep Sea Research Part I *Oceanographic Research Papers*, 55(1), 50-72.
- Pacheco P. (1505–1520). *Esmeralda De Situ Orbis*. London, Printed for the Hakluyt Society.
- Shargawy, M. H., Lienhard V., John, H. & Zubaer, S. M. (2010). The Thermo-Physical Properties of Sea Water. *A review of Existing Correlations and Data*. 16, 354-380.
- Talbot, P. A. (1932). *Tribes of the Niger Delta*, London's.



This page is intentionally left blank



GLOBAL JOURNAL OF RESEARCHES IN ENGINEERING: J
GENERAL ENGINEERING
Volume 24 Issue 1 Version 1.0 Year 2024
Type: Double Blind Peer Reviewed International Research Journal
Publisher: Global Journals
Online ISSN: 2249-4596 & Print ISSN: 0975-5861

Evolution of the use of Nanoparticles in Cancer Diagnosis and Treatment

By Camila Andrea Gualdría Sandoval, Esperanza del Pilar Infante Luna
& Luz Helena Camargo Casallas

Abstract- The use of nanoparticles in the health area is a research topic that has been increasing in recent years, from that perspective this work focused on making a characterization of nanoparticles, their evolution and interaction with blood, aspect addressed through the description of the biomagnetic fluid, focusing on characteristics such as viscosity and geometry. Also, the evolution of the applications or techniques in which nanoparticles have been used is presented, focusing the review on cancer treatments, for which the four progressive generations of this research field were considered, as well as the use of nanoparticles in diagnostic imaging. Finally, some fields of implementation and study in Colombia were identified. The review carried out allows concluding that the evolution of the use of nanoparticles.

Keywords: biomagnetic fluid, nanoparticles, magnetic nanoparticles, SPIONs

GJRE-J Classification: FOR Code: 0903



EVOLUTION OF THE USE OF NANOPARTICLES IN CANCER DIAGNOSIS AND TREATMENT

Strictly as per the compliance and regulations of:



RESEARCH | DIVERSITY | ETHICS

© 2024. Camila Andrea Gualdría Sandoval, Esperanza del Pilar Infante Luna & Luz Helena Camargo Casallas. This research/review article is distributed under the terms of the Attribution-NonCommercial-NoDerivatives 4.0 International (CC BY-NC-ND 4.0). You must give appropriate credit to authors and reference this article if parts of the article are reproduced in any manner. Applicable licensing terms are at <https://creativecommons.org/licenses/by-nc-nd/4.0/>.

Evolution of the use of Nanoparticles in Cancer Diagnosis and Treatment

Camila Andrea Gualdría Sandoval ^α, Esperanza del Pilar Infante Luna ^ο & Luz Helena Camargo Casallas ^ρ

Abstract- The use of nanoparticles in the health area is a research topic that has been increasing in recent years, from that perspective this work focused on making a characterization of nanoparticles, their evolution and interaction with blood, aspect addressed through the description of the biomagnetic fluid, focusing on characteristics such as viscosity and geometry. Also, the evolution of the applications or techniques in which nanoparticles have been used is presented, focusing the review on cancer treatments, for which the four progressive generations of this research field were considered, as well as the use of nanoparticles in diagnostic imaging. Finally, some fields of implementation and study in Colombia were identified. The review carried out allows concluding that the evolution of the use of nanoparticles.

Keywords: biomagnetic fluid, nanoparticles, magnetic nanoparticles, SPIONs.

I. INTRODUCTION

The term nanotechnology refers to a multidisciplinary field that deals with the research, design, synthesis, application of materials and functional systems by controlling substances at the nanometer level. The interest of nanotechnology is not only to manipulate matter on a small scale, but also to study the unique physical and chemical properties of nanostructures (e.g., surface properties, electrical conductivity and magnetic properties). In recent years, nanotechnology has had a major impact in areas such as biology and medicine (Rojas, Aguado, & González, 2016). With the aim of advancing in this field, a bibliographic review was carried out, oriented towards three topics: characterizing nanoparticles (np) and their evolution; describing the medium in which they move and therefore their interaction with it, and identifying the applications or techniques of nanotechnology in health sciences, specifically in cancer treatments (tumors), and the obtaining of diagnostic images through methods that use nanoscopic contrast agents or markers.

II. CHARACTERIZATION, DESCRIPTION AND EVOLUTION OF THE NP

The np are particles with dimensions of the order of $1 \text{ nm} = 1 \times 10^{-9} \text{ m}$, which facilitates their application to different fields of nanotechnology, in

medicine for example, they are used for the purpose of monitoring, control, construction or repair, defending or improving the human biological system at the molecular level (Wakaskar, 2018). Some of the np used in cancer treatments have been dendrimers, being np with three-dimensional tree-like structures in the range of 1-100 nm, they can host a variety of carrier molecules, both hydrophobic and hydrophilic and are useful delivery agents for genes, drugs and anticancer agents; thanks to their size and geometry they can be specifically controlled in groups, in order to possess pre-designed and specific physical and chemical properties (Alfonso & Casado, 2016).

On the other hand, micelles are hydrophobic spherical structures that are grouped to form the central core of the sphere in a liquid environment (Haley & Frenkel, 2008), so they are useful for the administration of water-insoluble drugs with sizes in the range of 10 - 50 nm (Urrejola et al., 2018). Nanospheres, on the other hand, are spherical structures composed of a matrix system where the surface can be modified by adding polymers and also biological materials, have a size in the range of 10 - 100 nm (Haley & Frenkel, 2008). From the perspective of their use as carriers, nanocapsules are vesicular systems with a central cavity or core to which it is possible to confine a drug, their size is in the range of 10 - 500 nm (Chávez, Olvera, Ganem, & Quintanar, 2002). Finally, we find the magnetic ones, on which we will go deeper, because their characteristics have made possible advances in the transport through the blood as a biomagnetic fluid.

a) Magnetic Nanoparticles (MNP)

They are np that are iron-based, therefore they can be manipulated by employing an external magnetic field (B) (Awwal et al., 2020). Magnetite (Fe_3O_4) is a black ferromagnetic iron oxide of Fe(II) and Fe(III), which has been the most studied, due to the potential to act as an electron donor (Mohammed, Gomaa, Ragab, & Zhu, 2017).

b) Ferrofluids

When talking about ferrofluids, we refer to a colloidal dispersion made by a special multidomain particles based on iron oxide and iron hydroxide by a wet chemical method, which facilitates the steering capability under the influence of a B (Lübbe, Bergemann, Riess, et al., 1996). Additionally, these colloidal magnetic np have unique surface properties

Author α σ ρ : e-mails: cagualdrias@correo.udistrital.edu.co, epinfantel@udistrital.edu.co, lhcamargoc@udistrital.edu.co

that allow biocompatibility and biodegradability in addition to having minimal toxicity, they are suitable as drug-delivery vehicles that have excellent magnetic saturation (Liu, Xu, Wang, & Ke, 2008).

c) *Superparamagnetic*

They are a unique type of MNP, because they have many desirable properties, from the point of view of biomedical applications, such as: biocompatibility, biodegradability and ease of synthesis, to which we must add their superparamagnetic nature. On the other hand, they do not produce hysteresis, since they leave a zero residual magnetization after an external B is removed, this feature helps to prevent coagulation, so compared to other MNP, it reduces the possibility of agglomeration in the body (Mohammed, Gomaa, Ragab, & Zhu, 2017).

The size of these particles influences both their physicochemical and pharmacokinetic properties, so two groups are classified: Spions: (superparamagnetic iron oxides) are np that in particular are generally based on inorganic iron oxide coated with hydrophilic polymers, whose size is larger than 50 nm (including the coating). USpions: (ultra-small superparamagnetic iron oxides) are np that have a size smaller than 50 nm, being blood pooling agents they could be used for perfusion imaging enabling the diagnosis of cerebral or myocardial ischemic diseases (Zhang et al., 2020).

III. CHARACTERIZATION AND INTERACTION OF THE ENVIRONMENT

Currently there is a field of research associated with the interaction of B with living beings, and in particular it has gained relevance in nanomedicine, from this perspective we can consider two basic areas: magnetobiology and biomagnetism. The former deals with the effects produced by magnetic fields on organisms, ranging from the orientation capacity of some animals, to the controversial damage to health caused by exposure to low-frequency electromagnetic waves. Biomagnetism, on the other hand, focuses on the study of the B associated to the organism itself, in particular, we refer to the biomagnetic fluid, which is found in organisms and reacts to the presence of a B. The results of these experimental fields are useful to obtain information that does not allow us to understand biophysical systems, to implement new clinical diagnostic techniques and to create new therapies centered on the use of np (Sosa, Alvarado, & Gonz, 2002).

a) *Blood as a Transport Medium for Nanoparticle*

The various applications of np as a means of transporting drugs or contrast chemicals, have led researchers to deepen both the knowledge of the blood, as the fluid through which these particles move, the interaction with the components thereof, and the

incidence of external magnetic fields applied, in this sense, Bose & Banerjee, (2015) mention measurements made to estimate the magnetic susceptibility of blood and reported that this is between 3.5×10^{-6} and 6.6×10^{-7} for venous and arterial blood, respectively, also Bartoszek & Drzazga, (1999) show an experimental study of the magnetic anisotropy of blood cells at a B of up to 1.8 T for a temperature range between 75 - 295 K, employing torsional magnetometry.

Ichioka & Ueno, (2000) conducted in vivo experiments using rats as subjects, which were subjected to magnetic fields of 8 T, showing a reduction in blood flow and temperature of the animal. In the same direction, the in vitro experiments conducted by Haik, Pai & Chen (1999), in which they used human blood samples subjected locally to a B of the same intensity, reduced by 30%, additionally established that as the biofluid enters and exits the gradient of B, In relation to the biomagnetic flux in narrow channels, Tzirtzilakis in 2005 found that these are affected by a constant and local B (Bose & Banerjee, 2015).

b) *Simulating Biomagnetic Fluid (Blood)*

Liu, Zhu, Rao, Clausen & Aidun, (2018) simulate the biotransport of np under a complex cell flow environment using a multiscale method based on the Lattice Boltzmann method (LBM), the basic components of which include liquid-phase LBM processing, the red blood cell spectrum linkage method (SLM), and the Langevin dynamics (LD) method to capture pauses of np motion. In addition, extensive bidirectional coupling schemes are established to capture precise interactions between each component and thus simulate np transport in cellular blood flow with high efficiency.

In turn, Lee, Ferrari & Decuzzi, (2009) present a general mathematical model to predict the transport behavior of particles with different physical properties: size (nano-microparticles) and shape, as well as the material in which they are immersed, considering a linear laminar flow. Their results show that non-spherical particles, under the concurrent action of inertial and hydrodynamic forces, can deflect laterally, an effect known as hydrodynamic margination, increasing the probability of interaction with the wall surface. Thus, in blood, np will periodically oscillate around their trajectory, thus reducing their distance from the vessel wall, while the particles may actually separate with a net lateral deflection.

On the other hand, Duncan & Bevan, (2015) generated a Monte Carlo simulation, measuring the net interactions between np "decorated" by ligands, which possess distinct chemical structures, providing multiple interactions in self-assembly, and membrane proteins on the surfaces of healthy and diseased cells. From their analysis, they identify that these ligand-functionalized np are able to selectively bind to populations of diseased cells rather than healthy cells, proving attractive for

improving the efficacy of drug therapies by using lower affinity ligands to target cancer cells with targeted membrane proteins.

Along the same lines, Müller, Fedosov & Gompper, (2014) performed simulations and attempted to study the marginal characteristics of carriers of different shapes and sizes using mesoscopic hydrodynamic simulations to explain the related physical mechanisms, finding that the properties of particle edges increase with increasing carrier size. The above results lead to the conclusion that addressing the various problems associated with drug delivery is a complex issue; its solution requires an interdisciplinary effort, including in vitro and in vivo experiments and realistic numerical simulations.

c) *Viscosity*

Blood viscosity and plasma viscosity are the best known parameters characterizing the properties of blood flow. Haik, Pai & Chen, (2001) conduct an investigation on the behavior of viscosity due to magnetic discharges in human blood, for which they carried out flow experiments on oxygenated blood in vitro and which is subjected to a B of up to 10 T. Additionally, they use a mathematical model to simulate biomagnetic fluid dynamics under similar conditions, which allows them to identify that the magnetization action will introduce a rotational motion to orient the magnetic fluid particles with the B (Afkhani & Renardy, 2017); however, the behavior and characteristics of the blood are unique to each patient. As a complement to the aforementioned computational experiments, Rukshin, Mohrenweiser, Yue & Afkhani, (2017) proposed a mathematical model describing the behavior of equations to visualize particle trajectories and calculate capture rates to assess the impact of various physical conditions on the success of magnetic drug targeting.

d) *Geometry of the Medium*

Another element to take into account in the characterization of the medium is the geometry, muscle arteries have three major geometrical differences with capillaries, for example in microvessels, the anti-slip boundary condition reduces the velocity of blood near the wall relative to the centerline and improves the ability to trap particles by weaker magnetic force due to lower resistance compared to millimeter vessels (Avilés et al., 2005). In this case, the force required is well below the maximum allowable exposure, however, due to the higher blood flow rate in muscles and blood vessels, the particles require a higher magnetic force to resist the "tenacity" that occurs in the opposite direction of particle motion.

IV. EVOLUTION OF APPLICATIONS IN CANCER TREATMENTS, USING NP

Cancer is a disease in which the cells of the human body acquire the ability to divide and multiply uncontrollably (Sharma, Sharma, Punj, & Priya, 2019), this condition acquired by the diseased cells through mutations of the genome, as the cancer cells divide, leads to the fact that the new cells will inherit the same growth capacity and increase the number of cancer cells (Miller, 2018). The treatments for this disease are diverse and in any case, side effects must be considered, therefore, targeted treatments are an important option for patients. In this sense, the evolution in the use of np is presented, which is approached through four generations, identifying the main investigations and their results.

a) *First Generation*

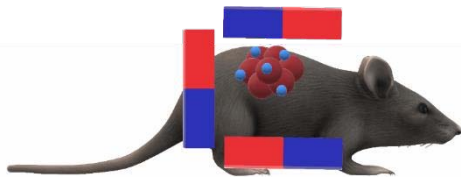
The first experiment was performed "in vivo" by Lübbe et al, (1996), who developed a magnetic fluid to which drugs, cytokines and other molecules can chemically bind to allow these agents to be directed into an organism by an external high-energy B. They used male rats and mice, kept in a controlled environment. For which they used male rats and mice, kept in a controlled environment. For the design of the external B, using high-energy permanent magnets made of rare earths (neodymium), they consisted of disks or blocks with variable thickness, configured in the shape of a column or a block (see Figure 1). In this way, the magnets could be arranged more closely around the individual tumor configuration, with a B between 0.2 - 0.5 T (depending on tumor size). They tested two forms of therapy with the magnetic fluid: treatment of tumors by mechanical occlusion with the ferrofluid in high concentrations; and magnetic therapy, using small amounts of the ferrofluid as a drug carrier vehicle, which allowed epirubicin to be concentrated locally in the tumors.

The first part of the study focused on tolerance to ferrofluid and magnetically bound epirubicin. The results show that hematological and blood chemistry values did not change from baseline after injection of different amounts of ferrofluid. On the other hand, epirubicin caused changes in hematological parameters. Histological data showed that the magnetic particles accumulated in the liver and spleen, without causing significant hepatosplenomegaly, the latter two results were within predicted. After the sixth week of observation, one animal in each high-dose group died, possibly due to cardiovascular failure caused by sepsis. In those groups in which the highdose epirubicin was administered, the animals died quickly; in the low-dose groups, they died somewhat later, around 4 - 6 weeks. In all other groups, including those receiving low levels of epirubicin, the animals survived the observation

period (Lübbe, Bergemann, Huhnt, Fricke, & Riess, 1996).

The second part of this investigation focused on the mechanical embolization by the ferrofluid after its injection and concentration in the tumor by means of an external B, regardless of the type of tumor, there was a rapid and constant decrease in tumor volume within 14 days after treatment. It was impossible to reproduce this tumor response in the animals given only epirubicin, although the tumors responded to the high dose of this drug, this was only for a brief period and most of the animals in this group died shortly thereafter.

Subsequent experiments by Lübbe led to the conclusion that magnetic fluid is a good agent to decrease tumor volume and with further studies, it can be used in different forms of local cancer treatment in conjunction with high-energy magnetic fields, avoiding mortality of the subject (Lübbe., Bergemann, Brock, & McClure, 1999).



Source: own

Fig. 1: Graphic Illustration of Placement of Rare Earth Magnets in Block form on the Tumor to be Treated

Thus, in the second experiment, Lübbe et al., (1999) chose their subjects with an eligibility criterion among them, seven patients with breast cancer, two with chondrosarcoma, two with parotid squamous cell carcinoma, one with Ewing's sarcoma and two with malignant tumor; with a life expectancy of at least three months and renal preservation. Continuing their line of research, they employed anticancer drugs that would reversibly bind to magnetic fluids, which were focused on locally advanced tumors through a B disposed on the tumor surface outside the body.

They tested for magnetite concentration in the tumor, and 10 of the 14 patients, had intact skin covering the tumors, the other four showed wound healing and open superficial wounds. In the first four cases, since the B will obscure the shape of the magnetic block attached to the tumor, it is easy to observe magnetite absorption into the tumor, this discoloration lasted for 24 - 36 hours and then disappeared completely, these areas were not locally toxic and ensured that the discoloration could not be removed to rule out the possibility of iron deposition from the magnetic lumps in the superficial layer of the skin. So the targeted magnetic drug with epirubicin was well tolerated and mild tumor reductions were achieved at day 10 and some small responses at day 40 (Lübbe. et al., 1999) (Lübbe, Bergemann, Riess, et al., 1996).

b) Second Generation

Based on the results described above, Alexiou et al. (2000) used mitoxantrone-linked ferrofluid (FF-MTX) to treat rabbits with squamous cell carcinoma and concentrated it under a B. When the tumor reaches a volume of 3500 mm³, FF-MTX is injected intra-arterially or intravenously. When an external B is focused on the tumor, it is activated by an electromagnet with a maximum flux density of 1.7 T, producing a non-uniform B, both in direction and magnitude, a feature that is crucial for the use of magnetic drugs. Magnetic drug targeting is a means of keeping the chemotherapeutic agent at the desired site of activity, thus increasing efficacy and decreasing systemic toxicity.

Only when the MTX dose was increased to 75% and 100%, tumor remission was observed, but this resulted in severe side effects (hair loss, ulcers and leukopenia). However, this "magnetically targeted drug" provides a unique opportunity to locally treat malignant tumors without systemic toxicity. In addition, it is possible to use these magnetic particles as "carrier systems" for various anticancer agents such as radionuclides, antibodies and cancer-specific genes (Alexiou et al., 2002).

c) Third Generation

Under another line of research, Gitter & Odenbac (2011) presented experimental results based on systematic "in vitro" quantitative measurements of a tube model simulating a Y-branched artery, in which they conclude that the success of particle orientation towards branching depends largely on the crossing point and the magnetic force at the site, elements that as previously mentioned must be evaluated.

For their part, Krukemeyer, Krenn, Jakobs & Wagner, (2011) performed a verification method on the effectiveness of cytostatic drugs coupled to ferromagnetic np and extracorporeal magnets, using 42 adult rats that were transfected with rhabdomyosarcoma. In the biodistribution assay, concentrations of mitoxantrone iron oxide and conventional mitoxantrone with and without 0.6 T magnets were measured in vitro in plasma and tumor tissue for one and two doses. During magnetic drug treatment, iron particles are rapidly removed and remain in the area where the tumor remained.

d) Fourth Generation

From the perspective of assessing patient safety, Attar et al., (2016) propose a configuration which investigates the thermal effect of superparamagnetic np on human cells, present a study considering general details on the design and construction of the configuration needed to generate a safe B to examine the thermal effect of superparamagnetic np on human cancer cells, then performed a series of experimental tests to study the effect of B on the cells for 30 minutes, which allowed them to calculate the temperature rise

and specific absorption. While it is true, hyperthermia treatment (Eivazzadeh-Keihan et al., 2019) is a mechanism to destroy malignant cells by increasing tissue temperature up to a range of 42 - 45°C, temperatures above 45 - 56°C, can cause necrotizing damage and subsequent tissue inflammation (Shabestari Khiabani, Farshbaf, Akbarzadeh, & Davaran, 2017). In this regard, ferromagnetic materials are commonly used to treat hyperthermia and the general procedure involves the allocation of magnetic particles of various sizes depending on the type of treatment to the tissue, then, when the particles generate heat through two mechanisms (including hysteresis and eddy currents), the tissue is exposed to an alternating B.

Among the advances in this fourth generation, it is important to mention the work of Al-Jamal et al., (2018), who performed in vivo experimentation based on a solid theoretical foundation for the design of a magnetic nanocarrier, capable of magnetizing uptake after intravenous administration, in order to elucidate the parameters necessary for the detection of magnetic tumors. Because long-circulating polymeric magnetic nanocarriers are capable of encapsulating increasing amounts of superparamagnetic iron oxide np (SPIONs) in a biocompatible oil carrier, they were able to study the effects of SPION loading and applied B intensity on magnetic tumor targeting in tumor-bearing mice.

Another important element is the fact that the high loading of SPIONs eliminates the need to use highly magnetized np and the oil core promotes high hydrophobic drug loading, compared to polymer-coated SPIONs. The objective of this experiment was to evaluate the key factors influencing magnetic targeting efficiency, including the loadings of SPIONs on m-NC (polymeric oil-core magnetic nanocapsules) and the magnitude of the magnetic force applied at a distance. Under controlled conditions, they quantified magnetic targeting in vivo and found that it was directly proportional to SPIONs loading and B intensity, however, higher SPIONs loading resulted in reduced blood circulation time and stabilization of magnetic targeting.

V. DIAGNOSTIC IMAGING WITH NP

Due to the physicochemical properties presented by nanomaterials, the development of nanodevices as contrast agents in medical imaging has clear advantages over traditional agents used in the diagnosis of diseases, among which we can mention: better optical dispersion (absorption of light in the material, with a clearer visual spectrum), increased biocompatibility, decreased probability of denaturation and especially, their ability to bind to ligands, which turns them into devices with multiple functions that bind to cells, simultaneously allowing imaging for diagnosis and transport of drugs to specific sites, thus, achieving

targeted and efficient treatment (Minbashi, Kordbacheh, Ghobadi, & Tuchin, 2020).

Nan, Suci, Ardelean, Senila & Turcu (2020), report a simple reaction strategy for the synthesis of magnetic iron oxide nps stabilized with ethylenediaminetetraacetic acid (EDTA) followed by the chelation reaction of gadolinium (Gd) ions. These results show that these magnetic nanosystems represent a promising dual-mode contrast in agents for MRI applications with biomedical applications in mind.

Another type of contrast agent used for feature detection are SPIONs, due to their long half-life and small diameter, they provide a variety of possibilities to visualize intracellular targets, they can also be coupled with fluorescent dyes so that these particles can be detected in vitro and in vivo by optical fluorescence methods.

In this technique, SPIONs are inhibited by the binding of polyethylene glycol (PEG) chains that are anchored by peptide substrates shed by proteases, in diagnostic imaging, dextran-coated SPIONs provide stability for imaging, such as magnetic resonance imaging, computed tomography and optical fluorescence (Cicha, Lyer, Alexiou, & Garlich, 2013).

In this direction, Nahrendorf et al., (2014) performed a study, where single-crystalline fluorochromelabeled SPIONs in the infrared were chelated with DTPA (diethylenetriaminepentaacetic acid) to allow binding of the PET radiotracer ^{64}Cu . While the iron oxide core provided the MRI contrast, the fluorochrome served for fluorescence imaging (fluorescence microscopy, flow cytometry and fluorescence mediated tomography), and the ^{64}Cu radiotracer allowed PET (positron emission tomography) imaging, while the iron oxide core provided the MRI contrast.

The reported results show a trend towards the increasing use of SPIONs in various biomedicine applications.

VI. IMPLEMENTATION IN COLOMBIA

Jaimez, Gonzales, Granados, Álvarez & Espitia, (2012) of the Pontificia Universidad Javeriana carried out a review article to see what advances and expectations there are in surgery to date, explaining what nanotechnology consists, its basic principles and some utilities in the field of surgery. On the other hand, Mendez and Muñoz [43] of the National University of Colombia wrote an article describing the clinical and molecular characteristics of premalignant lesions and oral cancer, as well as diagnostic methods using nanotechnology (nanochips, nanosensors, etc.) as an effective method for the early detection of cancer. Rodriguez, Moyano and Roa [44] from the Universidad Distrital Francisco Jose de Caldas, obtained a mathematical model and a computational simulation

describing the trajectory of magnetic np injected near the target tissue. The magnetic np propagate along the blood vessel in the Z-direction and point to the target area through a cylindrical magnet located outside the body generating a constant B.

Likewise, Gallo and Ossa [45] from the University of Antioquia carried out a study where they evaluated two silver np synthesis processes, using, in addition, a biofunctionalization process with polyethylene glycol (PEG) to improve the anchoring properties and biocompatibility of the np, for possible treatments against skin cancer.

In the master's thesis in engineering of Pantoja, (2020) of the Universidad Distrital Francisco José de Caldas, he has focused on proposing a mathematical model that can estimate the trajectory of NPM through the action of an external B and the blood flow is obtained through computational simulation. The model includes forces that significantly affect NPM dynamics, including magnetic fields generated by magnets, scattering forces, and drag. Molecular dynamics results show that NPM under the action of a B will be captured and attracted by it, so that they can be directed to the proposed target.

The reported results show that although there is no defined line of research on the use of np in Colombia, they nevertheless highlight the possibility of joining efforts to strengthen this field of knowledge.

VII. CONCLUSION

The np seen as drug nanocarriers play a leading role and it is in this direction in which research has been carried out, from this perspective to characterize the np and evaluate its evolution, it is identified that currently the work is focused on superparamagnetic np. The review carried out provides clarity regarding the evolution of np, as well as the importance of understanding how their kinematics are through the blood, seen as a biomagnetic fluid, a characteristic that has allowed the evaluation of strategies for directing nanoparticles that move through this medium, in this direction the main advances are associated with SPIONs for their biomedical application. There are many challenges from the treatment of diseases, starting from an accurate diagnosis to achieve an effective treatment, which involves a reduction of the adverse effects that these may have on the organism of the treated subject, in this sense the np offer a viable possibility both in diagnosis and therapy with low adverse effects, due to the possibility of targeting the treatment.

REFERENCES RÉFÉRENCES REFERENCIAS

1. Afkhami, S., & Renardy, Y. (2017). Ferrofluids and magnetically guided superparamagnetic particles in flows: a review of simulations and modeling. *Journal of Engineering Mathematics*, 107(1), 231–251. <https://doi.org/10.1007/s10665-017-9931-9>
2. Al-Jamal, K. T., Bai, J., Wang, J. T. W., Protti, A., Southern, P., Bogart, L., ... Pankhurst, Q. A. (2018). Magnetic Drug Targeting: Preclinical in Vivo Studies, Mathematical Modeling, and Extrapolation to Humans. *Nano Letters*, 16(9), 5652–5660. <https://doi.org/10.1021/acs.nanolett.6b02261>
3. Alexiou, C., Arnold, W., Klein, R. J., Parak, F. G., Hulin, P., Bergemann, C., ... Lubbe, A. S. (2000). Locoregional cancer treatment with magnetic drug targeting. *Cancer Research*, 60(23), 6641–6648.
4. Alexiou, Ch, Schmidt, A., Klein, R., Hulin, P., Bergemann, C., & Arnold, W. (2002). Magnetic drug targeting: Biodistribution and dependency on magnetic field strength. *Journal of Magnetism and Magnetic Materials*, 252(1-3 SPEC. ISS.), 363–366. [https://doi.org/10.1016/S0304-8853\(02\)00605-4](https://doi.org/10.1016/S0304-8853(02)00605-4)
5. Alfonso, B., & Casado, C. (2016). DENDRÍMEROS: MACROMOLÉCULAS VERSÁTILES CON INTERÉS INTERDISCIPLINAR. *Journal of Chemical Information and Modeling*, 01(01), 1689–1699.
6. Attar, M. M., Amanpour, S., Haghpanahi, M., Haddadi, M., Rezaei, G., Muhammadnejad, S., ... Javadi, S. (2016). Thermal analysis of magnetic nanoparticle in alternating magnetic field on human HCT-116 colon cancer cell line. *International Journal of Hyperthermia*, 32(8), 858–867. <https://doi.org/10.1080/02656736.2016.1204667>
7. Avilés, M. O., Ebner, A. D., Chen, H., Rosengart, A. J., Kaminski, M. D., & Ritter, J. A. (2005). Theoretical analysis of a transdermal ferromagnetic implant for retention of magnetic drug carrier particles. *Journal of Magnetism and Magnetic Materials*, 293(1), 605–615. <https://doi.org/10.1016/j.jmmm.2005.01.089>
8. Avval, Z. M., Malekpour, L., Raeisi, F., Babapoor, A., Mousavi, S. M., Hashemi, S. A., & Salari, M. (2020). Introduction of magnetic and supermagnetic nanoparticles in new approach of targeting drug delivery and cancer therapy application. *Drug Metabolism Reviews*, 52(1), 157–184. <https://doi.org/10.1080/03602532.2019.1697282>
9. Bartoszek, M., & Drzazga, Z. (1999).; *A study of magnetic anisotropy of blood cells*. 197, 573–575.
10. Bose, S., & Banerjee, M. (2015). Magnetic particle capture for biomagnetic fluid flow in stenosed aortic bifurcation considering particle-fluid coupling. *Journal of Magnetism and Magnetic Materials*, 385, 32–46. <https://doi.org/10.1016/j.jmmm.2015.02.060>
11. Chávez, F., Olvera, B. I., Ganem, A., & Quintanar, D. (2002). Liberación de sustancias lipofílicas a partir de nanocápsulas poliméricas. *Journal of the Mexican Chemical Society*, 46(4), 349–356.
12. Cicha, I., Lyer, S., Alexiou, C., & Garlich, C. D. (2013). Nanomedicine in diagnostics and therapy of cardiovascular diseases: Beyond atherosclerotic

- plaque imaging. *Nanotechnology Reviews*, 2(4), 449–472. <https://doi.org/10.1515/ntrev-2013-0009>
13. Duncan, G. A., & Bevan, M. A. (2015). Computational design of nanoparticle drug delivery systems for selective targeting. *Nanoscale*, 7(37), 15332–15340. <https://doi.org/10.1039/c5nr03691g>
 14. Eivazzadeh-Keihan, R., Radinekiyan, F., Maleki, A., Salimi Bani, M., Hajizadeh, Z., & Asgharnasl, S. (2019). A novel biocompatible core-shell magnetic nanocomposite based on cross-linked chitosan hydrogels for in vitro hyperthermia of cancer therapy. *International Journal of Biological Macromolecules*, 140, 407–414. <https://doi.org/10.1016/j.ijbiomac.2019.08.031>
 15. Gallo, J., & Ossa, C. (2019). Fabricación y caracterización de nanopartículas de plata con potencial uso en el tratamiento del cáncer de piel. *Ingeniería y Desarrollo*, 37(1), 88–104. <https://doi.org/10.14482/inde.37.1.6201>
 16. Gitter, K., & Odenbach, S. (2011). Experimental investigations on a branched tube model in magnetic drug targeting. *Journal of Magnetism and Magnetic Materials*, 323(10), 1413–1416. <https://doi.org/10.1016/j.jmmm.2010.11.061>
 17. Haik, Y., Pai, V., & Chen, C. J. (1999). Development of magnetic device for cell separation. *Journal of Magnetism and Magnetic Materials*, 194(1), 254–261. [https://doi.org/10.1016/S0304-8853\(98\)00559-9](https://doi.org/10.1016/S0304-8853(98)00559-9)
 18. Hajiaghajani, A., Hashemi, S., & Abdolali, A. (2017). Adaptable setups for magnetic drug targeting in human muscular arteries: Design and implementation. *Journal of Magnetism and Magnetic Materials*, 438, 173–180. <https://doi.org/10.1016/j.jmmm.2017.04.058>
 19. Haley, B., & Frenkel, E. (2008). Nanoparticles for drug delivery in cancer treatment. *Urologic Oncology: Seminars and Original Investigations*, 26(1), 57–64. <https://doi.org/10.1016/j.urolonc.2007.03.015>
 20. Jaimes, S., Gonzáles, A., Granados, C., Álvarez, D., & Espitia, E. (2012). Redalyc.Nanotecnología: avances y expectativas en cirugía. *Revista Colombiana de Cirugía*, 27, 158–166.
 21. Krukemeyer, M. G., Krenn, V., Jakobs, M., & Wagner, W. (2012). Mitoxantrone-iron oxide biodistribution in blood, tumor, spleen, and liver - Magnetic nanoparticles in cancer treatment. *Journal of Surgical Research*, 175(1), 35–43. <https://doi.org/10.1016/j.jss.2011.01.060>
 22. Lee, S. Y., Ferrari, M., & Decuzzi, P. (2009). Shaping nano-/micro-particles for enhanced vascular interaction in laminar flows. *Nanotechnology*, 20(49). <https://doi.org/10.1088/0957-4484/20/49/495101>
 23. Liu, H. D., Xu, W., Wang, S. G., & Ke, Z. J. (2008). Hydrodynamic modeling of ferrofluid flow in magnetic targeting drug delivery. *Applied Mathematics and Mechanics (English Edition)*, 29(10), 1341–1349. <https://doi.org/10.1007/s10483-008-1009-y>
 24. Liu, Zhu, Y., Rao, R. R., Clausen, J. R., & Aidun, C. K. (2018). Nanoparticle transport in cellular blood flow. *Computers and Fluids*, 172, 609–620. <https://doi.org/10.1016/j.compfluid.2018.03.022>
 25. Lübbe., Bergemann, C., Brock, J., & McClure, D. G. (1999). Physiological aspects in magnetic drug-targeting. *Journal of Magnetism and Magnetic Materials*, 194(1), 149–155. [https://doi.org/10.1016/S0304-8853\(98\)00574-5](https://doi.org/10.1016/S0304-8853(98)00574-5)
 26. Lübbe, A. S., Bergemann, C., Huhnt, W., Fricke, T., & Riess, H. (1996). *Lübbe1996_Preclinical*. 4694–4701.
 27. Lübbe, A. S., Bergemann, C., Riess, H., Schriever, F., Reichardt, P., Possinger, K., ... Huhn, D. (1996). Clinical experiences with magnetic drug targeting: A phase I study with 4'-epidoxorubicin in 14 patients with advanced solid tumors. *Cancer Research*, 56(20), 4686–4693.
 28. Méndez, B., & Muñoz, C. (2012). *Nanochips y nanosensores para el diagnóstico temprano de cáncer oral: una revisión*. (67), 131–147.
 29. Miller, M. E. (2018). *Human Diseases and Yeast*. Pdf (First edit). New York: Momentum Press Health.
 30. Mohammed, L., Gomaa, H. G., Ragab, D., & Zhu, J. (2017). Magnetic nanoparticles for environmental and biomedical applications: A review. *Particuology*, 30, 1–14. <https://doi.org/10.1016/j.partic.2016.06.001>
 31. Müller, K., Fedosov, D. A., & Gompper, G. (2014). Margination of micro- and nano-particles in blood flow and its effect on drug delivery. *Scientific Reports*, 4, 1–8. <https://doi.org/10.1038/srep04871>
 32. Nahrendorf, M., Zhang, H., Hembador, S., Panizzi, P., Sosnovik, D. E., Aikawa, E., ... Weissleder, R. (2008). Nanoparticle PET-CT imaging of macrophages in inflammatory atherosclerosis. *Circulation*, 117(3), 379–387. <https://doi.org/10.1161/CIRCULATIONAHA.107.741181>
 33. Nan, A., Suci, M., Ardelean, I., Şenilă, M., & Turcu, R. (2020). Characterization of the Nuclear Magnetic Resonance Relaxivity of Gadolinium Functionalized Magnetic Nanoparticles. *Analytical Letters*, 0(0), 1–16. <https://doi.org/10.1080/00032719.2020.1731522>
 34. Pantoja, J. (2020). *nanopartículas magnéticas en flujo sanguíneo para tratamiento de cáncer*. Universidad Distrital Francisco José de Caldas.
 35. Rodríguez, D., Moyano, J., & Roa, L. (2018). Estudio por dinámica molecular browniana de nanopartículas bajo efectos de campo magnéticos externos. *INGENIEROS MILITARES*, 13(9), 90–98.
 36. Rojas, Y., Aguado, K., & González, I. (2016). La nanomedicina y los sistemas de liberación de fármacos: ¿la revolución de la terapia contra el

- cáncer? *Educación Química*, 27 (4), 286–291. <https://doi.org/10.1016/j.eq.2016.07.002>
37. Rukshin, I., Mohrenweiser, J., Yue, P., & Afkhami, S. (2017). Modeling superparamagnetic particles in blood flow for applications in magnetic drug targeting. *Fluids*, 2(2), 1–12. <https://doi.org/10.3390/fluids2020029>
38. Shabestari Khiabani, S., Farshbaf, M., Akbarzadeh, A., & Davaran, S. (2017). Magnetic nanoparticles: preparation methods, applications in cancer diagnosis and cancer therapy. *Artificial Cells, Nanomedicine and Biotechnology*, 45(1), 6–17. <https://doi.org/10.3109/21691401.2016.1167704>
39. Sharma, V. R., Sharma, A. K., Punj, V., & Priya, P. (2019). Recent nanotechnological interventions targeting PI3K/Akt/mTOR pathway: A focus on breast cancer. *Seminars in Cancer Biology*, 59(July 2019), 133–146. <https://doi.org/10.1016/j.semcancer.2019.08.005>
40. Sosa, M., Alvarado, J. J. B., & Gonz, J. L. (2002). *Técnicas biomagnéticas y su comparación con los métodos bioeléctricos*. 48(5), 490–500.
41. Tong, S., Zhu, H., & Bao, G. (2019). Magnetic iron oxide nanoparticles for disease detection and therapy. *Materials Today*, 31(December), 86–99. <https://doi.org/10.1016/j.mattod.2019.06.003>
42. Urrejola, M. C., Soto, L. V., Zumarán, C. C., Peñaloza, J. P., Álvarez, B., Fuentesvilla, I., & Haidar, Z. S. (2018). Sistemas de Nanopartículas Poliméricas II: Estructura, Métodos de Elaboración, Características, Propiedades, Biofuncionalización y Tecnologías de Auto-Ensamblaje Capa por Capa (Layer-by-Layer Self-Assembly). *International Journal of Morphology*, 36(4), 1463–1471. <https://doi.org/10.4067/s0717-95022018000401463>
43. Wakaskar, R. R. (2018). General overview of lipid-polymer hybrid nanoparticles, dendrimers, micelles, liposomes, spongosomes and cubosomes. *Journal of Drug Targeting*, 26(4), 311–318. <https://doi.org/10.1080/1061186X.2017.1367006>
44. Zhang, G., Zhang, L., Si, Y., Li, Q., Xiao, J., Wang, B., Tian, G. (2020). Oxygen-enriched Fe₃O₄/Gd₂O₃ nanoporous for tumor-targeting MRI and ROS-triggered dual-modal cancer therapy through platinum (IV) prodrugs delivery. *Chemical Engineering Journal*, 388(February), 124269. <https://doi.org/10.1016/j.cej.2020.124269>



GLOBAL JOURNAL OF RESEARCHES IN ENGINEERING: J
GENERAL ENGINEERING
Volume 24 Issue 1 Version 1.0 Year 2024
Type: Double Blind Peer Reviewed International Research Journal
Publisher: Global Journals
Online ISSN: 2249-4596 & Print ISSN: 0975-5861

Effect of Interlayer Thickness on Mechanical Properties of Steel/Polymer/Steel Laminates Fabricated by Roll Bonding Technique

By Payam Maleki, Abbas Akbarzadeh & Mahdi Damghani

University of the West of England (UWE)

Abstract- Nowadays, metal/polymer/metal laminates are extensively used in various industries due to their unparalleled properties. In this study, the roll bonding process was employed for lamination of low carbon steel (St14) and semi-melted thermoplastic polyurethane sheets. The T-peel and Single Lap Shear (SLS) tests were conducted to determine the optimal rolling speed to achieve the highest bond strength between the polymer core and the steel skins. Then, with the goal of investigation of the effect of polymer volume fraction on the mechanical properties of laminates, the lamination process was performed at the optimal rolling speed and various thickness reductions. The uniaxial tensile tests were conducted at three directions of 0°, 45°, and 90° with respect to rolling direction for the skin sheet and four different laminates. The results of both T-peel and SLS tests recommend the lowest rolling speed (25 rpm) to acquire maximum bond strength. The results of tensile tests show that the mechanical properties of the laminates depend on the sample direction.

Keywords: metal/polymer/metal laminate sheet, roll bonding, thermoplastic polyurethane, low carbon steel sheet, mechanical properties.

GJRE-J Classification: LCC: TA401-492



EFFECT OF INTERLAYER THICKNESS ON MECHANICAL PROPERTIES OF STEEL/POLYMER/STEEL LAMINATES FABRICATED BY ROLL BONDING TECHNIQUE

Strictly as per the compliance and regulations of:



RESEARCH | DIVERSITY | ETHICS

© 2024. Payam Maleki, Abbas Akbarzadeh & Mahdi Damghani. This research/review article is distributed under the terms of the Attribution-NonCommercial-NoDerivatives 4.0 International (CC BY-NC-ND 4.0). You must give appropriate credit to authors and reference this article if parts of the article are reproduced in any manner. Applicable licensing terms are at <https://creativecommons.org/licenses/by-nc-nd/4.0/>.

Effect of Interlayer Thickness on Mechanical Properties of Steel/Polymer/Steel Laminates Fabricated by Roll Bonding Technique

Payam Maleki ^α, Abbas Akbarzadeh ^σ & Mahdi Damghani ^ρ

Abstract- Nowadays, metal/polymer/metal laminates are extensively used in various industries due to their unparalleled properties. In this study, the roll bonding process was employed for lamination of low carbon steel (St14) and semi-melted thermoplastic polyurethane sheets. The T-peel and Single Lap Shear (SLS) tests were conducted to determine the optimal rolling speed to achieve the highest bond strength between the polymer core and the steel skins. Then, with the goal of investigation of the effect of polymer volume fraction on the mechanical properties of laminates, the lamination process was performed at the optimal rolling speed and various thickness reductions. The uniaxial tensile tests were conducted at three directions of 0°, 45°, and 90° with respect to rolling direction for the skin sheet and four different laminates. The results of both T-peel and SLS tests recommend the lowest rolling speed (25 rpm) to acquire maximum bond strength. The results of tensile tests show that the mechanical properties of the laminates depend on the sample direction. It is also observed that as the volume fraction of the polymer in the laminate structure increases, the yield strength, tensile strength and elastic modulus decrease. The bond strength of the metal/ polymer interface is directly related to the ductility behavior of the laminates.

Keywords: metal/polymer/metal laminate sheet, roll bonding, thermoplastic polyurethane, low carbon steel sheet, mechanical properties.

I. INTRODUCTION

In recent years, there has been growing research in developing materials that are lightweight and have enhanced mechanical properties compared to traditional and conventional metallic structures such as aluminum, steel, titanium, etc. During the past decades, the widespread use of traditional metallic structures has led to an abundance of readily available design data supported by extensive and expensive experimental testing that makes designing and analyzing such structures safe and more convenient. For instance, the use of aluminum alloys for more than 70 years in the manufacture of aerostructures has led to a plethora of both available design data and past experiences. This makes it convenient and safe for designers and structural analysts to use such materials in the design of

aerostructures. Furthermore, the use of optimization techniques, i.e. topology, topography and size optimizations, has enabled structural designers and analysts to make metallic structures more lightweight. The use of modern manufacturing techniques such as Additive Layer Manufacturing (ALM) for metals has also contributed to making components that are lightweight. Whilst these approaches in design and manufacture are valid for single purpose structures, i.e. to be load bearing only, they are not suitable for when the structure has to be multi-functional. For instance, the metallic structures may exhibit desirable structural stiffness and strength but are not well suited for applications where high comparable specific stiffness and strength, improved isolation, superior vibration and sound damping properties and improved ductility are required [1]. Hence, scientists have resorted to alternative material systems and manufacturing methods. Amongst such material systems, hybridization has the potential to provide an economical mean [2], [3] to create material systems that can combine the advantages of miscellaneous materials, i.e. low density, high bending resistance, energy absorption, high load-capacity at low weight and etc., with each other and yield a material system that exploits the advantage of each constituent material meeting the required functions of a structure.

Amongst hybrid structures, three-layered metal/polymer/metal or multi-layer sheets, offer a great potential for the automotive, construction, naval industries and aerostructures. For instance, GLARE, a combination of aluminum layers and a Glass Fiber Reinforced Polymer (GFRP) has been applied in the construction of Airbus A380 double decker aircraft [1]. Another example is the use of Aramid Reinforced ALuminum Laminate (ARALL) for a damage tolerant wing design particularly areas prone to the fatigue loading [4]. It is worth noting that for newly adapted lightweight material systems, such as hybrid structures of metals-polymers, future gains are obtained with respect to environmental protection and sustainability. Metal/polymer/metal laminates as hybrid materials are also an alternative to homogeneous metal sheets that have polymeric properties as well as metallic characteristics. Good formability, excellent mechanical properties, lightweight, and acoustic and vibration

Author α σ: Department of Materials Science and Engineering, Sharif University of Technology, Tehran, Iran.

Author ρ: Department of Engineering, Design and Mathematics (EDM), University of the West of England (UWE), Bristol, UK.
e-mail: mahdi.damghani@uwe.ac.uk

damping are the three-layer sheets characteristics. The usage of these sheets is common in various industries.

Three-layered examples of metal/polymer/metal composites such as HYLITE have been used in automotive industry, due to their high mechanical and formability properties and being lightweight [5]. HYLITE is an aluminum/polypropylene/aluminum with thicknesses $0.2/0.8/0.2\text{mm}$ which was used in the construction of Audi A2. Another example is the use of BONDAL, a steel/polypropylene/steel composite known as steel counterpart to HYLITE, with a polymer core having approximate thickness of $50\ \mu\text{m}$. BONDAL has layer thicknesses of $0.5/0.5/0.5\ \text{mm}$ and is used for damping applications such as reducing radiating construction noise. It is worth noting that such composite material systems are being used in the aerospace industry as a result of their excellent compressive strength, high corrosion resistance, high toughness and workability. Furthermore, these sheets are currently being used in home appliances such as dishwashers and lawnmowers, where vibration and sound damping are crucial. Depending on the application of three-layer sandwich sheets in the industry, the ratio of the metal skin thickness to the polymer core, the type of metal and polymer, and the manufacturing and bonding of three-layer sheets are different.

Kim et al. [6] classified metal/polymer/metal three-layer laminates into three categories:

- Laminates with low-density polymeric core, containing 40% to 60% of the total thickness (lightweight).
- Laminates with thin polymeric core, containing 20% of the total thickness (acoustic damper).
- Laminates with very thin polymeric core (or without core) where the thickness and nature of the skins can be different (to take advantage of the different properties of both layers).

The three-layer composites metal skins mostly consist of steel sheets (often stainless steel) [7] or aluminum alloys such as AA5052 [8], AA5754 [9], and AA5182 [10] with different thicknesses. The most important criteria for selecting steel and aluminum sheets are high mechanical and formability properties [11], flexural stiffness, corrosion resistance, joinability, dent resistance, [12] and cost reduction [13]. Considering the superior inherent formability of the steel compared to aluminum, three-layer steel/polymer/steel sheets offer a higher stiffness-to-weight ratio than aluminum and steel monolithic sheets. In the assortment made by Hayashi et al. [14], specifically for laminated steel sheets, these laminates are divided into two categories; (i) vibration-damping sheets, i.e. with thickness composition of core = $0.03\ \text{mm} - 0.1\ \text{mm}$ and skin = $0.15\ \text{mm} - 1.6\ \text{mm}$, and (ii) lightweight laminate sheets, i.e. with thickness composition of core

= $0.2\ \text{mm} - 1\ \text{mm}$ and skin = $0.1\ \text{mm} - 0.4\ \text{mm}$. Moreover, there are a variety of polymers to be selected as the middle layer. Polypropylene [10], polyethylene [15], polyolefin (PP-PE) [7], and polyamide [16] are the most popular polymers used in three-layer laminates. The chief reasons for choosing these polymers are low density, good mechanical properties, good chemical stability, low cost, and high-temperature resistance [12]. These polymers usually have low wettability and bondability in contact with other surfaces due to their low-polarity behavior. Therefore, various adhesive films are used to attach the polymer core to metal adherends. Common adhesives used in the manufacturing of three-layer laminates are hot-melt polyethylene adhesive film [8], maleic polyethylene adhesive film [9], Ethylene-Vinyl Acetate (EVA) film [10], epoxy resin (koratac FL 201) [17] and Polypropylene Grafted Maleic Anhydride (PP-G-MA) thin film [18]. Due to the indirect bonding of the metal to the polymer and the presence of an additional layer and subsequently the dependence of metal/polymer interface strength on adhesive strength, and considering the subsequent mechanical and metallurgical processes, appropriate selection of the adhesive is crucial. In some studies, adhesives have been used directly as an intermediate layer (without the polymer core) between two metals [13]. The results show that the presence of adhesive between the two steel layers, while improving the laminate elongation, and delaying the necking, increases the formability of the three-layer sheet compared to the two-layer sheet without the adhesive. Adhesive bonding (manual lamination) [19], hot [17] and cold roll bonding [20], and hot pressing [9] are well-known processes in the production of metal/polymer/metal laminates. Carrado et al. [1], by comparing the roll bonded and hot-press bonded specimens of the same thickness, showed that the initial crack strength of the rolled sheet was higher than that of the hot-pressed sheet. Kazemi et al. [9] applied three-point bending test on the aluminum/polyurethan/aluminum three-layer sheet produced by the hot-pressing method. They related the debonding observed in the interface of aluminum/polyethylene to the creation, growth, and connection of micro-voids formed on the polymer surface during the hot pressing. The thickness and physical and mechanical properties of the polymer core and the bond strength affect the mechanical properties, formability, paintability, and weldability of the three-layer laminates sheet. Harhash et al. [7] reported the decrease in density and subsequently weight-saving as a positive and decrease in tensile and yield strength as an adverse effect of increasing the volume fraction of the polymer in the three-layer composite sheets (constant skins thickness). The importance of the polymeric layer shear strength is revealed where the shear force generated between the skin layers during the various forming processes (bending, drawing, etc.) overcomes the shear strength

of the polymer and interfacial delamination occurs. It was observed that weak polymer core causes skin sheets to slide on the other layer (lubricant-like behavior), resulting in a premature splitting [21]. By investigating the deep drawing process of the three-layer sheets with different polymer cores, Liu et al. [15] showed that the drawability of three-layer sheets becomes poor as the thickness and strength of the polymeric core increase. Kim et al. [10] attributed the improvement in the formability of the three-layer sheets to the high elongation of the polymer core and the high bond strength of the metal/polymer interface. It is demonstrated that for two laminate sheets of the same thickness and steel skins, the sheet with polypropylene core shows lower springback than the laminate with the Poly Vinyl Chloride (PVC) core [22]. This is attributed to higher strength of the PVC sheet compared to the polypropylene sheet. Since three-layer sheets in the car body are placed in the paint bath (temperature of 200°C for 30 minutes) after the forming stage, the polymeric core must have a melting temperature of more than 200°C to maintain its structure [23]. If the melting temperature of the polymer is less than the painting temperature, the polymer melts, and the flow of the polymer disturbs the structure of the part, and the paint bath becomes contaminated. Saito et al. [24] and Oberle et al. [25] in two separate investigations demonstrated that, since during spot welding process, the polymer core is heated and pressurized by the welding electrode, to improve the weldability of the three-layer sheet and the formation of an ideal weld, the polymer core must flow away from the welded area. As such, the flow properties of the polymeric core should be optimal so that the delamination does not occur in the composite during the welding and painting processes. Studies have shown that the surface treatment of the skin metal sheet such as corona treatment [1] and preheating plus wire brushing [26] effectively improves the surface energy and wettability and produces more contact surfaces. This leads to the enhancement of shear strength and formability of the three-layer sheet.

It is evident from the literature that the manufacture of multilayer composites is challenging because of significant differences in the mechanical properties and adhesion characteristics of polymeric core and metallic face sheets. This unique combination of materials requires advanced joining techniques to ensure a strong bond between the joining layers. Thus far, few studies have been carried out to consider the impact of fabrication methods, core volume fraction and orientation of Steel/Polymer/Steel (S/P/S) laminate sheets on its overall mechanical properties. Subsequently, considering that many parameters are involved in the manufacture and the final properties of this type of composite material systems, an exact evaluation is necessary to identify and achieve the

mechanical properties of the composite for each specific application.

The present study holds significant implications for the field of metal/polymer composites and endeavors to bridge the gap in knowledge. It also contributes to advancing the understanding of the direct roll bonding process and provides valuable insights for further optimizing the fabrication process, leading to the development of novel S/P/S composites with improved performance for various applications in automotive, aerospace, and structural engineering.

Thus, in this research, S/P/S laminates are manufactured by the roll-bonding process, without the use of adhesives (or reinforcements) and heated rollers (section 2). The authors attempt to achieve optimal mechanical properties. Three variables are considered:

- The polymer layer thickness (volume fraction of the core material)
- The rolling speed
- The rolling direction

Single Lap Shear (SLS) and T-peel tests were carried out to obtain the best rolling speed value for fabrication of four different laminate thicknesses by comparing the results of shear and bond strength, respectively. The effect(s) of the core volume fraction and rolling direction on the mechanical properties of the S/P/S sheet was studied by performing the uniaxial tensile test. The results were analyzed by examining the obtained data and the Scanning Electron Microscope (SEM) and are presented in section 3. Finally, the findings of the present work are concluded in section 4.

II. METHODOLOGY

a) *Laminate Manufacturing*

The Aluminum Killed (AK) low carbon steel St14 having 0.45 mm thickness was selected as the face sheet of the S/P/S laminate due to its good mechanical properties and excellent formability and weldability. The chemical composition of the St14 steel sheet is illustrated in Table 1. Furthermore, a Thermoplastic Polyurethane (TPU) sheet with an initial thickness of 2 mm was employed as the middle layer (core) of the three-layer sandwich sheet. Selection of the TPU sheet was due to its remarkable tensile and tear strengths, exceptional impact resistance, high chemical and corrosion resistance, excellent ductility over a vast temperature range, low weight and cost, and ultra-high adhesion with various surfaces [27]. Due to the importance of the working temperature of thermo-mechanical processes and changes in the polymer behavior at different temperatures, it is essential to know the rheology of the polymer. Thus, the Differential Scanning Calorimetry (DSC) analysis was performed on the TPU to determine the working temperature. The DSC curve of the TPU shows an endothermic peak at 226°C associated with the melting temperature (T_m), as shown

in Figure 1. The DSC curve of the TPU usually shows two glass transitions at -40°C and 95°C related to the soft and hard segments (T_g^{SS} and T_g^{HS}), respectively [10],

[22], [28]. Accordingly, the working temperature of this study was chosen between the highest glass transition (T_g^{HS}) and the melting temperature (T_m).

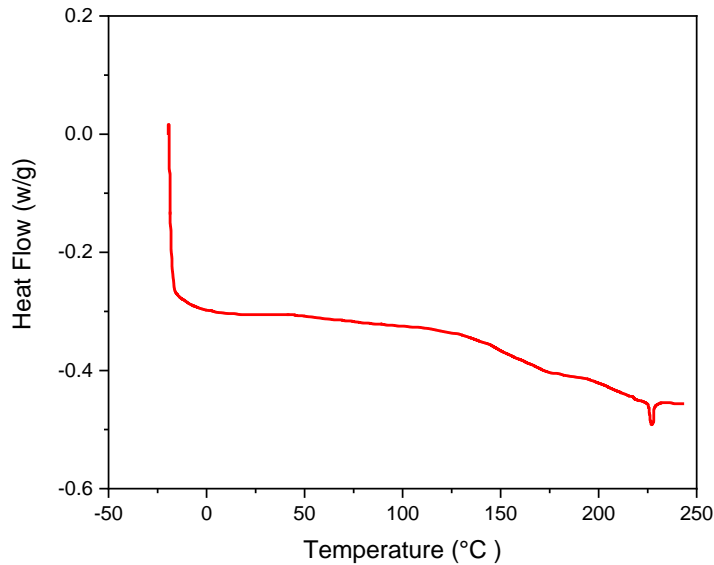


Figure 1: DSC curve of the TPU

Table 1: Chemical composition of the steel sheet

Fe	C *	Si	P	S	Cr	Ni	Mn	Mo	Al
Base	0.090	0.020	0.010	0.005	0.012	0.030	0.300	0.030	0.040

* numbers are in %

The three-layer S/P/S laminates were manufactured by the roll bonding process, without any adhesive or reinforcement. The following steps were conducted in hierarchal order:

- I. To increase the adhesion strength, the inner surfaces of both skin steel sheets were roughened in the rolling direction of sheet using stainless steel wire brush. Surface roughness was perfectly uniform and was measured by the Pocket-Surf®III roughness measuring mobile instrument after each brushing step. Post brushing, the average surface roughness of the St14 sheet was $R_a = 3.63 \mu\text{m}$. The optical graph of the brushed steel surface is shown in Figure 2.
- II. The contact surfaces (brushed side) of the two skin sheets and both sides of the TPU sheet were washed with acetone. The surfaces were air-dried to remove the surface contaminants and improve the quality of the bond.
- III. The TPU sheet was sandwiched between the two skin face sheets. The four corners of the laminated sheet were punched to prevent slipping of the layers during the process.

IV. The unbonded laminate was placed at 200°C fixed temperature oven for 5 minutes. The goal was to semi-melt the polymer to ease penetration of the rough surfaces into TPU surfaces leading to enhancement of the bond strength.

V. The sample was rolled immediately after removal from the oven to achieve the desired thickness. Considering the thickness of the unbonded laminate (2.9 mm), the three-layer laminates were fabricated at three rolling speeds and four rolling thickness reductions. The naming of test laminates was based on corresponding rolling speeds and thickness reductions, respectively (see Table 2). The cross-sectional view of four laminates with various thicknesses is presented in Figure 3.

b) Evaluation of the Mechanical Properties of the Base Sheets

To investigate the mechanical properties of metal and polymer sheets and compare them with different laminates, the uniaxial tensile test specimens were prepared according to ASTM E8/E8M and ASTM D638 (type IV) standards for steel and polymer sheets, respectively. Tensile tests of the steel sheet specimens along the rolling (RD), diagonal (DD), and transverse

(TD) directions, were conducted by the Hounsfield H10NKS machine with the test speed of 1 mm/min . The mechanical behavior of the TPU sheet was also obtained by the same machine with the test speed of 50 mm/min . Repeatability of the results was assured by performing at least three tensile tests for each condition.

Due to the importance of the polymer tear strength under tension and shear conditions, the tear strength test was conducted on the TPU sheet according to ASTM D624-00 (type C) standard and with the crosshead speed of 50 mm/min . It is worth noting that all tests were performed at room temperature.

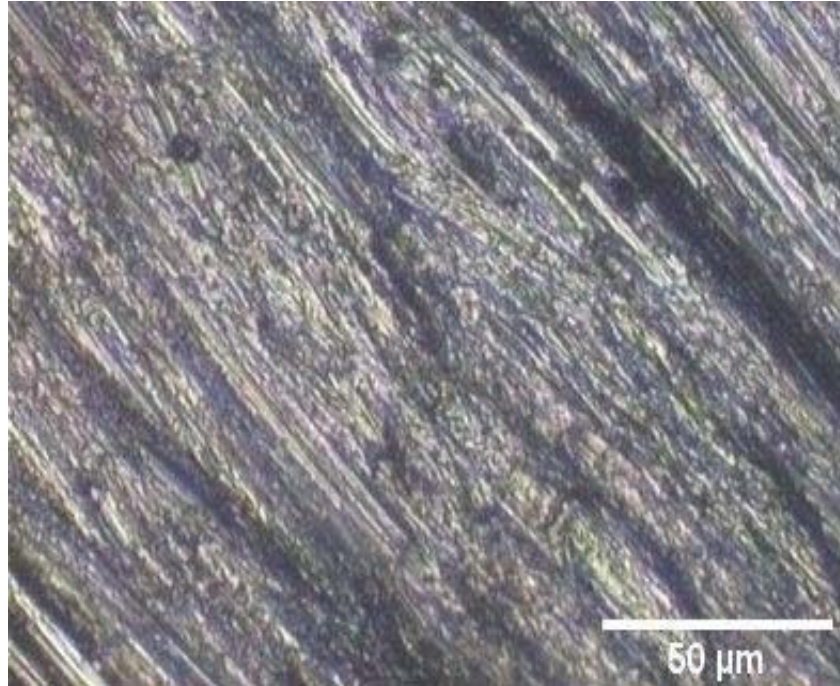


Figure 2: The optical micrograph of the roughened surface

Table 2: The laminates parameters and naming

Thickness Reduction (%)	Total Thickness (mm)	Core Volume Fraction (%)	Rolling Speed (rpm)		
			25	35	40
			Laminate Naming		
30	2.03	55.6	L-25-30	L-35-30	L-40-30
40	1.74	48.2	L-25-40	L-35-40	L-40-40
50	1.45	37.6	L-25-50	L-35-50	L-40-50
60	1.16	22.4	L-25-60	L-35-60	L-40-60

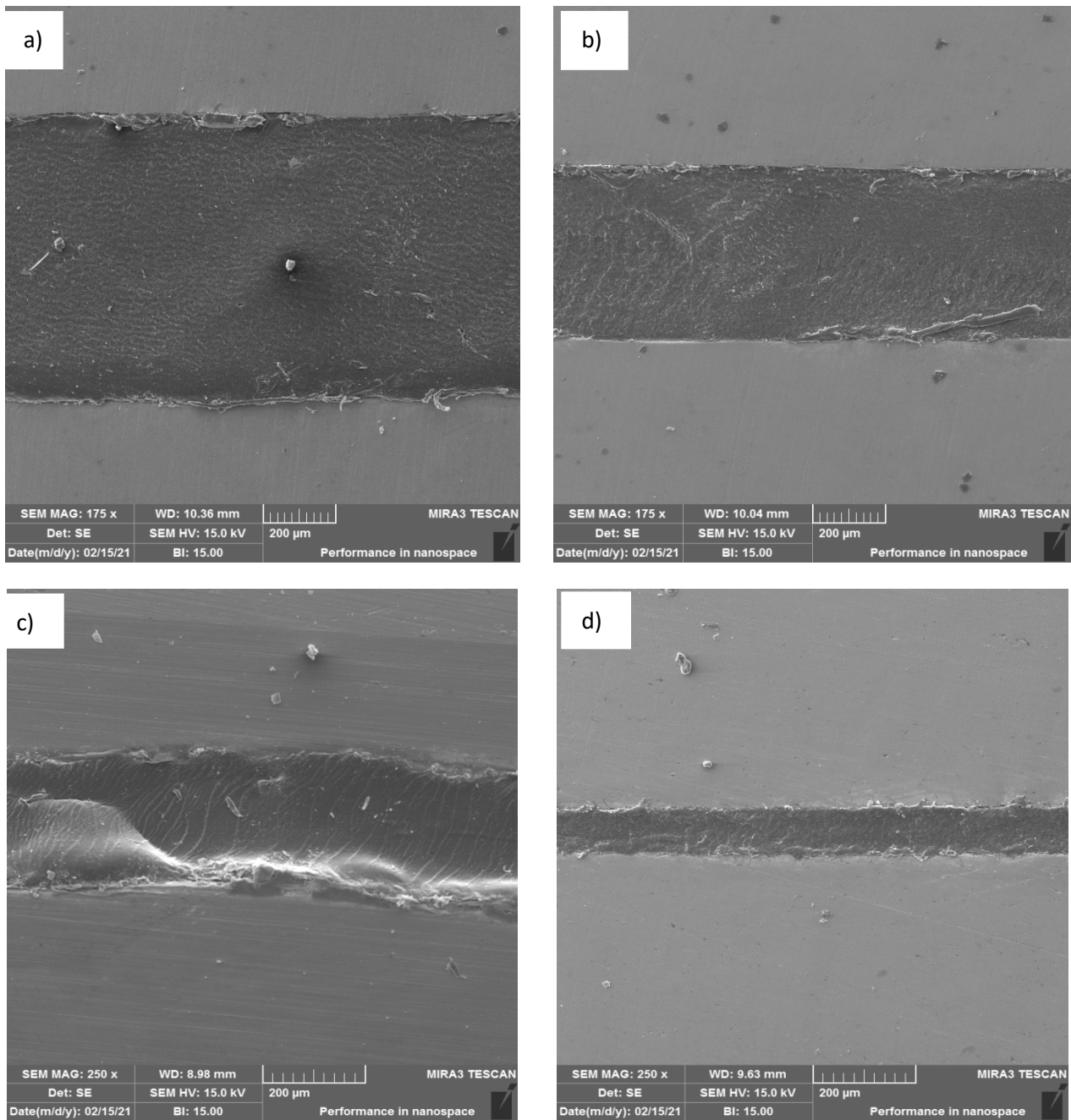


Figure 3: Cross sectional view of various laminates; (a) 30%, (b) 40%, (c) 50%, and (d) 60% thickness reduction

c) Rolling Speed Characterization

The optimal rolling speed is a key factor that has a significant impact on both the interfacial strength and fabrication of the three-layer laminates. Moreover, It can influence the mechanical and physical properties [29]. To determine the optimum rolling speed, bonding evaluation tests were carried out [30]. To evaluate the bond strength at skin-core interface of the different laminates under normal loading conditions, the T-peel and SLS tests were used. The T-peel test was performed according to the ASTM D1876-08 with the test speed of 20 mm/min. On the other hand, the SLS test was conducted according to ASTM D-3165-07 with

the crosshead speed of 1 mm/min to reflect the shear mechanical properties of the polymer layer. Figure 4 shows the geometric parameters of the T-peel and Lap-shear specimens. The size of specimens was modified in the small range. Due to the sensitivity of the results of these two tests and aiming to assure the accuracy of the results, the tests were repeated five times for each sample and the average values are reported.

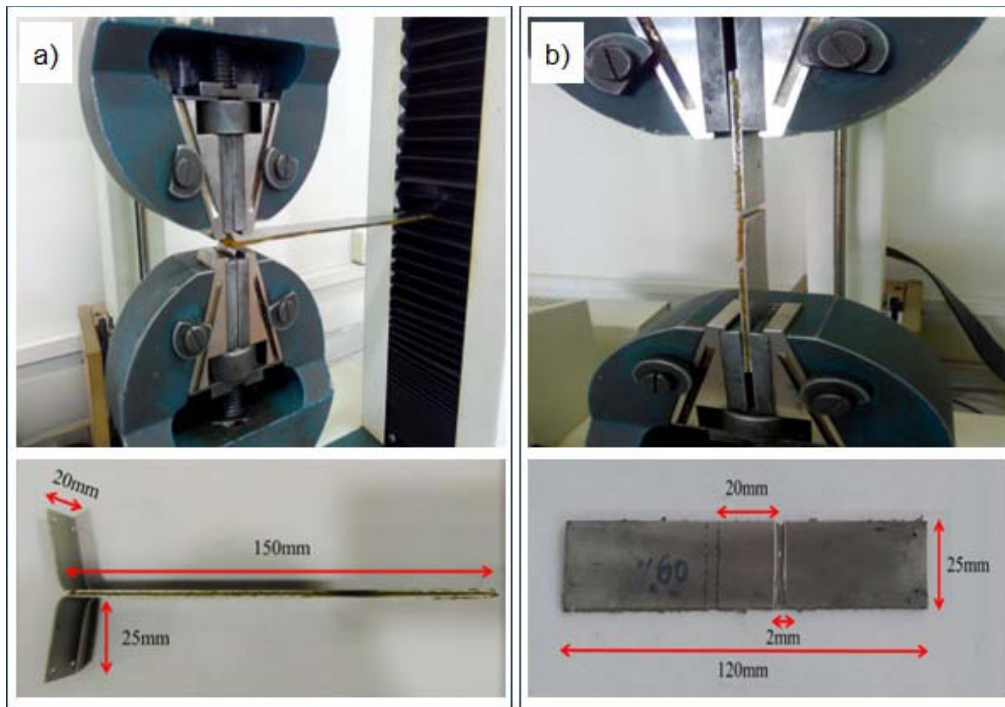


Figure 4: Experimental test set up and size of specimens for a) T-peel test and b) Single Lap Shear (SLS) test

d) *Characterization of the Mechanical Properties of the Laminates*

To study the impact of the core volume fraction and rolling direction on mechanical properties of three-layer laminates and its comparison with the monolithic steel sheet, the uniaxial tensile test was designed at three directions (RD, DD, and TD). To that end, the ASTM E8/E8M standard test method and constant crosshead speeds of 1 mm/min were chosen. Repeatability of the results was assured by performing at least three tensile tests for each direction, i.e. a total of 9 tensile tests.

e) *Analysis of the Results*

Due to thickness reduction of the polymeric core during the thermomechanical process and its impact on polymer microstructure, the density of different laminates may be different. Therefore, this property was experimentally investigated using a measuring cylinder and laboratory digital scale.

The experimental results were compared with those predicted using the rule of mixture for laminates [31]:

$$P_{SMS} = P_{Skin} \times V_{Skin} + P_{Core} \times V_{Core} \quad (1)$$

where P_{SMS} is the specific property of the laminate sheet, P_{Skin} and P_{Core} are that property for the skin sheet and polymeric core, respectively. V_{Skin} and V_{Core} are volume fractions of the skin sheet and polymeric core, respectively.

The bonding interface of the St14/TPU/St14 laminate sheet was investigated by using the Scanning Electron Microscope (SEM). Furthermore, the SEM was

utilized to examine the fracture surface of the specimens after performing the T-peel and SLS tests.

III. RESULTS AND DISCUSSIONS

a) *Mechanical Properties of the Core Sheet*

Since the mechanical properties of the core and the skin face sheets control the mechanical properties of three-layer laminates, a precise study of their mechanical behavior is required. Figure 5 shows the typical true strain-stress curve of the 2 mm thick TPU sheet.

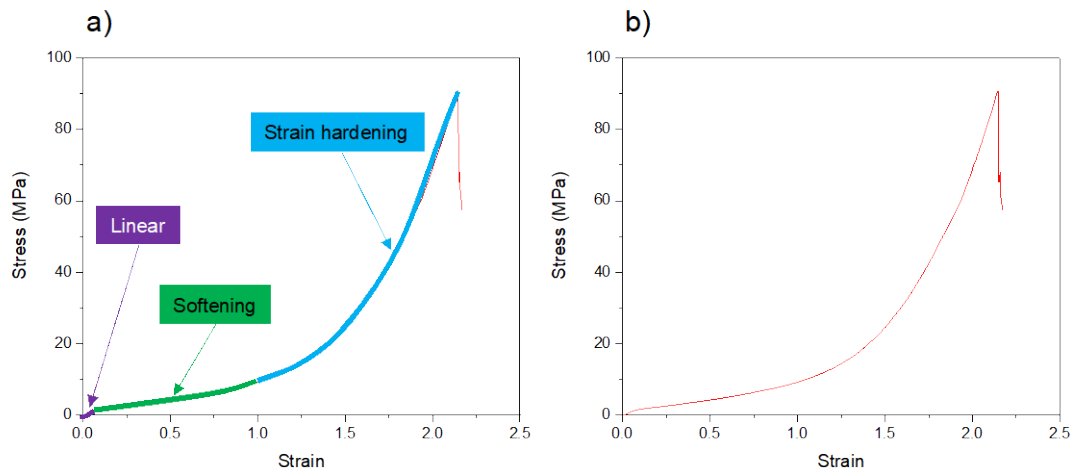


Figure 5: Stress-strain curve of the TPU sheet, a) characteristic areas of the graph, b) true stress-strain curve

The stress-strain behavior of the TPU is divided into three stages [32] as shown in Figure 5a. For the small strains, the curve is almost linear (purple region), and the specimen exhibits relatively stiff behavior. Material softening is the second phenomenon at the medium strain level (green region), and finally, strain hardening evolves progressively due to the strain-induced crystallization phenomenon at the largest strain (blue region). The combination of these three stages leads to the high strength of the polymer while maintaining considerably large elongation up to the point of failure.

The possibility of cutting, necking, and rupturing of the polyurethane sheet under tension or shear loading, increases the importance of the tear strength. The load-extension curve obtained from the tear test which is performed according to ASTM D-624-00 (Type C) is shown in Figure 6.

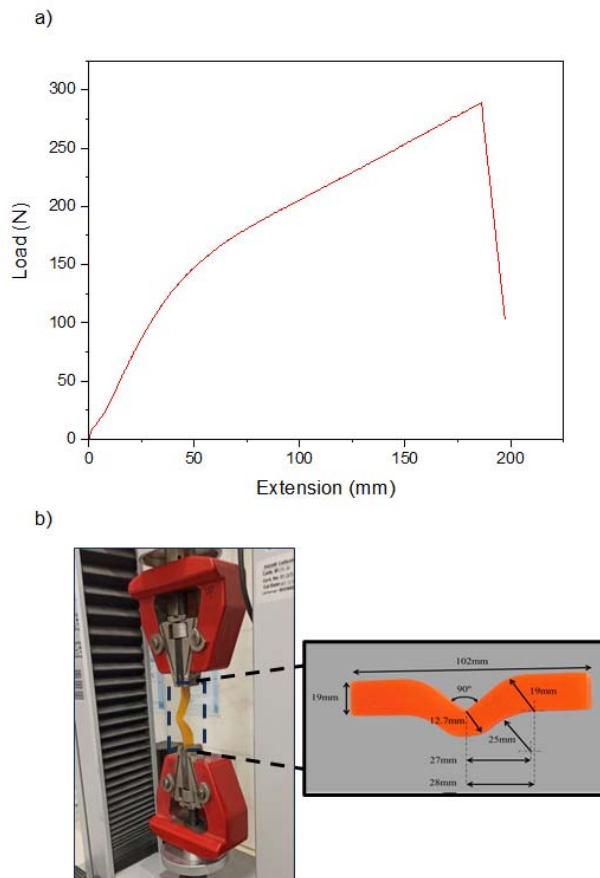


Figure 6: Illustration of tear test set up, a) Tear strength curve of the polymeric sheet, b) the experimental setup, and c) Dimensions of the sample based on ASTM D-624 (type C)

The change in the slope of the curve in the 50 mm extension is due to the change of loading conditions in the torn region of the test specimen. Tear strength of the TPU sheet is defined as the ratio of maximum load (286 N) at fracture point (≈ 186 mm extension) to the thickness of the specimen (2 mm). Therefore, the tear strength of ≈ 143 N/mm indicates high resistance of the TPU sheet to local deformation, and the extended tearing time (≈ 223 seconds) proves their superior level of stretchability, and excellent elongation.

b) *The Optimum Rolling Speed of S/P/S Laminate*

T-peel and SLS tests were performed on different laminates to determine the optimal rolling

speed. T-peel test and SLS test data reflect the normal and shear mechanical properties of the laminates, respectively. Hence, by evaluating and comparing the results of these tests, it is possible to determine the optimal rolling speed for fabricating the maximum-bond-strength laminates for further experiments. The typical load-extension curves resulted from the T-peel and the SLS tests are illustrated in Figure 7.

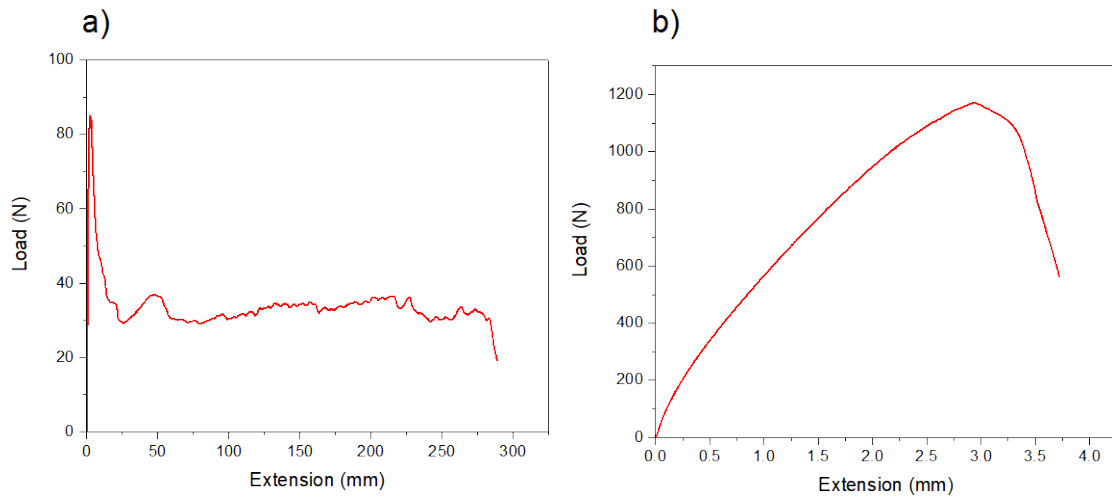


Figure 7: Load versus extension of, a) a T-peel test and b) SLS test

The Average Peel Strength (APS) can be calculated by [26]:

$$APS = \frac{\text{average load (N)}}{\text{bondwidth (mm)}} \quad (2)$$

where the average load is the average stable peel force after the first peak load.

Figure 8 shows the average peel strength at three various rolling speeds for four different laminates. Based on the figure, the bond strength decreases with increasing the rolling speed. The high bond strength at low rolling speed can be related to the longer time that the sample passes through the rollers. In general, in the rolling process of metallic sheets and composites which consists of two or more metallic sheets, the rolling speed before and after rolling (at the entrance and exit points) is not equal due to the occurrence of thickness reduction in the samples. In S/P/S laminates due to the fact that thickness reduction is only on the semi-melted polymer layer and the steel sheets pass through the rollers without any reduction in thickness, it can be assumed that in the rolling process of S/P/S laminates, the initial and final velocity of the rollers is equal.

Therefore, by converting the angular rolling speed to linear speed, it is possible to obtain the time that the samples pass through the rollers.



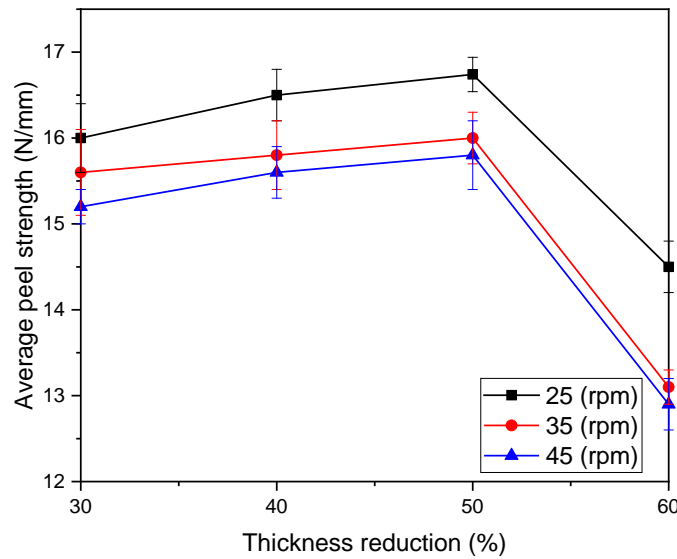


Figure 8: Comparison of the average peel strength at three various rolling speeds for four different laminate

The passage time is calculated by the following equation:

$$T = L \times 60 / V \times P \quad (3)$$

Where T represents the passage time (s), L is the sample length (mm), V is the angular rolling speed (rpm), and P is the roller perimeter. Figure 9 illustrates the schematic view of the roll bonding process of S/P/S laminates including these parameters.

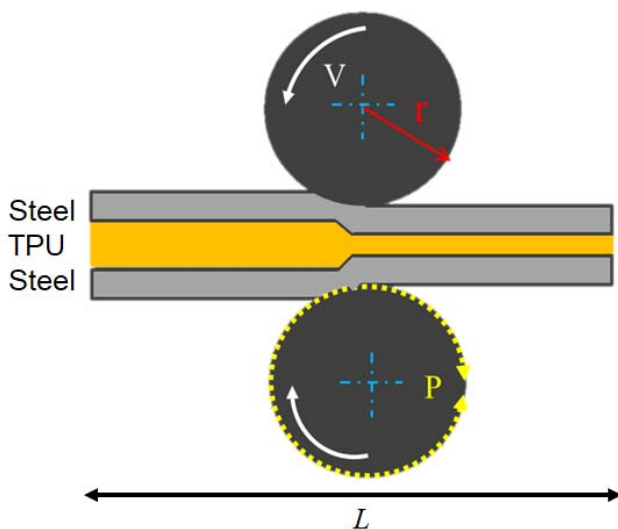


Figure 9: Schematic illustration of the roll bonding process

Therefore, the passage time of a 15 cm long T-peel sample between two rollers with a diameter of 15 cm at rolling speeds of 25, 35 and 45 rpm is 0.76,

0.54, and 0.42 seconds, respectively. This longer passage time guarantees uniform flow of the semi-melted polymer in the rolling direction between the two face sheets. Additionally, the low rolling speed prevents displacement and unwanted sliding of the two face sheets relative to each other and ensures the structural integrity of the laminates. Any sliding and movement of the face sheets relative to each other, which is probable at higher rolling speeds, can prevent the smooth flowing of the semi-melted polymer between them leading to formation of the cavities resulting in weakening of the bond strength. Therefore, the coincidence of brushed surfaces in rolling direction provides ducts for polymer flow in the same direction. This results in more engagement between the polymer and the roughened surfaces of the steel sheets. Consequently, this leads to improvement of the bond strength and minimizes the risk of delamination or separation. Andani et al. [33] have reported that the probability of formation of cavities at metal-polymer interface is higher as the semi-melted polymer flowed outside the laminate structure resulting in decreasing the bond strength. These cavities were formed in samples that were wire brushed first in the rolling direction and then perpendicular to the rolling direction. Therefore, it can be concluded that the smooth flow of the polymer in one direction can prevent the formation of these cavities and promote the cohesion of the bond.

At the exit of the rolling machine, the final temperature of the laminates that rolled at high rolling speed is higher than that of those rolled at low rolling speed. This is due to the short contact time of the preheated sample with the cold rollers. This

phenomenon elevates the potential of the generation of interlayer cavities by giving the warm polymer adequate time to undergo a gradual cooling process without the presence of external pressure. Andani et al. [33] demonstrated that at high rolling speed, the high temperature of the sample causes the polymer to become excessively soft, and the removal of the polymer from the sandwich structure is easier. Thus, there is not enough time for the polymer to penetrate the roughened surfaces, and consequently the bond strength decreases.

Furthermore, as Abbasi and Toroghinejad [34] observed, higher rolling speeds lead to shorter bond times to effectively apply pressure on the rolled sheets resulting in a sharp decrease in the adhesion strength. Thus, as the rolling speed decreases, the contact time

increases. Increasing the effective pressure of the rollers which is obtained by lowering the rolling speed, facilitates the squeezing, extruding, and penetrating of the semi-melt polyurethane into the brushed surface of skin sheets resulting in effective integration and generation of more mechanical interlocks.

Observation of the T-peel specimens after performing the test revealed both cohesive failure (fracture within the polymeric core) and adhesive failure (fracture along the interface between the polymeric core and skin sheets) modes. Samples with cohesive failure were associated to the result of optimum thickness reduction and low rolling speed, whereas the samples having adhesive failure were the result of suboptimal thickness reduction and high rolling speed (Figure 10).

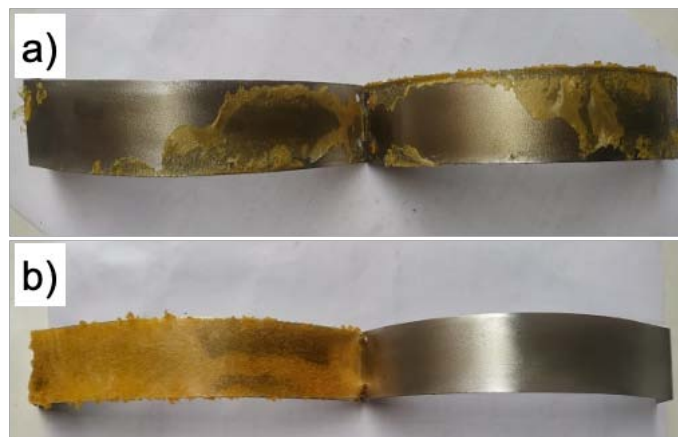


Figure 10: Failure of specimens after T-peel test, a) cohesive failure and (b) adhesive failure

Figure 11 shows the shear strength of S/P/S laminate for various thickness reductions. In this graph, the shear stress is calculated as:

$$\tau = F_{max} / A \quad (4)$$

Where F_{max} and A are the maximum load and the overlap area (400 mm^2), respectively. As shown in Figure 11, increase in rolling speed leads to reduction in shear strength. Moreover, for all rolling speeds, as the thickness of S/P/S laminates decreases (up to 50% thickness reduction), the single lap shear strength increases. This is attributed to the fact that thinner laminates have smaller load eccentricity. As such, joint bending moment caused by load eccentricity decreases leading to less peel stress at steel-polymer interface. It can be inferred that in S/P/S laminates, the volume fraction of micro pores and cavities and interfacial toughening, contribute to the resistance of the metal-polymer interface against crack initiation and propagation. In laminates with a high polymer volume fraction, the larger volume of micro pores and cavities within the polymer structure surpasses the benefits of interfacial toughening, subsequently reducing the resistance of the metal-polymer interface to crack

propagation. Conversely, in laminates with a low volume fraction of core material, although the volume of micro pores and cavities in the polymer structure is smaller, interfacial toughening is minimal, resulting in easier crack propagation. Therefore, achieving the highest level of crack resistance at metal-polymer interface requires optimizing both the volume fraction of micro-pores and the degree of interfacial toughening. Additionally, the optimum thickness of the core acts as a stress-absorbing element, effectively preventing crack initiation and arresting crack propagation at the interface, thereby improving the overall shear strength of the laminate. It is worth noting that laminates with 50% thickness reduction showed higher normal strength in T-peel test (see Figure 8). Hence, it could be inferred that, by striking a balance between interfacial toughening and the volume fraction of micro-cavities, laminates with a 50% thickness reduction exhibit the highest shear strength.

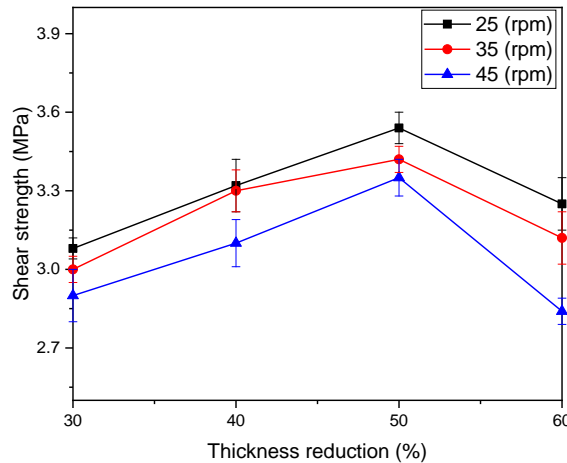


Figure 11: Comparison of the shear strength at three various rolling speeds for four different laminates

Figure 12 shows the fracture surfaces of the two SLS test specimens at the same thickness reduction (40%) at two rolling speeds of 25 rpm and 45 rpm. The magnitude of effective pressure applied to the specimen controls the volume fraction of the micro-cavities at the metal-polymer interface. It is suspected that there is an inverse correlation between the volume fraction of the micro-cavities at the metal-polymer interface and the effective contact surface and subsequently the bond

strength of the laminates. In other words, the higher metal-polymer interfacial volume fraction leads to low bond strength due to lower effective contact surface. Furthermore, lower rolling speeds are accompanied by higher effective pressure on the specimens, better penetration of the polymer to the rough surfaces of the skins, and thus reduction in volume fraction of the metal-polymer interfacial micro-cavities.

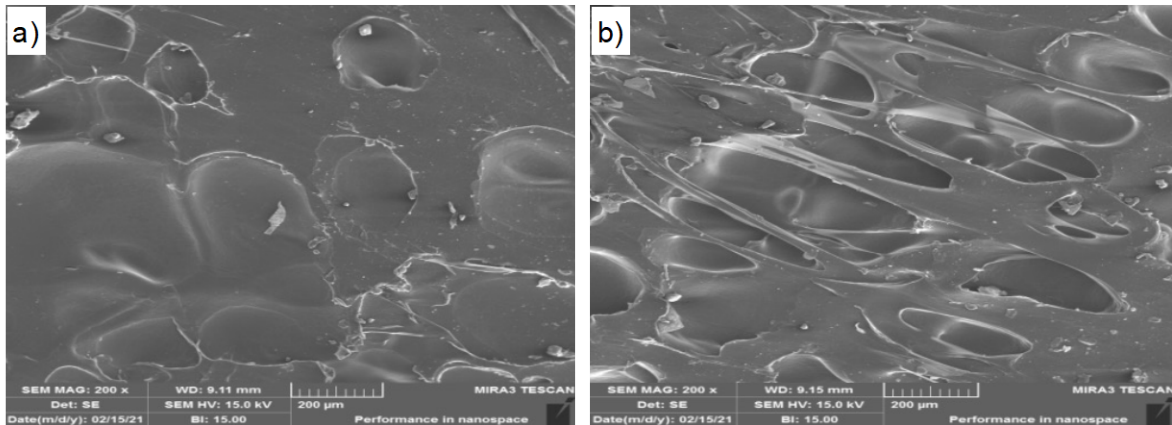


Figure 12: Fracture surfaces of the single lap shear specimens fabricated at rolling speed of: a) 25 rpm and b) 45 rpm

c) Mechanical Properties of the Laminate and Monolithic Steel Sheet

In this section, the effects of sample direction and volume fraction on the mechanical properties of laminates are discussed. The results provided hereafter are for steel sheet and four different laminates fabricated at optimum rolling speed of 25 rpm in three directions with respect to the rolling direction.

i. Effect of the Sample Direction

Figure 13 compares the typical stress-strain curve of both monolithic steel sheet (0.45 mm) and a

specific Steel/Polymer/Steel sheet (0.45/0.26/0.45 mm) under uniaxial tensile loading. Both materials initially display linear elastic behavior. Generally, the stress-strain curve of the laminate displays a more gradual transition from the elastic region to plastic deformation compared to that of a monolithic. As the steel sheet approaches ultimate failure, it exhibits a more abrupt necking behavior, resulting in a relatively sharp drop in stress. This brittle failure is characteristic of metallic materials, where the strong atomic bonds lead to sudden fracture under high strain. In contrast, the presence of the polymer layer in the S/P/S laminate

introduces a ductile behavior that enhances toughness and prevents rapid failure. The polymer layer provides additional energy absorption and deformation capacity,

resulting in a more gradual and controlled stress reduction prior to failure.

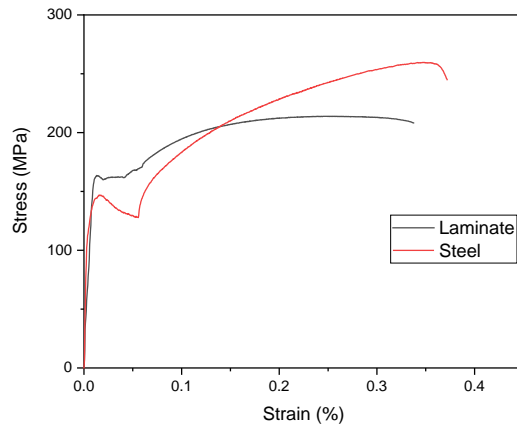


Figure 13: Stress-Strain curve of monolithic and laminated steel sheets

Figure 14 and Figure 15 show the yield and ultimate strength of laminates for various sample orientations with respect to RD and various thickness reductions, respectively.

As shown in the figures, there are considerable differences in the yield and ultimate tensile strengths for all four laminates compared to the monolithic steel sheet. Based on Figure 14, the yield strength of the monolithic steel sheet at all three directions (RD, DD, and TD) is higher than the three laminates L-25-30, L-25-40, and L-25-50. However, the yield strength of L-25-60 laminate is higher than that of the steel sheet. Similarity of the trends of L-25-50 and L-25-60 to the steel sheet curve suggests that the yield behavior of the thinner laminates is closer to that of the skin sheet due to reduced influence of polymer layer. While the polymer layer still contributes to factors such as interfacial adhesion and other mechanical properties of laminate,

its influence on the overall yield behavior diminishes as laminate thickness decreases. Increasing the volume fraction of the polymer leads to the same yield behavior in three directions.

Comparison of the results of Figure 15 shows that the tensile strength of the monolithic steel sheet in the DD is higher than that of all other laminates. However, for both RD and TD, the tensile strength of the steel sheet is lower than the L-25-60 and more than L-25-30, L-25-40, and L-25-50 laminates. The same trend of the steel sheet curve and all laminates exhibit the high dependence of the tensile strength of the laminates on the tensile strength of the skin sheets in all three directions. Consequently, this finding suggests that the mechanical properties of the steel face sheets exert a relatively greater impact on the UTS of the laminate compared to the polymeric core.

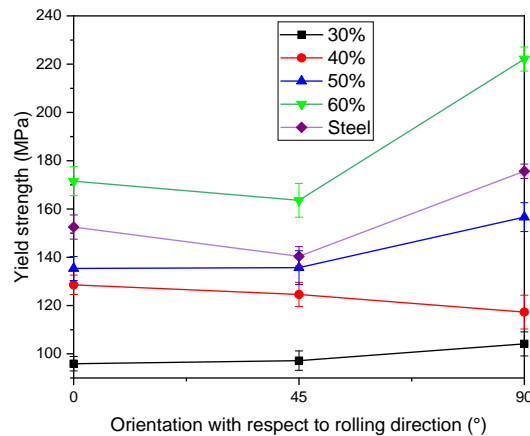


Figure 14: Effect of the angle of the sample axis with respect to RD on the yield strength (for various thickness reductions and bars on data points shows standard deviation of the test samples)

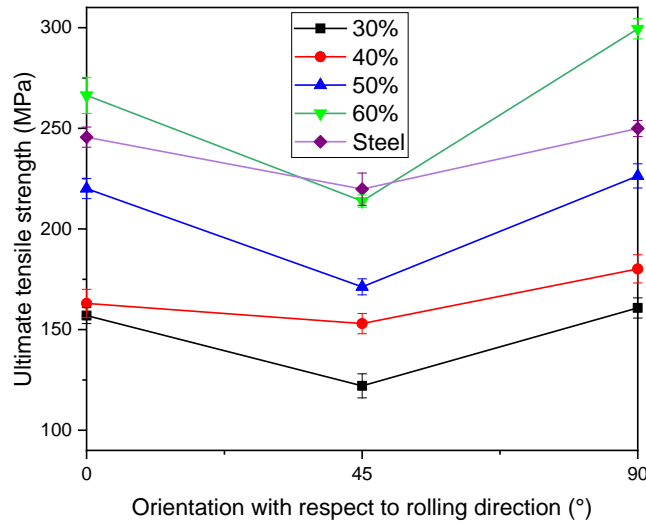


Figure 15: Effect of the angle of the sample axis with respect to RD on the ultimate tensile strength (for various thickness reductions and bars on data points shows standard deviation of the test samples)

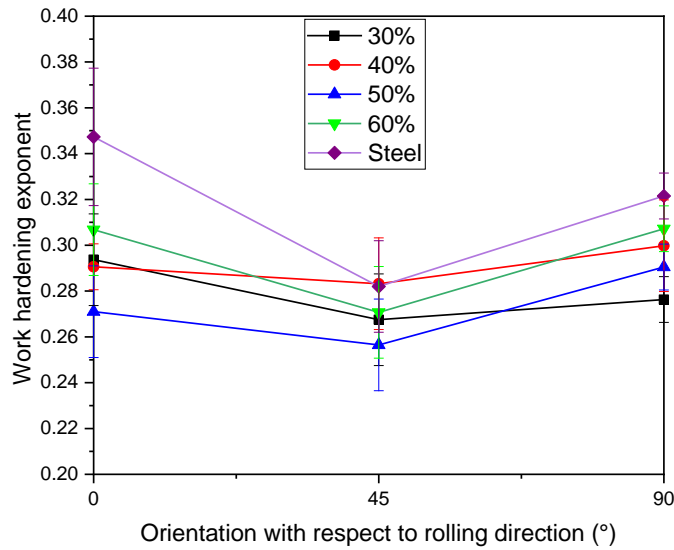


Figure 16: Effect of the angle of the sample axis with respect to RD on the work hardening exponent (for various thickness reductions and bars on data points shows standard deviation of the test samples)

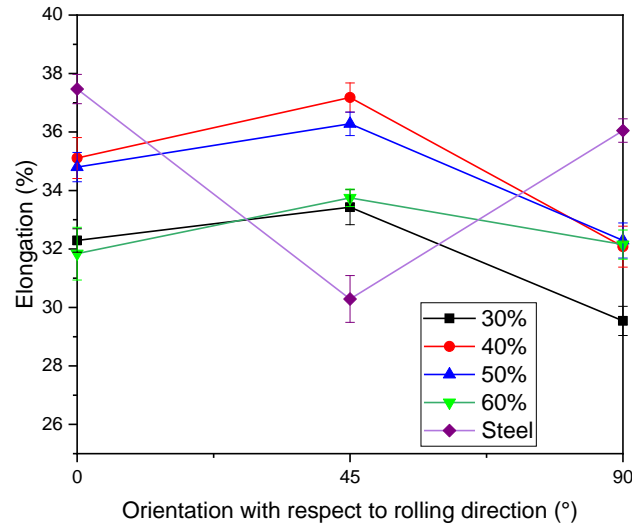


Figure 17: Effect of the angle of the sample axis with respect to RD on the ultimate elongation (for various thickness reductions and bars on data points shows standard deviation of the test samples)

The work hardening exponent measures the extent to which the material (monolithic and laminated steel sheet) undergo work hardening in response to uniaxial tensile load. Based on Considère criterion, the true strain (at maximum force) equates to the strain hardening exponent ($\epsilon_u = n$) at the onset of localized necking. The work hardening exponent parameter of both monolithic steel and S/P/S laminate is given in Figure 16. Based on the figure, the n value of monolithic steel face sheet in RD and TD directions is higher than that of all S/P/S laminates. Besides, in DD direction, n of monolithic steel face sheet is approximately equal to that of L-25-40 and higher than that of other laminates. It is worth noting that DiCello [35] attributed the low work hardening exponent of the laminate compared to that of skin face sheet to the thermal aging of the metal skin during the lamination process. On the other hand, Harhash et al. [7] and Forcellese and Simoncini [36] attributed such a result to the soft polymer core which negatively affects the strengthening behavior of the laminate sheets. Furthermore, according to the study by Kim et al. [10], the strain hardening exponent of the polypropylene was reported to be lower compared to that of the AA5182 skin. This resulted in the reduction of the overall strain-hardening exponent of the sandwich sheets compared to monolithic aluminum sheet.

By changing the direction of the tensile samples of all laminates from 0° to 45° , the work hardening exponent decreases. Then, the n value increases from 45° to 90° . The same trend of n value at three directions for the monolithic steel sheet indicates that the work hardening exponent of laminates is dependent on the skinsheet.

As shown in Figure 17, by increasing the angular orientation of the tensile samples from 0° to 90° , the elongation of all laminates first increases and then decreases while the skin sheet shows the opposite trend. Because the thicknesses of two skins of a laminate are equal and with same pressure on both sides of the polymer core, the metal-polymer interface strength of both sides is equal. It is suspected that, the occurrence of simultaneous necking of two steel skins in the same place increases the possibility of the premature fracture relative to the monolithic steel sheet. This simultaneous necking indicates a strong interaction between the skin layers, where they undergo a synchronized deformation mechanism. It can be influenced by various factors, such as the properties of the skin and polymer materials, their thicknesses, and the bonding strength between layers. At the DD, there is an improvement of this property for laminates. This can be related to high load bearing capacity (the ability of this specimen in distributing stress throughout the specimen length) of the metal-polymer interface samples at this direction. Forcellese and Simoncini [36] reported highest ultimate elongation value and post-necking deformation at 45° and similar elongation values for the 0° and 90° directions as well as lower post-necking deformation. They related this behavior to the lowest attitude to thinning owing to the highest normal anisotropy of the S/P/S sandwich composite occurring in the 45° angular orientation. Consequently, they observed the higher formability of samples at 45° orientation in the plane strain and drawing regions of Forming Limit Diagrams (FLD). Due to the significant difference between the elongation of the three-layer laminates and polymeric sheet, it can be concluded that

the two skin sheets strongly affect the three-layer sheet ductility behavior.

Figure 18 shows the Young's modulus (E , slope of linear portion of stress-strain curve) of S/P/S laminates and monolithic steel for various rolling directions. Based on the graph, E of S/P/S are lower

than that of monolithic steel sheet for all rolling directions. Furthermore, the value of E is insensitive to the rolling direction for all laminates and monolithic steel. This indicates that, in the present study, S/P/S laminates demonstrate an isotropic and macroscopically homogenous behavior.

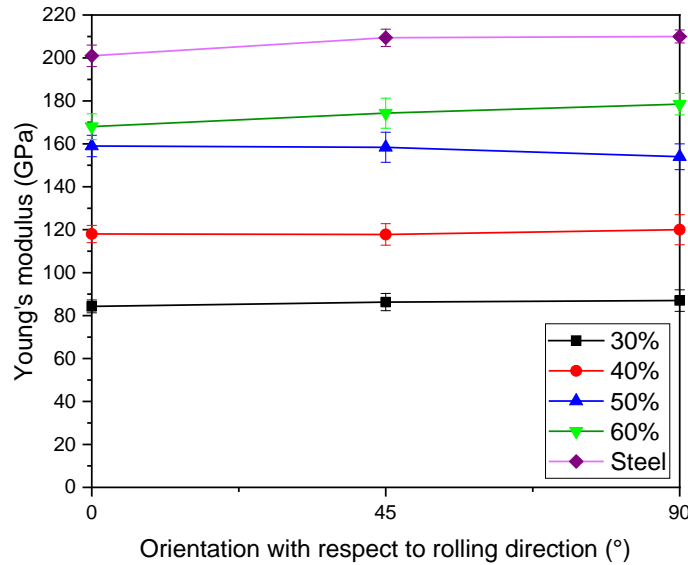


Figure 18: Effect of the angle of the sample axis with respect to RD on the Young's modulus (for various thickness reductions and bars on data points shows standard deviation of the test samples)

ii. Effect of the Polymer Volume Fraction

Figure 14 and Figure 15 show the increase in yield and tensile strength by decreasing the volume fraction of the polymer. Such result is in excellent agreement with those observed by Carrado et al. [1] and Harhash et al. [7].

Figure 19 shows the interface micrograph of all four laminates after lamination. According to the figure and the results of T-peel test (Figure 8), the mechanical interlocks have occurred between the rough surface of the skin sheet and the soft surface of the core sheet. This led to high bond strength at metal-polymer interface hindering the formation of delamination under tensile loading. On the other hand, the high tear strength of the polymeric sheet guarantees non-tearing along the width of the core sheet in the laminate structure. Therefore, all four laminates perform as an integrated sandwich structure. According to Figure 20, the ultimate tensile strength obtained from the tensile test (in the rolling direction) for two laminates L-25-50 and L-25-60 is higher than the calculated values obtained by the Rule Of Mixture (ROM). However, for L-25-30 and L-25-40, the experimental tensile strengths are lower than those obtained by ROM. It is observed that as the volume fraction of the polymer increases, the difference

between the experimental and predicted tensile strength decreases commensurately.

It should be noted that there is not a clear correlation between the polymer volume fraction and the work hardening exponent (Figure 16). The similarity of results of all four laminates at all three directions to those of the monolithic steel sheet indicates that S/P/S laminates have high strain distribution behavior and consequently possess high formability.

Additionally, the highest elongation at all rolling directions belongs to L-25-40 and L-25-50 (Figure 17). The high bond strength of these laminates can be the reason of high elongation and consequently their delayed fracture. A similar conclusion was reached in [19].

Figure 18 indicates that increasing the thickness of the polymeric core leads to a decrease in the Young's modulus of the S/P/S laminates. As the thickness of the polymeric core increases, the proportion of the steel layers decreases. The polymer layer, which typically has a lower Young's modulus than steel, becomes a larger component of the structure. As a result, the overall Young's modulus of the structure decreases. Young's modulus of S/M/S sandwich sheets are calculated following the rule of mixture based on the Young's modulus of St14 steel and TPU sheets which are

209.4 GPa and 12.35 MPa, respectively. Figure 21 exhibits the difference between experimental and ROM values of young's modulus of S/P/S samples in rolling direction. Since ROM does not account for the interfacial bonding strength, this difference can be attributed to interfacial properties of the laminates along with strain rate dependency of the TPU core.

Comparison of the experimental and predicted ROM results indicates that the higher the volume fraction of the polymer, the larger becomes the difference between the obtained and predicted elongations (Figure 22). Due to the lack of pressure on the laminated sheet during cooling, micro-cavities may form in the polymer structure. Thicker laminates have more microcavities due to their high polymer volume fraction. Increasing the difference between the experimental density and its predicted value by increasing the polymer volume fraction supports this hypothesis (Figure 23). The density of the monolithic steel and polymer sheets is 7.8 gr/cm^3 and 1.25 gr/cm^3 , respectively.

Figure 24 shows the effect of core volume fraction on the specific stiffness (Young's modulus/Density) of the S/P/S laminates and compares experimental and estimated (ROM) values. The lower specific stiffness of L25-30 may be due to the thicker core, which might not be as effective in distributing the load, especially when the core material has significantly lower stiffness ($0.0096 \text{ GPa/g.cm}^{-3}$) than the skin sheets ($26.84 \text{ GPa/g.cm}^{-3}$). L-25-40 and L-25-60 have specific stiffness values close to that of the steel skin sheet, suggesting effective load distribution and potentially good interfacial bonding. The highest specific stiffness of L-25-50 (28.95) could be due to an optimal combination of core thickness and material properties, maximizing the load distribution and minimizing stress concentrations. It can be concluded that L-25-50 is the sample with promising thickness combination, which maintains a reasonable weight saving in addition to higher specific stiffness. Harhash et al. [7] demonstrated that E/D of 316L/PP PE/316L decrease as core volume fraction increase due to dominant effect of the polymeric core.

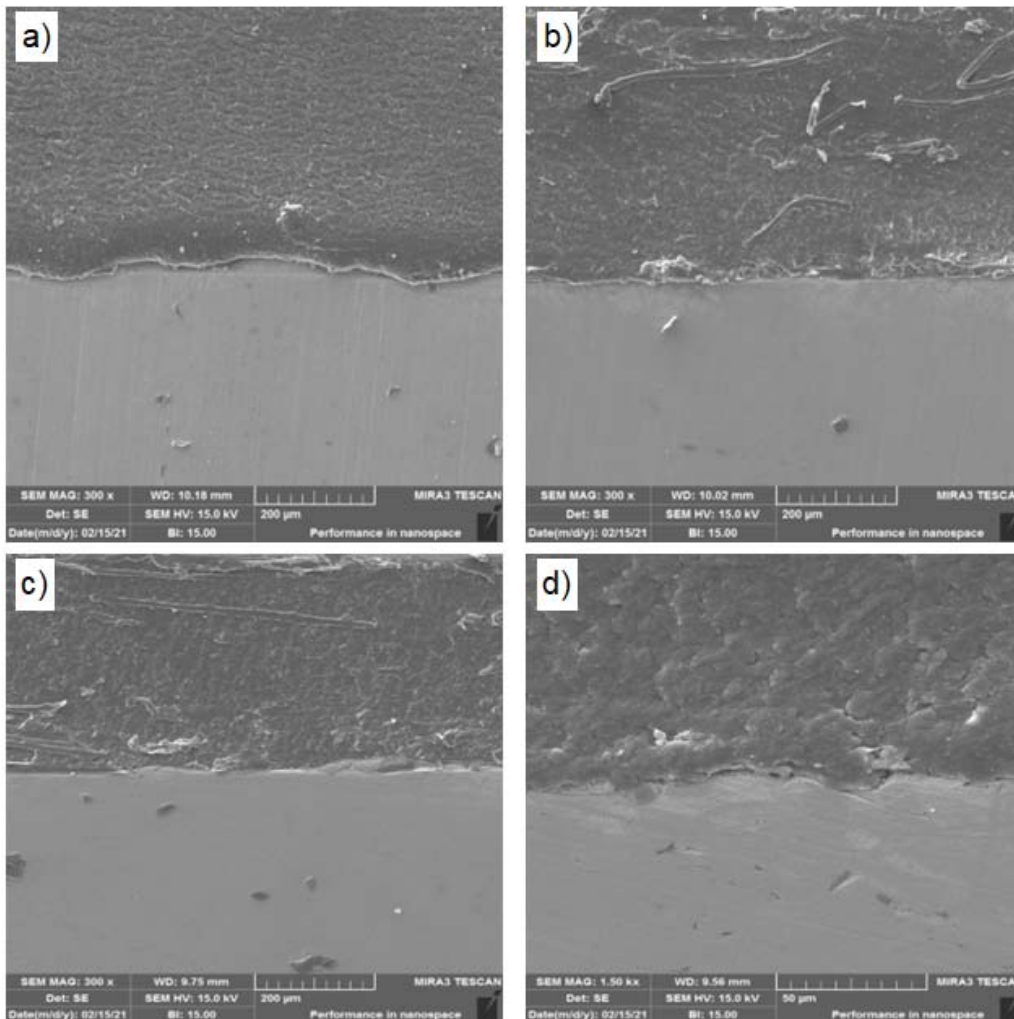


Figure 19: Metal/polymer interface of different laminates: (a) L-25-30, (b) L-25-40, (c) L-25-50, and (d) L-25-60 (Note: due to different thicknesses of specimens' different zooms and scales are used for each sample)

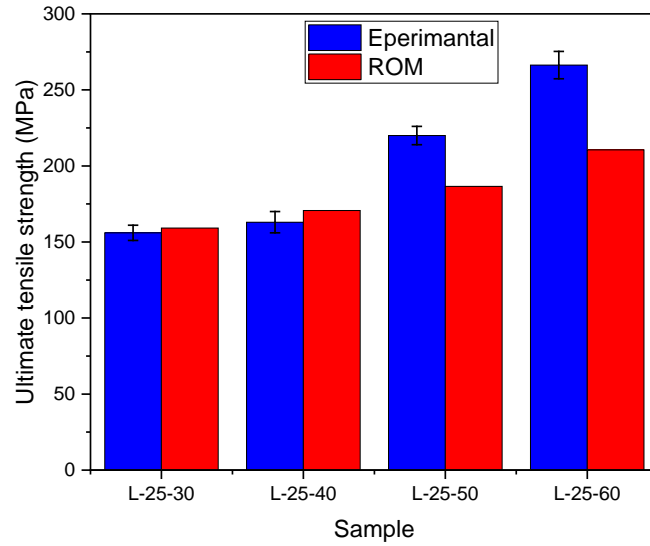


Figure 20: Comparison of the experimental and ROM results of UTS (at RD)

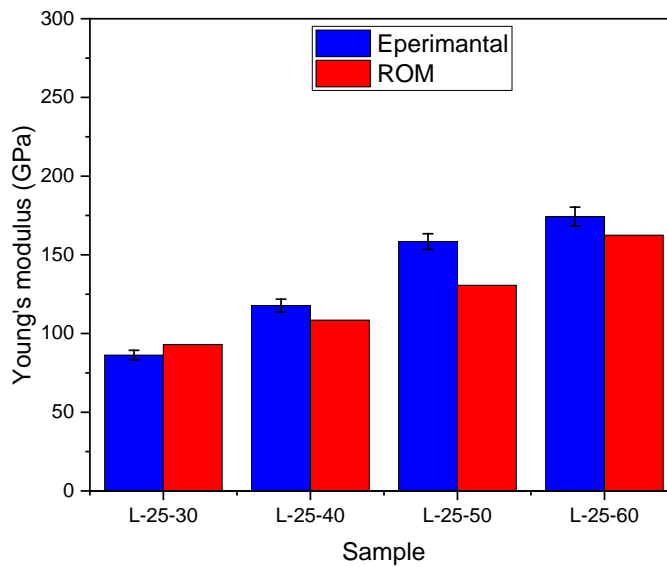


Figure 21: Comparison of the experimental and ROM results of young's modulus (at RD)

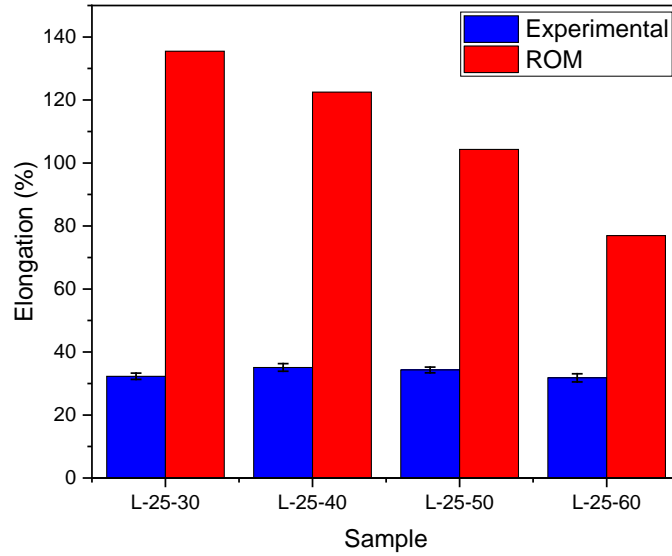


Figure 22: Comparison of the experimental and ROM results of elongation (at RD)

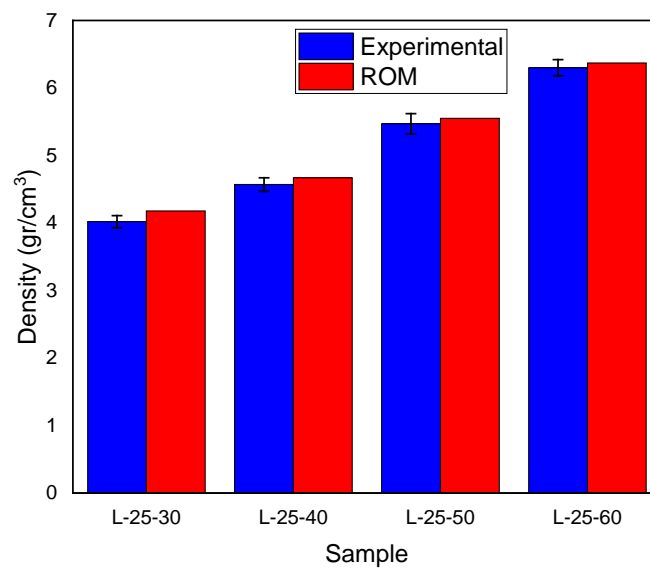


Figure 23: Comparison of the experimental and ROM results of density

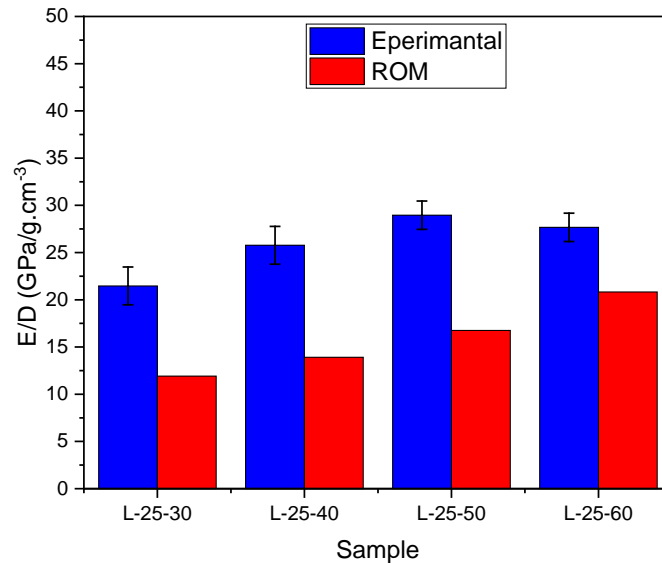


Figure 24: Comparison of the experimental and ROM results of specific stiffness

IV. CONCLUSIONS

A comprehensive experimental study was performed to investigate the effect(s) of the core volume fraction and rolling direction on the mechanical properties of the S/P/S composite laminate under uniaxial tensile loading. In the frame of the current study, the following conclusions are made:

1. Due to the higher passing time and consequently the higher effective pressure, the lower rolling speed leads to higher bond strength.
2. By increasing the polymer volume fraction in the laminate structure, the yield behavior becomes the same at RD, DD, and TD. On the other hand, S/P/S Laminates, like monolithic steel sheet exhibit higher ultimate tensile strength at 0° and 90° orientations, compared to the strength exhibited in a 45° orientation. As the volume fraction of the polymer increases, both yield and tensile strengths as well as elastic Young's modulus of laminates decreases.
3. The work hardening exponent (n) of all laminates is almost lower than that of monolithic steel sheet at all directions. Direct correlation between formability and n -value was observed. In other words, similarity of both the value and the trend of results obtained for low carbon steel and S/P/S laminates were indicative of high formability of laminates.
4. Increasing the angular orientation of the tensile samples from 0° to 90°, led too initial increase in the elongation of all laminates. However, the increase was succeeded by decreases in elongation while the skin sheet showed the opposite trend. Moreover high-bond strength laminates have higher elongation than low-bond strength laminates. The

difference between the obtained elongations and the calculated ones showed that thicker laminates had a larger volume fraction of micro-cavities that formed after lamination.

5. S/P/S laminates demonstrated homogeneous material behavior. This was the result of consistent stiffness properties in all directions relative to the rolling direction.
6. The likelihood of premature fracture in S/P/S laminates was higher than monolithic steel sheet thanks to occurrence of simultaneous necking of two steel face sheets at the same location.

Conducting experimental and finite element analysis to further understand the effect of interlayer thickness on formability, weldability, and impact resistance of this laminates is essential for improving their properties for various industrial applications. Additionally, the fracture mechanisms of the laminates need to be investigated under various loading conditions.

REFERENCES RÉFÉRENCES REFERENCIAS

1. A. Carradó, J. Faerber, S. Niemeyer, G. Ziegmann, and H. Palkowski, "Metal/polymer/metal hybrid systems: Towards potential formability applications," *Compos Struct*, vol. 93, no. 2, pp. 715–721, 2011, doi: <https://doi.org/10.1016/j.compstruct.2010.07.016>
2. M. Damghani, C. Wallis, J. Bakunowicz, and A. Murphy, "Experimental and numerical analysis for postbuckling behaviour of tailored hybrid composite laminates subjected to shear loading," *Compos Struct*, p. Accepted for publication, 2020.

3. M. Damghani, J. Saddler, E. Sammon, G. A. Atkinson, J. Matthews, and A. Murphy, "An experimental investigation of the impact response and Post-impact shear buckling behaviour of hybrid composite laminates," *Compos Struct*, vol. 305, p. 116506, 2023, doi: <https://doi.org/10.1016/j.compstruct.2022.116506>
4. A. Kwakernaak, J. Hofstede, J. Poulis, and R. Benedictus, "8 - Improvements in bonding metals for aerospace and other applications," in *Woodhead Publishing Series in Welding and Other Joining Technologies*, M. C. B. T.-W. and J. of A. M. Chaturvedi, Ed., Woodhead Publishing, 2012, pp. 235–287. doi: <https://doi.org/10.1533/9780857095169.2.235>
5. I. Burchitz, R. Boesenkool, S. van der Zwaag, and M. Tassoul, "Highlights of designing with Hylite – a new material concept," *Mater Des*, vol. 26, no. 4, pp. 271–279, 2005, doi: <https://doi.org/10.1016/j.matdes.2004.06.021>
6. J.-K. Kim and T.-X. Yu, "Forming and failure behaviour of coated, laminated and sandwiched sheet metals: a review," *J Mater Process Technol*, vol. 63, no. 1, pp. 33–42, 1997, doi: [https://doi.org/10.1016/S0924-0136\(96\)02596-4](https://doi.org/10.1016/S0924-0136(96)02596-4)
7. M. Harhash, O. Sokolova, A. Carradó, and H. Palkowski, "Mechanical properties and forming behaviour of laminated steel/polymer sandwich systems with local inlays – Part 1," *Compos Struct*, vol. 118, pp. 112–120, 2014, doi: <https://doi.org/10.1016/j.compstruct.2014.07.011>
8. J. Liu, W. Liu, and W. Xue, "Forming limit diagram prediction of AA5052/polyethylene/AA5052 sandwich sheets," *Materials & Design (1980-2015)*, vol. 46, pp. 112–120, 2013, doi: <https://doi.org/10.1016/j.matdes.2012.09.057>
9. F. Kazemi, R. Hashemi, and S. A. Niknam, "Formability and fractography of AA5754/polyethylene/AA5754 sandwich composites," *Mechanics Based Design of Structures and Machines*, vol. 50, no. 4, pp. 1253–1267, Apr. 2022, doi: [10.1080/15397734.2020.1747488](https://doi.org/10.1080/15397734.2020.1747488)
10. K. J. Kim *et al.*, "Formability of AA5182/polypropylene/AA5182 sandwich sheets," *J Mater Process Technol*, vol. 139, no. 1, pp. 1–7, 2003, doi: [https://doi.org/10.1016/S0924-0136\(03\)00173-0](https://doi.org/10.1016/S0924-0136(03)00173-0)
11. K. Logesh and V. K. B. Raja, "Formability analysis for enhancing forming parameters in AA8011/PP/AA1100 sandwich materials," *The International Journal of Advanced Manufacturing Technology*, vol. 93, no. 1, pp. 113–120, 2017, doi: [10.1007/s00170-015-7832-5](https://doi.org/10.1007/s00170-015-7832-5)
12. K. J. Kim *et al.*, "Development of application technique of aluminum sandwich sheets for automotive hood," *International Journal of Precision Engineering and Manufacturing*, vol. 10, no. 4, pp. 71–75, 2009, doi: [10.1007/s12541-009-0073-5](https://doi.org/10.1007/s12541-009-0073-5)
13. V. Satheeshkumar and R. G. Narayanan, "Investigation on the influence of adhesive properties on the formability of adhesive-bonded steel sheets," *Proc Inst Mech Eng C J Mech Eng Sci*, vol. 228, no. 3, pp. 405–425, May 2013, doi: [10.1177/0954406213488727](https://doi.org/10.1177/0954406213488727)
14. H. Hayashi and T. Nakagawa, "Recent trends in sheet metals and their formability in manufacturing automotive panels," *J Mater Process Technol*, vol. 46, no. 3, pp. 455–487, 1994, doi: [https://doi.org/10.1016/0924-0136\(94\)90128-7](https://doi.org/10.1016/0924-0136(94)90128-7)
15. J. Liu and L. Zhuang, "Cylindrical cup-drawing characteristics of aluminum-polymer sandwich sheet," *The International Journal of Advanced Manufacturing Technology*, vol. 97, no. 5, pp. 1885–1896, 2018, doi: [10.1007/s00170-018-2077-8](https://doi.org/10.1007/s00170-018-2077-8)
16. M. Nourjani Pourmoghadam, R. Shahrokh Esfahani, M. R. Morovati, and B. Nekooei Rizi, "Bifurcation analysis of plastic wrinkling formation for anisotropic laminated sheets (AA2024–Polyamide–AA2024)," *Comput Mater Sci*, vol. 77, pp. 35–43, 2013, doi: <https://doi.org/10.1016/j.commatsci.2013.03.037>
17. M. Harhash, A. Carradó, and H. Palkowski, "DEEP-AND STRETCH-FORMING OF STEEL/POLYMER/STEEL LAMINATES," in *Euro Hybrid Materials and Structures*, Kaiserslautern (Germany), 2016.
18. B. Rezaei Anvar and A. Akbarzadeh, "Roll bonding of AA5052 and polypropylene sheets: Bonding mechanisms, microstructure and mechanical properties," *J Adhes*, vol. 93, no. 7, pp. 550–574, Jun. 2017, doi: [10.1080/00218464.2015.1116067](https://doi.org/10.1080/00218464.2015.1116067)
19. S. Nambu, M. Michiuchi, J. Inoue, and T. Koseki, "Effect of interfacial bonding strength on tensile ductility of multilayered steel composites," *Compos Sci Technol*, vol. 69, no. 11, pp. 1936–1941, 2009, doi: <https://doi.org/10.1016/j.compscitech.2009.04.013>
20. H. Park, S.-J. Kim, J. Lee, J. H. Kim, and D. Kim, "Characterization of the Mechanical Properties of a High-Strength Laminated Vibration Damping Steel Sheet and Their Application to Formability Prediction," *Metals and Materials International*, vol. 25, no. 5, pp. 1326–1340, 2019, doi: [10.1007/s12540-019-00281-8](https://doi.org/10.1007/s12540-019-00281-8)
21. R. B. Ruokolainen and D. R. Sigler, "The Effect of Adhesion and Tensile Properties on the Formability of Laminated Steels," *J Mater Eng Perform*, vol. 17, no. 3, pp. 330–339, 2008, doi: [10.1007/s11665-008-9207-7](https://doi.org/10.1007/s11665-008-9207-7)
22. M. Weiss, B. Rolfe, M. Dingle, and P. Hodgson, "The influence of interlayer thickness and properties on spring-back of SPS- (steel/polymer/steel) laminates.," *Steel grips*, vol. 2, pp. 445–449, 2004, [Online]. Available: https://dro.deakin.edu.au/article/es/journal_contribution/The_influence_of_interlayer_thickness_and_properties_on_spring-back_of_SPS_steel_polymer_steel_laminates_/20537805

23. F. Avril, R. Rahmé, M. Doux, D. Verchere, D. Sage, and P. Cassagnau, "New Polymer Materials for Steel/Polymer/Steel Laminates in Automotive Applications," *Macromol Mater Eng*, vol. 298, no. 6, pp. 644–652, Jun. 2013, doi: <https://doi.org/10.1002/mame.201200058>
24. T. Saito and N. Mizuhashi, "Resistance welding of vibration-damped steel sheet," *Welding International*, vol. 4, no. 12, pp. 993–997, Jan. 1990, doi: [10.1080/09507119009453040](https://doi.org/10.1080/09507119009453040)
25. H. Oberle, C. Commaret, C. Minier, R. Magnaud, and G. Pradere, "Optimizing resistance spot welding parameters for vibration damping steel sheets," *Weld J*, vol. 77, 1998, [Online]. Available: <https://api.semanticscholar.org/CorpusID:136653269>
26. S. Mousa and G.-Y. Kim, "Direct Adhesion of Warm Roll-Bonded Al1100/Polyurethane/Al1100 Sandwich Composite," in *Proceedings of the ASME 2015 International Manufacturing Science and Engineering Conference*, North Carolina (USA), Jun. 2015. doi: [10.1115/MSEC2015-9467](https://doi.org/10.1115/MSEC2015-9467)
27. W. Lin, X. Li, W. Dong, Y. Zhao, M. Li, and Y. Wang, "Ultrahigh bonding strength and excellent corrosion resistance of Al-TPU hybrid induced by microstructures and silane layer," *J Mater Process Technol*, vol. 296, p. 117180, 2021, doi: <https://doi.org/10.1016/j.jmatprotec.2021.117180>
28. M. Yahiaoui, J. Denape, J.-Y. Paris, A. G. Ural, N. Alcalá, and F. J. Martínez, "Wear dynamics of a TPU/steel contact under reciprocal sliding," *Wear*, vol. 315, no. 1, pp. 103–114, 2014, doi: <https://doi.org/10.1016/j.wear.2014.04.005>
29. J. Liu, Q. Zhang, B. Zhang, and M. Yu, "The Influence of the Roll-Laminating Process on the Bonding Quality of Polymer-Coated Steel Interface," *Coatings*, vol. 11, no. 4, 2021. doi: [10.3390/coatings11040472](https://doi.org/10.3390/coatings11040472)
30. S. Mousa, N. Scheirer, and G.-Y. Kim, "Roll-bonding of metal-polymer-metal sandwich composites reinforced by glass whiskers at the interface," *J Mater Process Technol*, vol. 255, pp. 463–469, 2018, doi: <https://doi.org/10.1016/j.jmatprotec.2017.12.039>
31. M. Harhash, R. R. Gilbert, S. Hartmann, and H. Palkowski, "Experimental characterization, analytical and numerical investigations of metal/polymer/metal sandwich composites – Part 1: Deep drawing," *Compos Struct*, vol. 202, pp. 1308–1321, 2018, doi: <https://doi.org/10.1016/j.compstruct.2018.06.066>
32. A. Frick, M. Borm, N. Kaoud, J. Kolodziej, and J. Neudeck, "Microstructure and thermomechanical properties relationship of segmented thermoplastic polyurethane (TPU)," *AIP Conf Proc*, vol. 1593, no. 1, pp. 520–525, May 2014, doi: [10.1063/1.4873835](https://doi.org/10.1063/1.4873835)
33. M. Kamali Andani, H. Daneshmanesh, and S. A. Jenabali Jahromi, "Investigation of the bonding strength of the stainless steel 316L/polyurethane/stainless steel 316L tri-layer composite produced by the warm rolling process," *Journal of Sandwich Structures & Materials*, vol. 22, no. 3, pp. 728–742, Apr. 2018, doi: [10.1177/1099636218770911](https://doi.org/10.1177/1099636218770911)
34. M. Abbasi and M. R. Toroghinejad, "Effects of processing parameters on the bond strength of Cu/Cu roll-bonded strips," *J Mater Process Technol*, vol. 210, no. 3, pp. 560–563, 2010, doi: <https://doi.org/10.1016/j.jmatprotec.2009.11.003>
35. J. A. DiCello, "Steel-Polypropylene-Steel Laminate – A New Weight Reduction Material," in *1980 Automotive Engineering Congress and Exposition*, SAE International, Feb. 1980. doi: <https://doi.org/10.4271/800078>
36. A. Forcellese and M. Simoncini, "Mechanical properties and formability of metal–polymer–metal sandwich composites," *The International Journal of Advanced Manufacturing Technology*, vol. 107, no. 7, pp. 3333–3349, 2020, doi: [10.1007/s00170-020-05245-6](https://doi.org/10.1007/s00170-020-05245-6)

GLOBAL JOURNALS GUIDELINES HANDBOOK 2024

WWW.GLOBALJOURNALS.ORG

MEMBERSHIPS

FELLOWS/ASSOCIATES OF ENGINEERING RESEARCH COUNCIL

FERC/AERC MEMBERSHIPS

INTRODUCTION



FERC/AERC is the most prestigious membership of Global Journals accredited by Open Association of Research Society, U.S.A (OARS). The credentials of Fellow and Associate designations signify that the researcher has gained the knowledge of the fundamental and high-level concepts, and is a subject matter expert, proficient in an expertise course covering the professional code of conduct, and follows recognized standards of practice. The credentials are designated only to the researchers, scientists, and professionals that have been selected by a rigorous process by our Editorial Board and Management Board.

Associates of FERC/AERC are scientists and researchers from around the world are working on projects/researches that have huge potentials. Members support Global Journals' mission to advance technology for humanity and the profession.

FERC

FELLOW OF ENGINEERING RESEARCH COUNCIL

FELLOW OF ENGINEERING RESEARCH COUNCIL is the most prestigious membership of Global Journals. It is an award and membership granted to individuals that the Open Association of Research Society judges to have made a 'substantial contribution to the improvement of computer science, technology, and electronics engineering.

The primary objective is to recognize the leaders in research and scientific fields of the current era with a global perspective and to create a channel between them and other researchers for better exposure and knowledge sharing. Members are most eminent scientists, engineers, and technologists from all across the world. Fellows are elected for life through a peer review process on the basis of excellence in the respective domain. There is no limit on the number of new nominations made in any year. Each year, the Open Association of Research Society elect up to 12 new Fellow Members.



BENEFITS

TO THE INSTITUTION

GET LETTER OF APPRECIATION

Global Journals sends a letter of appreciation of author to the Dean or CEO of the University or Company of which author is a part, signed by editor in chief or chief author.



EXCLUSIVE NETWORK

GET ACCESS TO A CLOSED NETWORK

A FERC member gets access to a closed network of Tier 1 researchers and scientists with direct communication channel through our website. Fellows can reach out to other members or researchers directly. They should also be open to reaching out by other.

Career

Credibility

Exclusive

Reputation



CERTIFICATE

CERTIFICATE, LOR AND LASER-MOMENTO

Fellows receive a printed copy of a certificate signed by our Chief Author that may be used for academic purposes and a personal recommendation letter to the dean of member's university.

Career

Credibility

Exclusive

Reputation



DESIGNATION

GET HONORED TITLE OF MEMBERSHIP

Fellows can use the honored title of membership. The "FERC" is an honored title which is accorded to a person's name viz. Dr. John E. Hall, Ph.D., FERC or William Walldroff, M.S., FERC.

Career

Credibility

Exclusive

Reputation

RECOGNITION ON THE PLATFORM

BETTER VISIBILITY AND CITATION

All the Fellow members of FERC get a badge of "Leading Member of Global Journals" on the Research Community that distinguishes them from others. Additionally, the profile is also partially maintained by our team for better visibility and citation. All fellows get a dedicated page on the website with their biography.

Career

Credibility

Reputation

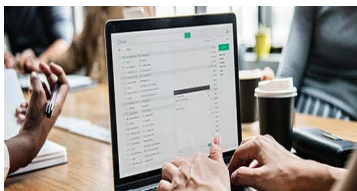
FUTURE WORK

GET DISCOUNTS ON THE FUTURE PUBLICATIONS

Fellows receive discounts on the future publications with Global Journals up to 60%. Through our recommendation programs, members also receive discounts on publications made with OARS affiliated organizations.

Career

Financial



GJ ACCOUNT

UNLIMITED FORWARD OF EMAILS

Fellows get secure and fast GJ work emails with unlimited storage of emails that they may use them as their primary email. For example, john [AT] globaljournals [DOT] org.

Career

Credibility

Reputation



PREMIUM TOOLS

ACCESS TO ALL THE PREMIUM TOOLS

To take future researches to the zenith, fellows receive access to all the premium tools that Global Journals have to offer along with the partnership with some of the best marketing leading tools out there.

Financial

CONFERENCES & EVENTS

ORGANIZE SEMINAR/CONFERENCE

Fellows are authorized to organize symposium/seminar/conference on behalf of Global Journal Incorporation (USA). They can also participate in the same organized by another institution as representative of Global Journal. In both the cases, it is mandatory for him to discuss with us and obtain our consent. Additionally, they get free research conferences (and others) alerts.

Career

Credibility

Financial

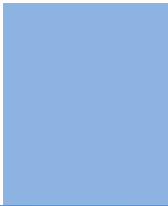
EARLY INVITATIONS

EARLY INVITATIONS TO ALL THE SYMPOSIUMS, SEMINARS, CONFERENCES

All fellows receive the early invitations to all the symposiums, seminars, conferences and webinars hosted by Global Journals in their subject.

Exclusive





PUBLISHING ARTICLES & BOOKS

EARN 60% OF SALES PROCEEDS

Fellows can publish articles (limited) without any fees. Also, they can earn up to 70% of sales proceeds from the sale of reference/review books/literature/publishing of research paper. The FERC member can decide its price and we can help in making the right decision.

Exclusive Financial

REVIEWERS

GET A REMUNERATION OF 15% OF AUTHOR FEES

Fellow members are eligible to join as a paid peer reviewer at Global Journals Incorporation (USA) and can get a remuneration of 15% of author fees, taken from the author of a respective paper.

Financial

ACCESS TO EDITORIAL BOARD

BECOME A MEMBER OF THE EDITORIAL BOARD

Fellows may join as a member of the Editorial Board of Global Journals Incorporation (USA) after successful completion of three years as Fellow and as Peer Reviewer. Additionally, Fellows get a chance to nominate other members for Editorial Board.

Career Credibility Exclusive Reputation

AND MUCH MORE

GET ACCESS TO SCIENTIFIC MUSEUMS AND OBSERVATORIES ACROSS THE GLOBE

All members get access to 5 selected scientific museums and observatories across the globe. All researches published with Global Journals will be kept under deep archival facilities across regions for future protections and disaster recovery. They get 10 GB free secure cloud access for storing research files.



ASSOCIATE OF ENGINEERING RESEARCH COUNCIL

ASSOCIATE OF ENGINEERING RESEARCH COUNCIL is the membership of Global Journals awarded to individuals that the Open Association of Research Society judges to have made a 'substantial contribution to the improvement of computer science, technology, and electronics engineering.

The primary objective is to recognize the leaders in research and scientific fields of the current era with a global perspective and to create a channel between them and other researchers for better exposure and knowledge sharing. Members are most eminent scientists, engineers, and technologists from all across the world. Associate membership can later be promoted to Fellow Membership. Associates are elected for life through a peer review process on the basis of excellence in the respective domain. There is no limit on the number of new nominations made in any year. Each year, the Open Association of Research Society elect up to 12 new Associate Members.



BENEFITS

TO THE INSTITUTION

GET LETTER OF APPRECIATION

Global Journals sends a letter of appreciation of author to the Dean or CEO of the University or Company of which author is a part, signed by editor in chief or chief author.



EXCLUSIVE NETWORK

GET ACCESS TO A CLOSED NETWORK

A AERC member gets access to a closed network of Tier 1 researchers and scientists with direct communication channel through our website. Associates can reach out to other members or researchers directly. They should also be open to reaching out by other.

Career

Credibility

Exclusive

Reputation



CERTIFICATE

CERTIFICATE, LOR AND LASER-MOMENTO

Associates receive a printed copy of a certificate signed by our Chief Author that may be used for academic purposes and a personal recommendation letter to the dean of member's university.

Career

Credibility

Exclusive

Reputation



DESIGNATION

GET HONORED TITLE OF MEMBERSHIP

Associates can use the honored title of membership. The "AERC" is an honored title which is accorded to a person's name viz. Dr. John E. Hall, Ph.D., AERC or William Walldroff, M.S., AERC.

Career

Credibility

Exclusive

Reputation

RECOGNITION ON THE PLATFORM

BETTER VISIBILITY AND CITATION

All the Associate members of AERC get a badge of "Leading Member of Global Journals" on the Research Community that distinguishes them from others. Additionally, the profile is also partially maintained by our team for better visibility and citation. All associates get a dedicated page on the website with their biography.

Career

Credibility

Reputation

FUTURE WORK

GET DISCOUNTS ON THE FUTURE PUBLICATIONS

Associates receive discounts on the future publications with Global Journals up to 60%. Through our recommendation programs, members also receive discounts on publications made with OARS affiliated organizations.

Career

Financial



GJ ACCOUNT

UNLIMITED FORWARD OF EMAILS

Associates get secure and fast GJ work emails with unlimited storage of emails that they may use them as their primary email. For example, john [AT] globaljournals [DOT] org..

Career

Credibility

Reputation



PREMIUM TOOLS

ACCESS TO ALL THE PREMIUM TOOLS

To take future researches to the zenith, associates receive access to all the premium tools that Global Journals have to offer along with the partnership with some of the best marketing leading tools out there.

Financial

CONFERENCES & EVENTS

ORGANIZE SEMINAR/CONFERENCE

Associates are authorized to organize symposium/seminar/conference on behalf of Global Journal Incorporation (USA). They can also participate in the same organized by another institution as representative of Global Journal. In both the cases, it is mandatory for him to discuss with us and obtain our consent. Additionally, they get free research conferences (and others) alerts.

Career

Credibility

Financial

EARLY INVITATIONS

EARLY INVITATIONS TO ALL THE SYMPOSIUMS, SEMINARS, CONFERENCES

All associates receive the early invitations to all the symposiums, seminars, conferences and webinars hosted by Global Journals in their subject.

Exclusive





PUBLISHING ARTICLES & BOOKS

EARN 30-40% OF SALES PROCEEDS

Associates can publish articles (limited) without any fees. Also, they can earn up to 30-40% of sales proceeds from the sale of reference/review books/literature/publishing of research paper.

Exclusive

Financial

REVIEWERS

GET A REMUNERATION OF 15% OF AUTHOR FEES

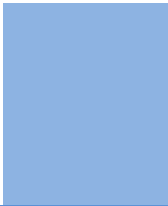
Associate members are eligible to join as a paid peer reviewer at Global Journals Incorporation (USA) and can get a remuneration of 15% of author fees, taken from the author of a respective paper.

Financial

AND MUCH MORE

GET ACCESS TO SCIENTIFIC MUSEUMS AND OBSERVATORIES ACROSS THE GLOBE

All members get access to 2 selected scientific museums and observatories across the globe. All researches published with Global Journals will be kept under deep archival facilities across regions for future protections and disaster recovery. They get 5 GB free secure cloud access for storing research files.



ASSOCIATE	FELLOW	RESEARCH GROUP	BASIC
<p>\$4800 lifetime designation</p> <hr/> <p>Certificate, LoR and Momento 2 discounted publishing/year Gradation of Research 10 research contacts/day 1 GB Cloud Storage GJ Community Access</p>	<p>\$6800 lifetime designation</p> <hr/> <p>Certificate, LoR and Momento Unlimited discounted publishing/year Gradation of Research Unlimited research contacts/day 5 GB Cloud Storage Online Presense Assistance GJ Community Access</p>	<p>\$12500.00 organizational</p> <hr/> <p>Certificates, LoRs and Momentos Unlimited free publishing/year Gradation of Research Unlimited research contacts/day Unlimited Cloud Storage Online Presense Assistance GJ Community Access</p>	<p>APC per article</p> <hr/> <p>GJ Community Access</p>



PREFERRED AUTHOR GUIDELINES

We accept the manuscript submissions in any standard (generic) format.

We typeset manuscripts using advanced typesetting tools like Adobe In Design, CorelDraw, TeXnicCenter, and TeXStudio. We usually recommend authors submit their research using any standard format they are comfortable with, and let Global Journals do the rest.

Alternatively, you can download our basic template from <https://globaljournals.org/Template.zip>

Authors should submit their complete paper/article, including text illustrations, graphics, conclusions, artwork, and tables. Authors who are not able to submit manuscript using the form above can email the manuscript department at submit@globaljournals.org or get in touch with chiefeditor@globaljournals.org if they wish to send the abstract before submission.

BEFORE AND DURING SUBMISSION

Authors must ensure the information provided during the submission of a paper is authentic. Please go through the following checklist before submitting:

1. Authors must go through the complete author guideline and understand and *agree to Global Journals' ethics and code of conduct*, along with author responsibilities.
2. Authors must accept the privacy policy, terms, and conditions of Global Journals.
3. Ensure corresponding author's email address and postal address are accurate and reachable.
4. Manuscript to be submitted must include keywords, an abstract, a paper title, co-author(s) names and details (email address, name, phone number, and institution), figures and illustrations in vector format including appropriate captions, tables, including titles and footnotes, a conclusion, results, acknowledgments and references.
5. Authors should submit paper in a ZIP archive if any supplementary files are required along with the paper.
6. Proper permissions must be acquired for the use of any copyrighted material.
7. Manuscript submitted *must not have been submitted or published elsewhere* and all authors must be aware of the submission.

Declaration of Conflicts of Interest

It is required for authors to declare all financial, institutional, and personal relationships with other individuals and organizations that could influence (bias) their research.

POLICY ON PLAGIARISM

Plagiarism is not acceptable in Global Journals submissions at all.

Plagiarized content will not be considered for publication. We reserve the right to inform authors' institutions about plagiarism detected either before or after publication. If plagiarism is identified, we will follow COPE guidelines:

Authors are solely responsible for all the plagiarism that is found. The author must not fabricate, falsify or plagiarize existing research data. The following, if copied, will be considered plagiarism:

- Words (language)
- Ideas
- Findings
- Writings
- Diagrams
- Graphs
- Illustrations
- Lectures



- Printed material
- Graphic representations
- Computer programs
- Electronic material
- Any other original work

AUTHORSHIP POLICIES

Global Journals follows the definition of authorship set up by the Open Association of Research Society, USA. According to its guidelines, authorship criteria must be based on:

1. Substantial contributions to the conception and acquisition of data, analysis, and interpretation of findings.
2. Drafting the paper and revising it critically regarding important academic content.
3. Final approval of the version of the paper to be published.

Changes in Authorship

The corresponding author should mention the name and complete details of all co-authors during submission and in manuscript. We support addition, rearrangement, manipulation, and deletions in authors list till the early view publication of the journal. We expect that corresponding author will notify all co-authors of submission. We follow COPE guidelines for changes in authorship.

Copyright

During submission of the manuscript, the author is confirming an exclusive license agreement with Global Journals which gives Global Journals the authority to reproduce, reuse, and republish authors' research. We also believe in flexible copyright terms where copyright may remain with authors/employers/institutions as well. Contact your editor after acceptance to choose your copyright policy. You may follow this form for copyright transfers.

Appealing Decisions

Unless specified in the notification, the Editorial Board's decision on publication of the paper is final and cannot be appealed before making the major change in the manuscript.

Acknowledgments

Contributors to the research other than authors credited should be mentioned in Acknowledgments. The source of funding for the research can be included. Suppliers of resources may be mentioned along with their addresses.

Declaration of funding sources

Global Journals is in partnership with various universities, laboratories, and other institutions worldwide in the research domain. Authors are requested to disclose their source of funding during every stage of their research, such as making analysis, performing laboratory operations, computing data, and using institutional resources, from writing an article to its submission. This will also help authors to get reimbursements by requesting an open access publication letter from Global Journals and submitting to the respective funding source.

PREPARING YOUR MANUSCRIPT

Authors can submit papers and articles in an acceptable file format: MS Word (doc, docx), LaTeX (.tex, .zip or .rar including all of your files), Adobe PDF (.pdf), rich text format (.rtf), simple text document (.txt), Open Document Text (.odt), and Apple Pages (.pages). Our professional layout editors will format the entire paper according to our official guidelines. This is one of the highlights of publishing with Global Journals—authors should not be concerned about the formatting of their paper. Global Journals accepts articles and manuscripts in every major language, be it Spanish, Chinese, Japanese, Portuguese, Russian, French, German, Dutch, Italian, Greek, or any other national language, but the title, subtitle, and abstract should be in English. This will facilitate indexing and the pre-peer review process.

The following is the official style and template developed for publication of a research paper. Authors are not required to follow this style during the submission of the paper. It is just for reference purposes.



Manuscript Style Instruction (Optional)

- Microsoft Word Document Setting Instructions.
- Font type of all text should be Swis721 Lt BT.
- Page size: 8.27" x 11", left margin: 0.65, right margin: 0.65, bottom margin: 0.75.
- Paper title should be in one column of font size 24.
- Author name in font size of 11 in one column.
- Abstract: font size 9 with the word "Abstract" in bold italics.
- Main text: font size 10 with two justified columns.
- Two columns with equal column width of 3.38 and spacing of 0.2.
- First character must be three lines drop-capped.
- The paragraph before spacing of 1 pt and after of 0 pt.
- Line spacing of 1 pt.
- Large images must be in one column.
- The names of first main headings (Heading 1) must be in Roman font, capital letters, and font size of 10.
- The names of second main headings (Heading 2) must not include numbers and must be in italics with a font size of 10.

Structure and Format of Manuscript

The recommended size of an original research paper is under 15,000 words and review papers under 7,000 words. Research articles should be less than 10,000 words. Research papers are usually longer than review papers. Review papers are reports of significant research (typically less than 7,000 words, including tables, figures, and references)

A research paper must include:

- a) A title which should be relevant to the theme of the paper.
- b) A summary, known as an abstract (less than 150 words), containing the major results and conclusions.
- c) Up to 10 keywords that precisely identify the paper's subject, purpose, and focus.
- d) An introduction, giving fundamental background objectives.
- e) Resources and techniques with sufficient complete experimental details (wherever possible by reference) to permit repetition, sources of information must be given, and numerical methods must be specified by reference.
- f) Results which should be presented concisely by well-designed tables and figures.
- g) Suitable statistical data should also be given.
- h) All data must have been gathered with attention to numerical detail in the planning stage.

Design has been recognized to be essential to experiments for a considerable time, and the editor has decided that any paper that appears not to have adequate numerical treatments of the data will be returned unrefereed.

- i) Discussion should cover implications and consequences and not just recapitulate the results; conclusions should also be summarized.
- j) There should be brief acknowledgments.
- k) There ought to be references in the conventional format. Global Journals recommends APA format.

Authors should carefully consider the preparation of papers to ensure that they communicate effectively. Papers are much more likely to be accepted if they are carefully designed and laid out, contain few or no errors, are summarizing, and follow instructions. They will also be published with much fewer delays than those that require much technical and editorial correction.

The Editorial Board reserves the right to make literary corrections and suggestions to improve brevity.



FORMAT STRUCTURE

It is necessary that authors take care in submitting a manuscript that is written in simple language and adheres to published guidelines.

All manuscripts submitted to Global Journals should include:

Title

The title page must carry an informative title that reflects the content, a running title (less than 45 characters together with spaces), names of the authors and co-authors, and the place(s) where the work was carried out.

Author details

The full postal address of any related author(s) must be specified.

Abstract

The abstract is the foundation of the research paper. It should be clear and concise and must contain the objective of the paper and inferences drawn. It is advised to not include big mathematical equations or complicated jargon.

Many researchers searching for information online will use search engines such as Google, Yahoo or others. By optimizing your paper for search engines, you will amplify the chance of someone finding it. In turn, this will make it more likely to be viewed and cited in further works. Global Journals has compiled these guidelines to facilitate you to maximize the web-friendliness of the most public part of your paper.

Keywords

A major lynchpin of research work for the writing of research papers is the keyword search, which one will employ to find both library and internet resources. Up to eleven keywords or very brief phrases have to be given to help data retrieval, mining, and indexing.

One must be persistent and creative in using keywords. An effective keyword search requires a strategy: planning of a list of possible keywords and phrases to try.

Choice of the main keywords is the first tool of writing a research paper. Research paper writing is an art. Keyword search should be as strategic as possible.

One should start brainstorming lists of potential keywords before even beginning searching. Think about the most important concepts related to research work. Ask, "What words would a source have to include to be truly valuable in a research paper?" Then consider synonyms for the important words.

It may take the discovery of only one important paper to steer in the right keyword direction because, in most databases, the keywords under which a research paper is abstracted are listed with the paper.

Numerical Methods

Numerical methods used should be transparent and, where appropriate, supported by references.

Abbreviations

Authors must list all the abbreviations used in the paper at the end of the paper or in a separate table before using them.

Formulas and equations

Authors are advised to submit any mathematical equation using either MathJax, KaTeX, or LaTeX, or in a very high-quality image.

Tables, Figures, and Figure Legends

Tables: Tables should be cautiously designed, uncrowned, and include only essential data. Each must have an Arabic number, e.g., Table 4, a self-explanatory caption, and be on a separate sheet. Authors must submit tables in an editable format and not as images. References to these tables (if any) must be mentioned accurately.



Figures

Figures are supposed to be submitted as separate files. Always include a citation in the text for each figure using Arabic numbers, e.g., Fig. 4. Artwork must be submitted online in vector electronic form or by emailing it.

PREPARATION OF ELECTRONIC FIGURES FOR PUBLICATION

Although low-quality images are sufficient for review purposes, print publication requires high-quality images to prevent the final product being blurred or fuzzy. Submit (possibly by e-mail) EPS (line art) or TIFF (halftone/ photographs) files only. MS PowerPoint and Word Graphics are unsuitable for printed pictures. Avoid using pixel-oriented software. Scans (TIFF only) should have a resolution of at least 350 dpi (halftone) or 700 to 1100 dpi (line drawings). Please give the data for figures in black and white or submit a Color Work Agreement form. EPS files must be saved with fonts embedded (and with a TIFF preview, if possible).

For scanned images, the scanning resolution at final image size ought to be as follows to ensure good reproduction: line art: >650 dpi; halftones (including gel photographs): >350 dpi; figures containing both halftone and line images: >650 dpi.

Color charges: Authors are advised to pay the full cost for the reproduction of their color artwork. Hence, please note that if there is color artwork in your manuscript when it is accepted for publication, we would require you to complete and return a Color Work Agreement form before your paper can be published. Also, you can email your editor to remove the color fee after acceptance of the paper.

TIPS FOR WRITING A GOOD QUALITY ENGINEERING RESEARCH PAPER

Techniques for writing a good quality engineering research paper:

1. Choosing the topic: In most cases, the topic is selected by the interests of the author, but it can also be suggested by the guides. You can have several topics, and then judge which you are most comfortable with. This may be done by asking several questions of yourself, like "Will I be able to carry out a search in this area? Will I find all necessary resources to accomplish the search? Will I be able to find all information in this field area?" If the answer to this type of question is "yes," then you ought to choose that topic. In most cases, you may have to conduct surveys and visit several places. Also, you might have to do a lot of work to find all the rises and falls of the various data on that subject. Sometimes, detailed information plays a vital role, instead of short information. Evaluators are human: The first thing to remember is that evaluators are also human beings. They are not only meant for rejecting a paper. They are here to evaluate your paper. So present your best aspect.

2. Think like evaluators: If you are in confusion or getting demotivated because your paper may not be accepted by the evaluators, then think, and try to evaluate your paper like an evaluator. Try to understand what an evaluator wants in your research paper, and you will automatically have your answer. Make blueprints of paper: The outline is the plan or framework that will help you to arrange your thoughts. It will make your paper logical. But remember that all points of your outline must be related to the topic you have chosen.

3. Ask your guides: If you are having any difficulty with your research, then do not hesitate to share your difficulty with your guide (if you have one). They will surely help you out and resolve your doubts. If you can't clarify what exactly you require for your work, then ask your supervisor to help you with an alternative. He or she might also provide you with a list of essential readings.

4. Use of computer is recommended: As you are doing research in the field of research engineering then this point is quite obvious. Use right software: Always use good quality software packages. If you are not capable of judging good software, then you can lose the quality of your paper unknowingly. There are various programs available to help you which you can get through the internet.

5. Use the internet for help: An excellent start for your paper is using Google. It is a wondrous search engine, where you can have your doubts resolved. You may also read some answers for the frequent question of how to write your research paper or find a model research paper. You can download books from the internet. If you have all the required books, place importance on reading, selecting, and analyzing the specified information. Then sketch out your research paper. Use big pictures: You may use encyclopedias like Wikipedia to get pictures with the best resolution. At Global Journals, you should strictly follow [here](#).



6. Bookmarks are useful: When you read any book or magazine, you generally use bookmarks, right? It is a good habit which helps to not lose your continuity. You should always use bookmarks while searching on the internet also, which will make your search easier.

7. Revise what you wrote: When you write anything, always read it, summarize it, and then finalize it.

8. Make every effort: Make every effort to mention what you are going to write in your paper. That means always have a good start. Try to mention everything in the introduction—what is the need for a particular research paper. Polish your work with good writing skills and always give an evaluator what he wants. Make backups: When you are going to do any important thing like making a research paper, you should always have backup copies of it either on your computer or on paper. This protects you from losing any portion of your important data.

9. Produce good diagrams of your own: Always try to include good charts or diagrams in your paper to improve quality. Using several unnecessary diagrams will degrade the quality of your paper by creating a hodgepodge. So always try to include diagrams which were made by you to improve the readability of your paper. Use of direct quotes: When you do research relevant to literature, history, or current affairs, then use of quotes becomes essential, but if the study is relevant to science, use of quotes is not preferable.

10. Use proper verb tense: Use proper verb tenses in your paper. Use past tense to present those events that have happened. Use present tense to indicate events that are going on. Use future tense to indicate events that will happen in the future. Use of wrong tenses will confuse the evaluator. Avoid sentences that are incomplete.

11. Pick a good study spot: Always try to pick a spot for your research which is quiet. Not every spot is good for studying.

12. Know what you know: Always try to know what you know by making objectives, otherwise you will be confused and unable to achieve your target.

13. Use good grammar: Always use good grammar and words that will have a positive impact on the evaluator; use of good vocabulary does not mean using tough words which the evaluator has to find in a dictionary. Do not fragment sentences. Eliminate one-word sentences. Do not ever use a big word when a smaller one would suffice.

Verbs have to be in agreement with their subjects. In a research paper, do not start sentences with conjunctions or finish them with prepositions. When writing formally, it is advisable to never split an infinitive because someone will (wrongly) complain. Avoid clichés like a disease. Always shun irritating alliteration. Use language which is simple and straightforward. Put together a neat summary.

14. Arrangement of information: Each section of the main body should start with an opening sentence, and there should be a changeover at the end of the section. Give only valid and powerful arguments for your topic. You may also maintain your arguments with records.

15. Never start at the last minute: Always allow enough time for research work. Leaving everything to the last minute will degrade your paper and spoil your work.

16. Multitasking in research is not good: Doing several things at the same time is a bad habit in the case of research activity. Research is an area where everything has a particular time slot. Divide your research work into parts, and do a particular part in a particular time slot.

17. Never copy others' work: Never copy others' work and give it your name because if the evaluator has seen it anywhere, you will be in trouble. Take proper rest and food: No matter how many hours you spend on your research activity, if you are not taking care of your health, then all your efforts will have been in vain. For quality research, take proper rest and food.

18. Go to seminars: Attend seminars if the topic is relevant to your research area. Utilize all your resources.

19. Refresh your mind after intervals: Try to give your mind a rest by listening to soft music or sleeping in intervals. This will also improve your memory. Acquire colleagues: Always try to acquire colleagues. No matter how sharp you are, if you acquire colleagues, they can give you ideas which will be helpful to your research.

20. Think technically: Always think technically. If anything happens, search for its reasons, benefits, and demerits. Think and then print: When you go to print your paper, check that tables are not split, headings are not detached from their descriptions, and page sequence is maintained.



21. Adding unnecessary information: Do not add unnecessary information like "I have used MS Excel to draw graphs." Irrelevant and inappropriate material is superfluous. Foreign terminology and phrases are not apropos. One should never take a broad view. Analogy is like feathers on a snake. Use words properly, regardless of how others use them. Remove quotations. Puns are for kids, not grunt readers. Never oversimplify: When adding material to your research paper, never go for oversimplification; this will definitely irritate the evaluator. Be specific. Never use rhythmic redundancies. Contractions shouldn't be used in a research paper. Comparisons are as terrible as clichés. Give up ampersands, abbreviations, and so on. Remove commas that are not necessary. Parenthetical words should be between brackets or commas. Understatement is always the best way to put forward earth-shaking thoughts. Give a detailed literary review.

22. Report concluded results: Use concluded results. From raw data, filter the results, and then conclude your studies based on measurements and observations taken. An appropriate number of decimal places should be used. Parenthetical remarks are prohibited here. Proofread carefully at the final stage. At the end, give an outline to your arguments. Spot perspectives of further study of the subject. Justify your conclusion at the bottom sufficiently, which will probably include examples.

23. Upon conclusion: Once you have concluded your research, the next most important step is to present your findings. Presentation is extremely important as it is the definite medium through which your research is going to be in print for the rest of the crowd. Care should be taken to categorize your thoughts well and present them in a logical and neat manner. A good quality research paper format is essential because it serves to highlight your research paper and bring to light all necessary aspects of your research.

INFORMAL GUIDELINES OF RESEARCH PAPER WRITING

Key points to remember:

- Submit all work in its final form.
- Write your paper in the form which is presented in the guidelines using the template.
- Please note the criteria peer reviewers will use for grading the final paper.

Final points:

One purpose of organizing a research paper is to let people interpret your efforts selectively. The journal requires the following sections, submitted in the order listed, with each section starting on a new page:

The introduction: This will be compiled from reference matter and reflect the design processes or outline of basis that directed you to make a study. As you carry out the process of study, the method and process section will be constructed like that. The results segment will show related statistics in nearly sequential order and direct reviewers to similar intellectual paths throughout the data that you gathered to carry out your study.

The discussion section:

This will provide understanding of the data and projections as to the implications of the results. The use of good quality references throughout the paper will give the effort trustworthiness by representing an alertness to prior workings.

Writing a research paper is not an easy job, no matter how trouble-free the actual research or concept. Practice, excellent preparation, and controlled record-keeping are the only means to make straightforward progression.

General style:

Specific editorial column necessities for compliance of a manuscript will always take over from directions in these general guidelines.

To make a paper clear: Adhere to recommended page limits.

Mistakes to avoid:

- Insertion of a title at the foot of a page with subsequent text on the next page.
- Separating a table, chart, or figure—confine each to a single page.
- Submitting a manuscript with pages out of sequence.
- In every section of your document, use standard writing style, including articles ("a" and "the").
- Keep paying attention to the topic of the paper.

- Use paragraphs to split each significant point (excluding the abstract).
- Align the primary line of each section.
- Present your points in sound order.
- Use present tense to report well-accepted matters.
- Use past tense to describe specific results.
- Do not use familiar wording; don't address the reviewer directly. Don't use slang or superlatives.
- Avoid use of extra pictures—include only those figures essential to presenting results.

Title page:

Choose a revealing title. It should be short and include the name(s) and address(es) of all authors. It should not have acronyms or abbreviations or exceed two printed lines.

Abstract: This summary should be two hundred words or less. It should clearly and briefly explain the key findings reported in the manuscript and must have precise statistics. It should not have acronyms or abbreviations. It should be logical in itself. Do not cite references at this point.

An abstract is a brief, distinct paragraph summary of finished work or work in development. In a minute or less, a reviewer can be taught the foundation behind the study, common approaches to the problem, relevant results, and significant conclusions or new questions.

Write your summary when your paper is completed because how can you write the summary of anything which is not yet written? Wealth of terminology is very essential in abstract. Use comprehensive sentences, and do not sacrifice readability for brevity; you can maintain it succinctly by phrasing sentences so that they provide more than a lone rationale. The author can at this moment go straight to shortening the outcome. Sum up the study with the subsequent elements in any summary. Try to limit the initial two items to no more than one line each.

Reason for writing the article—theory, overall issue, purpose.

- Fundamental goal.
- To-the-point depiction of the research.
- Consequences, including definite statistics—if the consequences are quantitative in nature, account for this; results of any numerical analysis should be reported. Significant conclusions or questions that emerge from the research.

Approach:

- Single section and succinct.
- An outline of the job done is always written in past tense.
- Concentrate on shortening results—limit background information to a verdict or two.
- Exact spelling, clarity of sentences and phrases, and appropriate reporting of quantities (proper units, important statistics) are just as significant in an abstract as they are anywhere else.

Introduction:

The introduction should "introduce" the manuscript. The reviewer should be presented with sufficient background information to be capable of comprehending and calculating the purpose of your study without having to refer to other works. The basis for the study should be offered. Give the most important references, but avoid making a comprehensive appraisal of the topic. Describe the problem visibly. If the problem is not acknowledged in a logical, reasonable way, the reviewer will give no attention to your results. Speak in common terms about techniques used to explain the problem, if needed, but do not present any particulars about the protocols here.

The following approach can create a valuable beginning:

- Explain the value (significance) of the study.
- Defend the model—why did you employ this particular system or method? What is its compensation? Remark upon its appropriateness from an abstract point of view as well as pointing out sensible reasons for using it.
- Present a justification. State your particular theory(-ies) or aim(s), and describe the logic that led you to choose them.
- Briefly explain the study's tentative purpose and how it meets the declared objectives.



Approach:

Use past tense except for when referring to recognized facts. After all, the manuscript will be submitted after the entire job is done. Sort out your thoughts; manufacture one key point for every section. If you make the four points listed above, you will need at least four paragraphs. Present surrounding information only when it is necessary to support a situation. The reviewer does not desire to read everything you know about a topic. Shape the theory specifically—do not take a broad view.

As always, give awareness to spelling, simplicity, and correctness of sentences and phrases.

Procedures (methods and materials):

This part is supposed to be the easiest to carve if you have good skills. A soundly written procedures segment allows a capable scientist to replicate your results. Present precise information about your supplies. The suppliers and clarity of reagents can be helpful bits of information. Present methods in sequential order, but linked methodologies can be grouped as a segment. Be concise when relating the protocols. Attempt to give the least amount of information that would permit another capable scientist to replicate your outcome, but be cautious that vital information is integrated. The use of subheadings is suggested and ought to be synchronized with the results section.

When a technique is used that has been well-described in another section, mention the specific item describing the way, but draw the basic principle while stating the situation. The purpose is to show all particular resources and broad procedures so that another person may use some or all of the methods in one more study or referee the scientific value of your work. It is not to be a step-by-step report of the whole thing you did, nor is a methods section a set of orders.

Materials:

Materials may be reported in part of a section or else they may be recognized along with your measures.

Methods:

- Report the method and not the particulars of each process that engaged the same methodology.
- Describe the method entirely.
- To be succinct, present methods under headings dedicated to specific dealings or groups of measures.
- Simplify—detail how procedures were completed, not how they were performed on a particular day.
- If well-known procedures were used, account for the procedure by name, possibly with a reference, and that's all.

Approach:

It is embarrassing to use vigorous voice when documenting methods without using first person, which would focus the reviewer's interest on the researcher rather than the job. As a result, when writing up the methods, most authors use third person passive voice.

Use standard style in this and every other part of the paper—avoid familiar lists, and use full sentences.

What to keep away from:

- Resources and methods are not a set of information.
- Skip all descriptive information and surroundings—save it for the argument.
- Leave out information that is immaterial to a third party.

Results:

The principle of a results segment is to present and demonstrate your conclusion. Create this part as entirely objective details of the outcome, and save all understanding for the discussion.

The page length of this segment is set by the sum and types of data to be reported. Use statistics and tables, if suitable, to present consequences most efficiently.

You must clearly differentiate material which would usually be incorporated in a study editorial from any unprocessed data or additional appendix matter that would not be available. In fact, such matters should not be submitted at all except if requested by the instructor.



Content:

- Sum up your conclusions in text and demonstrate them, if suitable, with figures and tables.
- In the manuscript, explain each of your consequences, and point the reader to remarks that are most appropriate.
- Present a background, such as by describing the question that was addressed by creation of an exacting study.
- Explain results of control experiments and give remarks that are not accessible in a prescribed figure or table, if appropriate.
- Examine your data, then prepare the analyzed (transformed) data in the form of a figure (graph), table, or manuscript.

What to stay away from:

- Do not discuss or infer your outcome, report surrounding information, or try to explain anything.
- Do not include raw data or intermediate calculations in a research manuscript.
- Do not present similar data more than once.
- A manuscript should complement any figures or tables, not duplicate information.
- Never confuse figures with tables—there is a difference.

Approach:

As always, use past tense when you submit your results, and put the whole thing in a reasonable order.

Put figures and tables, appropriately numbered, in order at the end of the report.

If you desire, you may place your figures and tables properly within the text of your results section.

Figures and tables:

If you put figures and tables at the end of some details, make certain that they are visibly distinguished from any attached appendix materials, such as raw facts. Whatever the position, each table must be titled, numbered one after the other, and include a heading. All figures and tables must be divided from the text.

Discussion:

The discussion is expected to be the trickiest segment to write. A lot of papers submitted to the journal are discarded based on problems with the discussion. There is no rule for how long an argument should be.

Position your understanding of the outcome visibly to lead the reviewer through your conclusions, and then finish the paper with a summing up of the implications of the study. The purpose here is to offer an understanding of your results and support all of your conclusions, using facts from your research and generally accepted information, if suitable. The implication of results should be fully described.

Infer your data in the conversation in suitable depth. This means that when you clarify an observable fact, you must explain mechanisms that may account for the observation. If your results vary from your prospect, make clear why that may have happened. If your results agree, then explain the theory that the proof supported. It is never suitable to just state that the data approved the prospect, and let it drop at that. Make a decision as to whether each premise is supported or discarded or if you cannot make a conclusion with assurance. Do not just dismiss a study or part of a study as "uncertain."

Research papers are not acknowledged if the work is imperfect. Draw what conclusions you can based upon the results that you have, and take care of the study as a finished work.

- You may propose future guidelines, such as how an experiment might be personalized to accomplish a new idea.
- Give details of all of your remarks as much as possible, focusing on mechanisms.
- Make a decision as to whether the tentative design sufficiently addressed the theory and whether or not it was correctly restricted. Try to present substitute explanations if they are sensible alternatives.
- One piece of research will not counter an overall question, so maintain the large picture in mind. Where do you go next? The best studies unlock new avenues of study. What questions remain?
- Recommendations for detailed papers will offer supplementary suggestions.



Approach:

When you refer to information, differentiate data generated by your own studies from other available information. Present work done by specific persons (including you) in past tense.

Describe generally acknowledged facts and main beliefs in present tense.

THE ADMINISTRATION RULES

Administration Rules to Be Strictly Followed before Submitting Your Research Paper to Global Journals Inc.

Please read the following rules and regulations carefully before submitting your research paper to Global Journals Inc. to avoid rejection.

Segment draft and final research paper: You have to strictly follow the template of a research paper, failing which your paper may get rejected. You are expected to write each part of the paper wholly on your own. The peer reviewers need to identify your own perspective of the concepts in your own terms. Please do not extract straight from any other source, and do not rephrase someone else's analysis. Do not allow anyone else to proofread your manuscript.

Written material: You may discuss this with your guides and key sources. Do not copy anyone else's paper, even if this is only imitation, otherwise it will be rejected on the grounds of plagiarism, which is illegal. Various methods to avoid plagiarism are strictly applied by us to every paper, and, if found guilty, you may be blacklisted, which could affect your career adversely. To guard yourself and others from possible illegal use, please do not permit anyone to use or even read your paper and file.



CRITERION FOR GRADING A RESEARCH PAPER (COMPILATION)
BY GLOBAL JOURNALS

Please note that following table is only a Grading of "Paper Compilation" and not on "Performed/Stated Research" whose grading solely depends on Individual Assigned Peer Reviewer and Editorial Board Member. These can be available only on request and after decision of Paper. This report will be the property of Global Journals.

Topics	Grades		
	A-B	C-D	E-F
<i>Abstract</i>	Clear and concise with appropriate content, Correct format. 200 words or below	Unclear summary and no specific data, Incorrect form Above 200 words	No specific data with ambiguous information Above 250 words
<i>Introduction</i>	Containing all background details with clear goal and appropriate details, flow specification, no grammar and spelling mistake, well organized sentence and paragraph, reference cited	Unclear and confusing data, appropriate format, grammar and spelling errors with unorganized matter	Out of place depth and content, hazy format
<i>Methods and Procedures</i>	Clear and to the point with well arranged paragraph, precision and accuracy of facts and figures, well organized subheads	Difficult to comprehend with embarrassed text, too much explanation but completed	Incorrect and unorganized structure with hazy meaning
<i>Result</i>	Well organized, Clear and specific, Correct units with precision, correct data, well structuring of paragraph, no grammar and spelling mistake	Complete and embarrassed text, difficult to comprehend	Irregular format with wrong facts and figures
<i>Discussion</i>	Well organized, meaningful specification, sound conclusion, logical and concise explanation, highly structured paragraph reference cited	Wordy, unclear conclusion, spurious	Conclusion is not cited, unorganized, difficult to comprehend
<i>References</i>	Complete and correct format, well organized	Beside the point, Incomplete	Wrong format and structuring



INDEX

A

Acenaphthylene · 36, 40
Aliphatic · 39
Anthracene · 36, 37, 40

B

Brines · 32

C

Canoe · 33
Concentric · 18

F

Fluoranthene · 36, 37, 40

P

Phenanthrene · 36, 40
Polyaromatic · 32, 36, 39
Primordial · 18
Pristine · 37

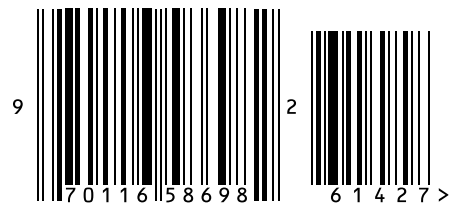


save our planet



Global Journal of Researches in Engineering

Visit us on the Web at www.GlobalJournals.org | www.EngineeringResearch.org
or email us at helpdesk@globaljournals.org



ISSN 9755861

© Global Journals